Cambridge, Massachusetts
July 1951

Professor J. S. Newell
Secretary of the Faculty
Massachusetts Institute of Technology
Cambridge 39, Massachusetts

Dear Sir :

In accordance with the requirements for the degree of Master of Science in Marine Engineering, I submit herewith a thesis entitled CALCULATION OF CAVITATING PROPELLER CHARACTERISTICS.

Respectfully,

Alexander J. Tachmindji

CALCULATION OF CAVITATING PROPELLER CHARACTERISTICS.

by

ALEXANDER J. TACHMINDJI

B.Sc., University of Durham, 1949

SUBMITTED IN PARTIAL FULFILLMENT OF THE
REQUIREMENTS FOR THE DEGREE OF
MASTER OF SCIENCE
in
MARINE ENGINEERING
at the
MASSACHUSETTS INSTITUTE OF TECHNOLOGY
1951

Signature of Author .....

Department of Naval Architecture and Marine Engineering
July 1951

Thesis Supervisor .....

Signature of Chairman of Departmental
Committee on Graduate Students .....

CALCULATION OF CAVITATING PROPELLER CHARACTERISTICS.

by

A. J. Tachmindji

Submitted for the degree of Master of Science
in the Department of Naval Architecture
and Marine Engineering.
July 1951.

Abstract.

The thesis deals with a method of calculating the performance of propellers operating in the cavitating region. The analysis is based on the theory developed for a screw operating under high loading in conjunction with two-dimensional characteristics of single sections in cavitation. Allowance has been made for the cascade effect in the propeller and the formation of cavities around the blade. Such cavities modify the apparent outline of the blade and the section, increasing the cascade correction which has to be applied to a single section.

The present analysis which is limited to ogival sections due to the lack of data for aerofoil profiles, has shown that it is possible to determine the performance provided that back cavitation only is present.

Values of lift and drag coefficients and the increase in solidity under cavitation are given for a number of cavitation indices. A calculation has been performed for a severely cavitating screw, the results indicating that the presence of vapor pockets do not essentially modify the propeller theory and that the cavitating region can be considered as an extension to the normal operation.

ACKNOWLEDGMENT.

The author would like to acknowledge the help of Professor F.M. Lewis of the Department of Naval Architecture and Marine Engineering, for his active interest and valuable suggestions in connection with this work.

TABLE OF CONTENTS.

LIST OF FIGURES.

INTRODUCTION.

Since the formulation of the vortex theory for screw propellers, a number of attempts have been made in predicting the performance characteristics, with a view towards providing a method for improving the design features and obtaining the most efficient distribution of blade elements. Such treatments have been concerned with the performance of propellers in the non-cavitating condition, and are based on extensions of the Lanchester-Prandtl aerofoil theory. The application of such a theory for lightly loaded propellers was developed by Betz (Ref. 1) establishing the best distribution of thrust along the blades for minimum induced drag. In the succeeding period various papers were published by Helmboldt, Glauert, Pistolesi, Kawada, Burrill and Hill (Ref. 2, 3, 4, 5, 6 and 7) applying the above theory to the analysis of propeller problems and the prediction of propeller performances.

Such applications were, however, limited in predicting the performances in the non-cavitating region and in general for the case of lightly loaded propellers. While the majority of screws are designed to operate with no cavitation, there are instances where some form of cavitation has to be accepted during operating conditions and it is for such cases that the present analysis nas been made. It is also realised, that a more complete knowledge of the results of cavitation might lead to a comprehensive method of incorporating, during the design procedure, features which may retard the onset of cavitation or in any event may decrease the effect which cavitation has upon thrust and torque.

The theory with which the initial developments were made

is based on the conception that the induced velocities are those formed by a system of free vortices which are initiated from the blades and thus constitute the slipstream of the propeller. This system of free vortices takes the form of helicoidal vortex sheets which originate from the trailing edge of each blade and pass down aft of the propeller with a pitch slightly greater than that of the blades. In an ideal propeller with an infinite number of blades, these helicoidal vortex sheets will be very close together and can thus be considered as being equivalent to a compact system of cylindrical vortex sheets. Further, in place of the closely spaced helical vortex lines which constitute these cylindrical sheets at each radius, the vorticity corresponding to each annulus of the propeller can be considered to be made up of a close succession of transverse vortex rings whose vorticity represents the increased axial velocity of the slipstream, and a cylindrical surface formed by longitudinal vortex lines whose vorticity represents the rotation of the slipstream. A knowledge of the induced velocities formed by the vortex system, affords a method of determining the hydrodynamic reaction on any blade from the modified velocities in association with the aerofoil characteristics corresponding to a two-dimensional flow.

The effect of cavitation of the blade will not modify the above mechanism but will introduce additional factors which have to be considered. In the case of a lightly loaded screw propeller the contraction of the slipstream may be neglected, but by the introduction of cavitation, the vortex sheet angle will be considerably affected. In addition, due to the formation of a cavity at the blade section the effective blade outline as well as the section outline will be changed in such a way so as to reduce the thrust and

torque characteristics of the screw. The presence of cavities will effectively modify the propeller and may produce the same effect as a screw with blade sections and an outline which includes the cavities. This change is not, however, always truly defined owing to the fact that cavitation may appear in laminar or bubble type, and in the latter case while the effective thickness of the section may be actually considered as being increased, the amount of increment in that section is indeterminate. It is, therefore, logical that the above viewpoint has to be limited to a laminar type cavitation where the changes in the section outline are definite. Further, as the amount of bubble cavitation is directly dependant on the air content in the water (Ref.8) while this has relatively little effect on laminar cavitation, it would be necessary to introduce a parameter involving air content when presenting the performance characteristics in the cavitating condition. Such a parameter, however, has not yet been developed and a correction for bubble cavitation would be unwarranted.

The effect of cavitation on the blade will modify both the angle of the vortex sheets and the magnitude of the induced velocities, but these effects are automatically introduced when the characteristics of the section in the two-dimensional flow are considered. It is only necessary, therefore, to develop the theory for a heavily loaded but non-cavitating screw, the effect of cavitation and the necessary corrections for blade width augmentation being introduced during the calculation process.

The lack of two-dimensional data for aerofoil sections in the cavitating region has limited this analysis to propellers having ogival sections only. In the light of further developments, however, the analysis can be extended for aerofoil sections, provided that the necessary characteristics of the sections are known.

PROCEDURE.

ANALYSIS OF THEORY.

The development of the theory which has been used*, is the one introduced by Burrill (Ref. 6) and is essentially similar to Glauert's (Ref. 12) and to Lock's (Ref. 13 and 14) except for a few minor modifications. The elements of thrust at any radius can be obtained on the basis of the vortex theory or the simple momentum theory due allowance being made for a propeller having a finite number of blades. The Goldstein correction factor is in this case introduced as a factor in the velocity rather than in the circulation, a complete discussion on this subject being given in Appendix A. This analysis takes account of the change in the angle of the vortex sheets from ϕ to ϵ due to the contraction of the slipstream and hence of a modification of the Goldstein factor k_ϕ to k_ϵ. If a is the axial inflow factor, then the element of thrust dT at any radius r, is given by :

$$\frac{dT}{dr} = 4\pi.r.\rho.V^2(1 + k_\phi.a).k_\epsilon.a \quad * \quad .....(1)$$

This expression which has been derived by the simple momentum theory can also be determined when based on other considerations. Burrill (Ref. 6) derives equation (1) on the basis of pressure rise across the propeller, while similar expressions can also be obtained from considerations of the vortex theory method of approach by comparing the thrust at the blades to the thrust in terms of the mean circulation in the ultimate wake.

---

* See Appendix B for derivation.

It will be noticed that expression (1) is slightly different from the one derived by Lock (Ref. 14) using the Kutta-Joukowski law. In terms of the notation used in this development, Lock gets a thrust distribution given by :

$$\frac{dT}{dr} = 4\pi.r.\rho.V^2(1 + a).k_\phi.a \qquad .....(2)$$

The above expression assumes that there is no contraction of the slipstream and hence that the angle ϕ and ϵ are equal. A calculation with expression (2) has yielded that the thrust at any radius is about 5% greater than that given by equation (1).

Another expression can be developed, on the assumption that the mean inflow at the screw is half of that at the ultimate wake, thus neglecting the increment in hydrodynamic pitch angle between the propeller and the slipstream at infinity behind. On the basis of such an assumption the thrust will be given by :

$$\frac{dT}{dr} = 4\pi.r.\rho.V^2(1 + k_\phi.a).k_\phi.a \qquad .....(3)$$

the values derived from this expression being 3% greater than those calculated from equation (1) for the usual values of advance ratio.

In view of the above considerations, equation (1) has been used as the expression giving the thrust distribution at any radius. It is now possible to equate (1) with an expression for the elementary thrust in terms of the lift and drag coefficient at that radius and thus to obtain the values of the axial and rotational inflow factors a and a', as well as the value of the lift coefficient. As shown in Appendix B,

$$a = \frac{\tan\phi - \tan\psi}{\tan\psi\{1 + \tan\phi.\tan(\phi + \gamma)\}} \qquad .....(4)$$

$$a' = \frac{\{\tan\phi - \tan\psi\}\tan(\phi+\gamma)}{1 + \tan\phi.\tan(\phi+\gamma)} \quad \ldots\ldots\ldots(5)$$

$$C_L = \frac{4}{s}.k_\epsilon.\sin\phi.\tan\beta.\left\{1 - \frac{\tan\beta}{\tan\phi}\left(1 - k_\phi\right)\right\} \quad \ldots(6)$$

(See Appendix A for Nomenclature and definition of Angles)

It will be noticed that these expressions are functions of the hydrodynamic pitch angle ϕ, the advance angle ψ, the hydrodynamic inflow angle β, the drag-lift ratio $\tan\gamma$, the solidity s and the Goldstein factor k_ϕ and k_ϵ, all of which are known or determinable if ϕ is known. The elementary thrust and torque coefficients K_{Tx} and K_{Qx} can be expressed as

$$K_{Tx} = \frac{s}{4}\pi^3.x^3.(1 - a')^2(1 + \tan^2\phi).C_L\frac{\cos(\phi+\gamma)}{\cos\gamma} \quad \ldots(7)$$

and $$K_{Qx} = \frac{s}{8}\pi^3.x^4.(1 - a')^2(1 + \tan^2\phi).C_L\frac{\sin(\phi+\gamma)}{\cos\gamma} \quad \ldots(8)$$

The value of the lift coefficient can be obtained through a process of trial anf error if the two-dimensional characteristics of the sections are known. In such a case a value for the angle of attack of the section can be assumed, and it is thus possible to compare the lift coefficient obtained from expression (6) and from the experimental curves. If the two lift coefficients do not agree then a change in the assumed angle of attack is necessary until such agreement is reached.

The pitch angle ϵ of the vortex sheets in the slipstream of the propeller will be slightly greater than the one at the propeller plane owing to the contraction of the slipstream. The value of such an angle can be obtained in terms of the inflow velocities and the hydrodynamic pitch angle at the propeller, and as shown in Appendix B is given by :

$$\tan\epsilon = \frac{1}{(1 - 2a')}\left\{2(1 - a').\tan\phi - \tan\psi\right\} \quad \ldots\ldots(9)$$

This expression cannot, however, be evaluated in the initial stages of the calculation but if the angle γ is neglected in comparison with ϕ, it may be approximated to

$$\epsilon \doteq \phi + \beta \quad \ldots\ldots\ldots\ldots\ldots\ldots\ldots(10)$$

Effect of pressure drop in the ultimate wake.

The rotation of the slipstream with an angular velocity varying at each radius will produce a reduction in pressure in the final wake and will, therefore, have some influence on the thrust and torque. This influence is, however, extremely small in the outer parts of the propeller, a position at which the majority of the thrust is concentrated. The pressure drop will have an appreciable effect on the angles of incidence, lift coefficients and efficiencies of the inner sections and in the case of an unusual propeller designed to give an approximately constant thrust distribution over the blade it might be desirable to include such effect. For normal screws the effect may be safely neglected (Ref. 15) and in the present calculation such effect has been entirely omitted.

It may be possible, if such a correction is warranted, to introduce it by considering the total pressure drop across the propeller to be altered by the dynamic pressure $\frac{1}{2} \cdot (1 - k_c \cdot a')^2 \cdot \Omega^2 r^2$. The efficiency of the section will, therefore, be decreased by the term $(1 - k_c \cdot a')$. As the efficiency of any section is

$$e_x = \frac{\tan \psi}{\tan(\phi + \gamma)}$$

the term $\tan(\phi + \gamma)$ will be changed and will be given by

$$\tan(\phi + \gamma) \text{ with rotation} = (1 - k_c \cdot a') \tan(\phi + \gamma) \text{ without rotation}$$

If the drag-lift ratio γ was constant the solution would be simple, but as γ is itself a function of the angle of attack and hence ϕ, a series of γ values have to be assumed and the corresponding angle of incidence calculated until the above equation is satisfied.

Such an analysis, however, introduces a very small

correction and due to the fact that the theory is in itself an approximation, such corrections are not warranted for the usual type propellers.

Cavitation index.

The usual cavitation index is based on the dynamic pressure corresponding only to the axial velocity of advance, though there have been some advocates (Ref. 16) stating that such an index should be based on the total dynamic pressure, considering both the rotational and the axial velocity. The usual cavitation index, hereby denoted by σ_v, is therefore only a comparative number. In the M.I.T. propeller tunnel the index σ_n is used for ease in experimenting and which is based on the rotational component only. This index has an additional advantage in that it is possible to distinguish the onset of face cavitation when the characteristics of a propeller are plotted with such a parameter. During this analysis, therefore, calculations have been performed for constant σ_n values, though the corresponding σ_v values have also been given.

The cavitation index σ_x for any section has, however, to be based on the dynamic pressure of the resultant component of both velocities at that section, as only such resultant is measured during two-dimensional flow experimentation.

The relation between σ_x and σ_v is derived in Appendix B and is given by :

$$\sigma_x = \frac{\sigma_v}{(1 - a')^2 \left\{ \frac{\tan^2\phi}{\tan^2\psi} + \frac{(\pi.x)^2}{J^2} \right\}} \qquad \ldots\ldots(11)$$

The above equation can be simplified by neglecting the

inflow velocities, and then

$$\sigma_x \doteq \frac{\sigma_v}{1 + \frac{(\pi . x)^2}{J^2}} \qquad \text{.....(12)}$$

such expression being used as a first approximation.

TWO-DIMENSIONAL CHARACTERISTICS OF BLADE SECTIONS.

From considerations of the developed propeller theory it is seen that two-dimensional characteristics for sections under cavitating conditions are necessary in order to calculate the values of the lift and drag coefficients. Such data is, however, extremely rare and only a limited number of tests have been carried out for sections under fully developed cavitating conditions, the majority of experimenters being contended with tests up to the onset of cavitation. The influence of complete cavitation on the lift and drag characteristics has only been investigated by Walchner, Ackeret, Hinterthan and Martyrer (Ref. 17, 18, 19, 20 and 21) for a limited number of sections. Due to the lack of data on aerofoil profiles, it was decided to perform the analysis for a propeller having ogival sections. This was also substantiated by the ease in combining the characteristics of such sections, as the only necessary parameter is the thickness-chord ratio. Some characteristics for sections used in turbine blading (Ref. 22) were compared to those directly applicable to propeller sections and found to be in general agreement.

The data is plotted in Fig.(16) through Fig.(35) on the basis of thickness-chord ratio for each cavitation index. Such data has been obtained from Walchner's, Hinterthan's

LIFT COEFFICIENT, C_L
-0.8
-0.4
0
0.4
0.8
1.2
1.6
$C_{L_{max}}$
$\alpha_{C_{L_{max}}}$
$\alpha_{C_{L_0}}$
$\alpha_{C_{L_{min}}}$
$C_{L_{min}}$
LIFT COEFFICIENT
FIG. 1
$C_{L_{max}} = 0.934$

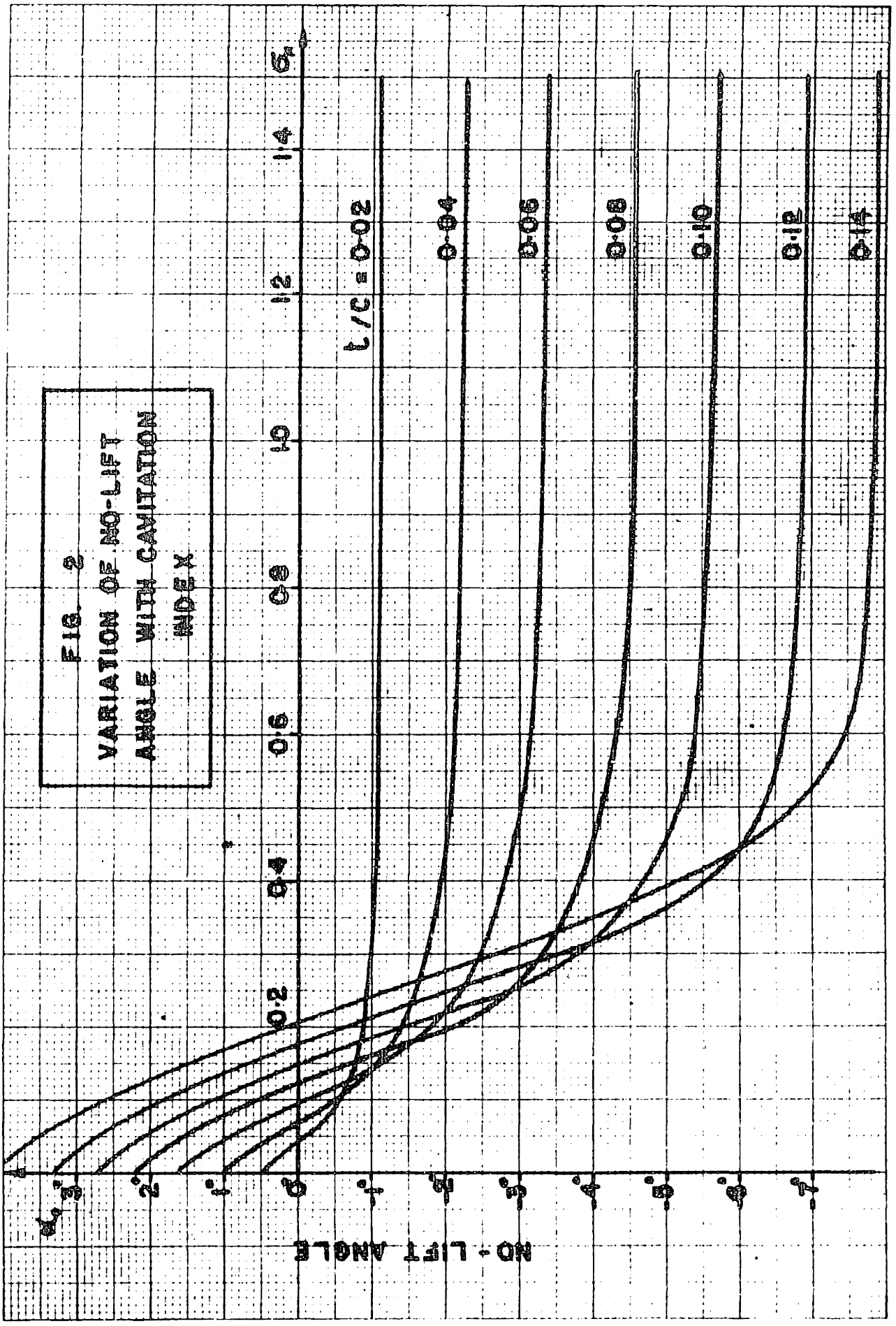

FIG. 2
VARIATION OF NO-LIFT ANGLE WITH CAVITATION INDEX σ

and Martyrer's tests for ogival sections, though it must be realised that the number of sections tested is inadequate to certify these results. The plots are faired through the experimental points giving a range of thickness-chord ratio from 0.025 to 0.15 which represents the common values for marine propeller sections. The cavitation index refers to that of the section and is based on the total velocity that the section encounters. The dotted line on the lift coefficient curves represents the approximate angle of attack for a given thickness-chord ratio at which the section will start to cavitate, while the chain-dotted lines on the drag curves are those for negative angles of attack and are plotted to an inverted scale in order to avoid confusion with the positive angle of attack curves.

Fig. (1) shows the relationship between cavitation index and lift coefficient for one thickness-chord ratio and it will be seen that in general such a relationship is a straight line so that linear interpolation may be used between the Fig. (16) - (35) for cases of intermediate cavitation indices. If some doubt, however, exists as to whether the section operates at, or near, the peak it is advisable to make an auxiliary plot for that particular section and for the desired angle of attack and thus determine the value of the lift coefficient at the desired σ_x value.

The variation of the no-lift angle as the cavitation increases is shown by the contours in Fig.(2). It will be noticed that as the cavitation index is decreased the position of the no-lift line moves from the back to the face of the section. This indicates that in order to obtain the same lift coefficient under cavitating conditions as that existing during normal operation, the angle must be increased by an amount, at least, equal to the change in the no-lift angle.

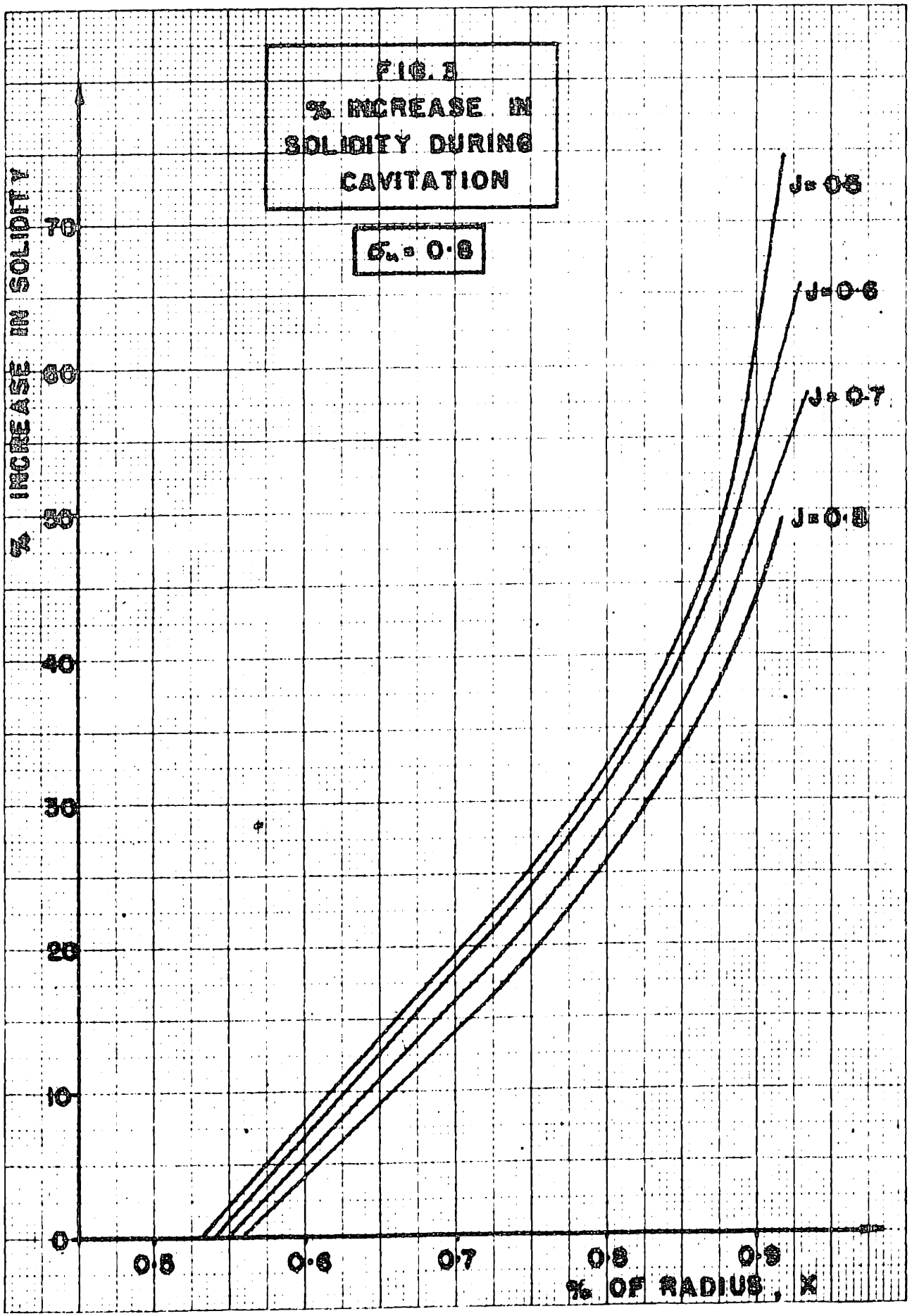
FIG. 8
% INCREASE IN SOLIDITY DURING CAVITATION
σ_n = 0·8
% INCREASE IN SOLIDITY
70
60
50
40
30
20
10
0
J = 0·5
J = 0·6
J = 0·7
J = 0·8
0·5
0·6
0·7
0·8
0·9
% OF RADIUS, X

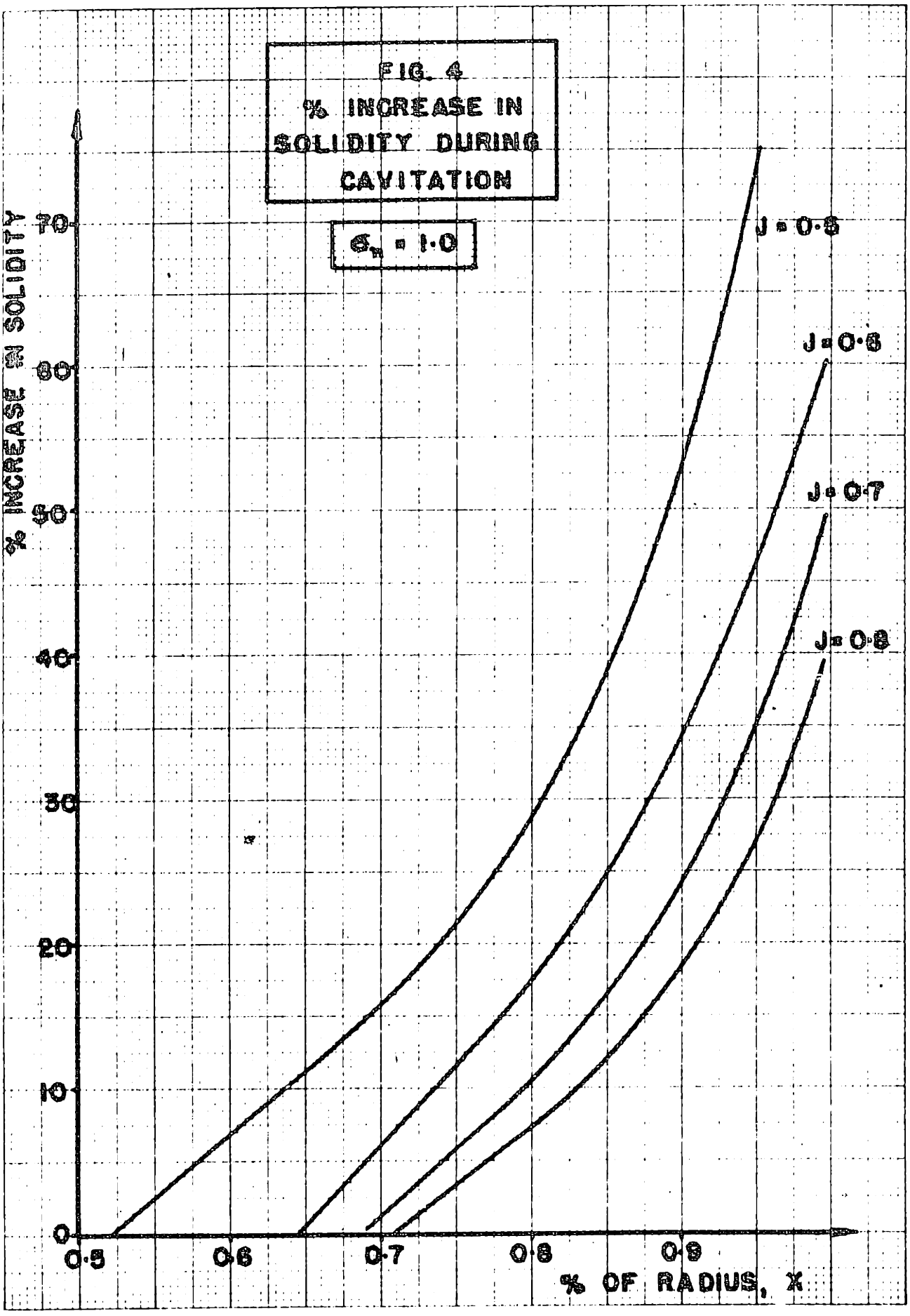
FIG. 4
% INCREASE IN SOLIDITY DURING CAVITATION
σ_n = 1·0
% INCREASE IN SOLIDITY
70
60
50
40
30
20
10
0
J = 0·5
J = 0·6
J = 0·7
J = 0·8
0·5
0·6
0·7
0·8
0·9
% OF RADIUS, X

CASCADE CORRECTION UNDER CAVITATION.

As in the case of non-cavitating operation a correction factor must be applied to the two-dimensional characteristics of a single section, in order to account for the cascade interference in the blades. The formation of a cavity around the blade will accentuate that effect and will modify the section, increasing both the thickness and the chord and thus producing an effectively smaller gap ratio between the blades. The magnitude of such an effect is quite considerable decreasing the lift coefficient by as much as 50% when the presence of the cavity is taken into account.

Unfortunately, however, no tests in cascade under cavitating conditions have been performed and the correction for cavity formation has to be done artificially. This correction is introduced as an increase in chord, neglecting the increment in thickness, and thus accounting for the formation of back cavitation. Face cavitation, will in the majority of cases, take the form of an increase in thickness except under extreme conditions where the cavity might extend beyond the trailing edge of the section, and will only then produce an effective chord length which is greater than the actual.

Knowing the effectively increased chord length it is possible to obtain an effective solidity for the propeller at that radius and using that value determine the cascade factor from non-cavitating tests. The increment in chord length, plotted as an increment in solidity, is shown in Fig.(3) and (4) for different conditions of operation but for one particular propeller and has been obtained from observations in the propeller tunnel. Such data has also been compared to Walchner's observations for single sections and is shown in Fig.(5) plotted against angle of attack for

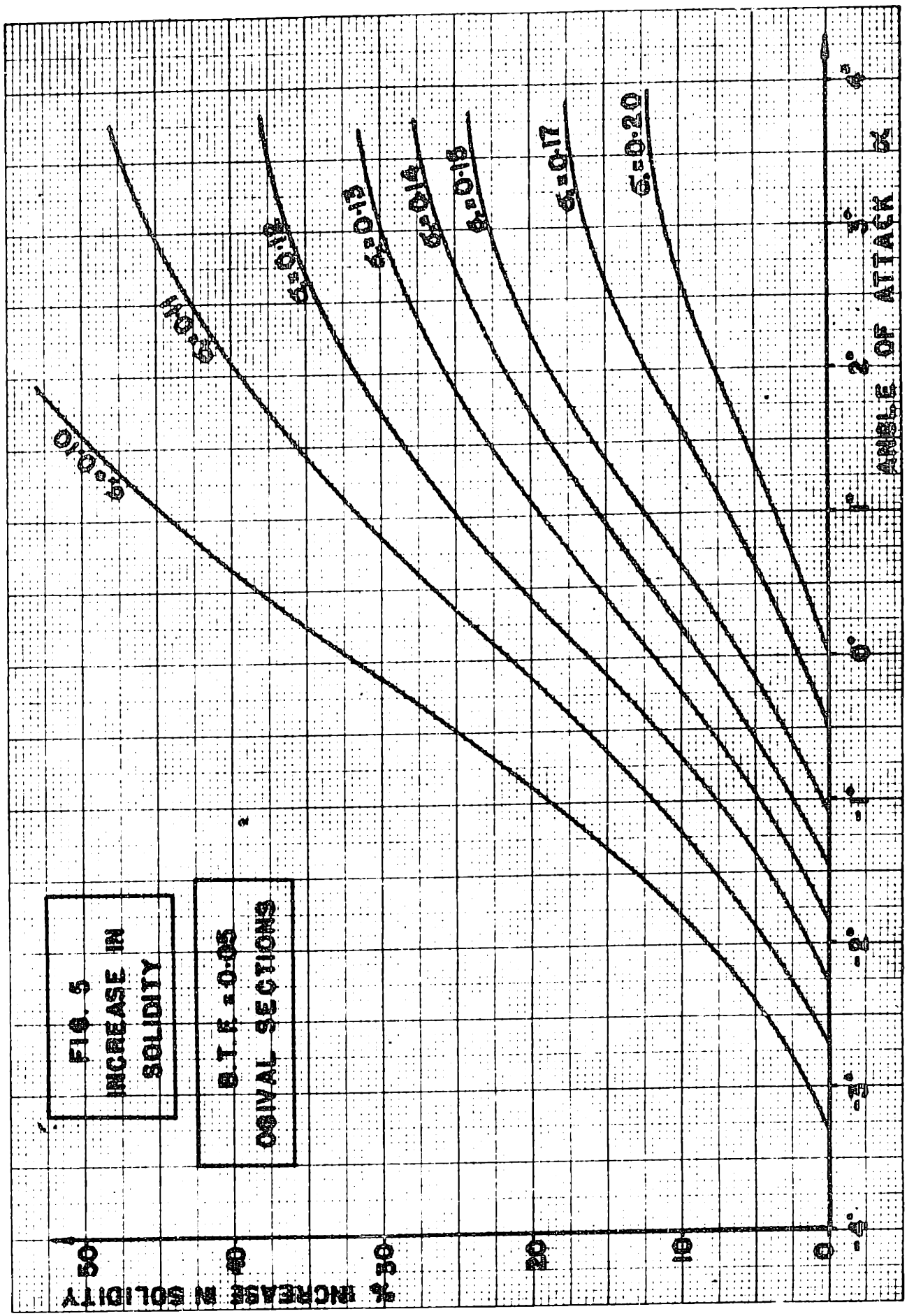

Fig. 5
INCREASE IN SOLIDITY

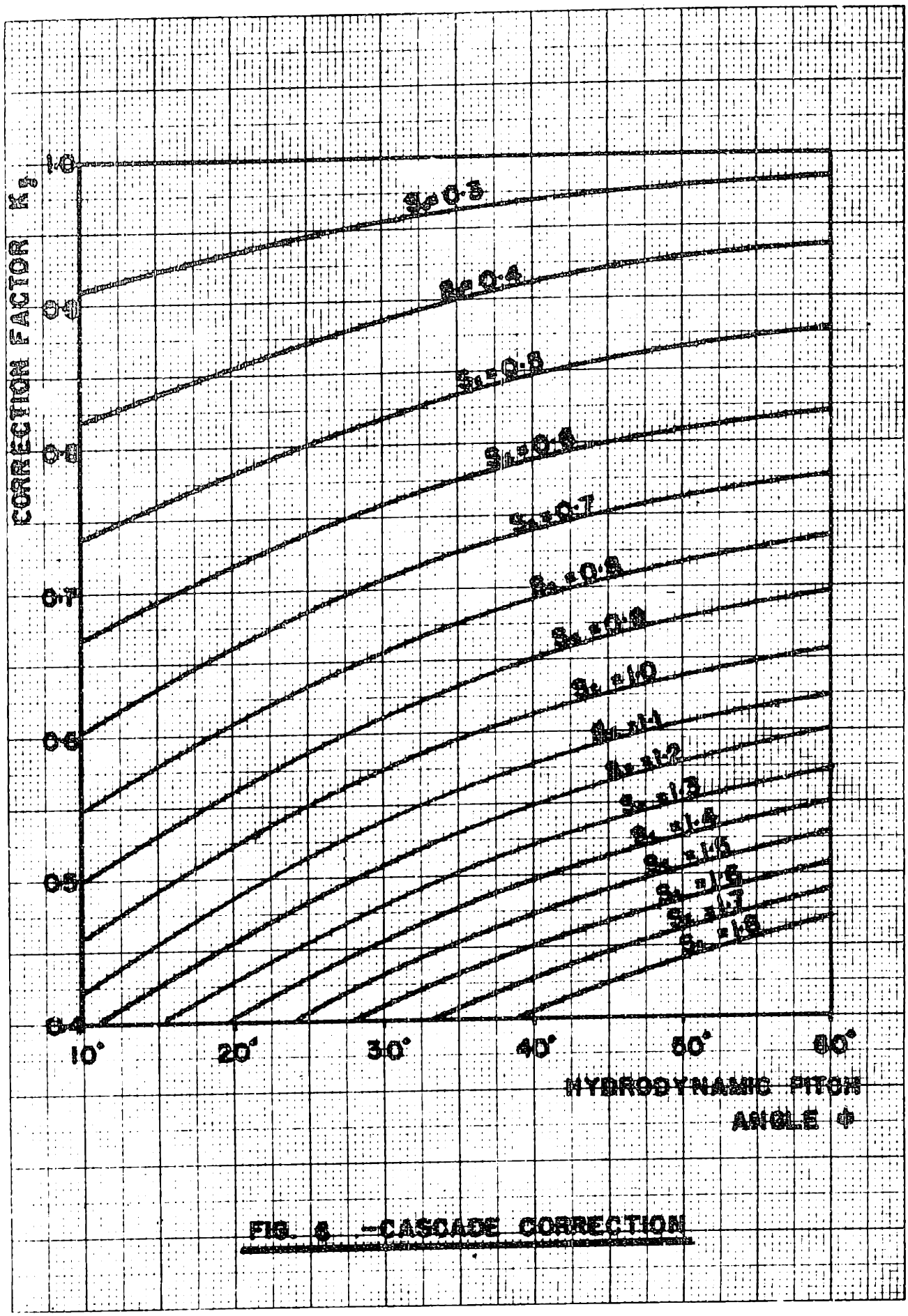

FIG. 6 —CASCADE CORRECTION

contours of cavitation indices.

It must be realised, however, that such values are liable to an error which may amount to 5% for certain conditions of operation, as the data is obtained by visual observation or photographs and the end of the cavity is not always clearly defined.

Using the actual solidity, increased by the amount given in Fig.(5), it is now possible to obtain the cascade correction factor, Fig.(6), which has been derived from Gutsche's original cascade tests and reproduced from Ref.6.

OUTLINE OF CALCULATION PROCEDURE.

The procedure for calculating the characteristics of a propeller consists in determining the elements of thrust and torque at a number of radii along the length of the blade and integrating such results. This involves a knowledge of the lift coefficient or the angle of attack of the sections and such values can only be computed by a process of trial and error. The cavitation index at which a section operates being approximately known,(equation (12)), an angle of attack has to be tried until the lift coefficient obtained from equation (6) and from the characteristics of the section are equal. The effective solidity of the section can then be computed, the cascade correction factor determined and the value of the drag coefficient read from Fig.(16)-(35).

The process is reasonably quick, and it has been found that usually two trials for the angle of attack will determine the lift within one per cent. This is due to the fact that the value of the lift coefficient calculated and determined from the charts converges from two opposite

directions.

A closer approximation can be calculated, if desired, by using the values obtained during the first computation for the hydrodynamic pitch angle at the propeller and in the slipstream. In that case it is possible to use the correct expression for the cavitation index (equation (11)) instead of the approximate one (equation (12)), but it will be found that such correction will only amount to an increment of 1% to 2%. As, however, the lift and drag characteristics of the section cannot be certified to such an accuracy, it is considered sufficient to use the approximate expressions.

A detailed procedure and a sample calculation are given in Appendix D.

RESULTS.

The calculation was performed on a 4-bladed merchant propeller having ogival sections and features as shown in Fig. (7) and (8). The propeller was specially chosen for its ability of producing severe cavitation under comparatively high cavitation indices. Data pertaining to the propeller is given in Appendix C.

Calculated characteristics have been obtained for the non-cavitating condition in order to test the validity of the theory and determine whether any modifications are necessary. It has been found, however, that the calculated results were consistent with the derived experimental values. The cavitating operation was investigated for two constant σ_n values, 1.0 and 0.8, over a range of J values such that the amount of cavitation was unduly severe extending over both the face and the back of the sections. Detail values obtained during the calculations are given in Tables III-XII, Appendix F, while the thrust and torque distributions are given in Fig. (36)-(45).

The propeller was also tested in the cavitation tunnel in order to determine experimentally the characteristics under both cavitating and non-cavitating conditions, the results being shown in Fig. (9), (10) and (11) on which the calculated points have also been plotted. The extend of cavitation is shown in Photographs (1)-(8) which have been obtained for the conditions under which the calculations have been performed.

During the calculation the approximate expressions for the cavitation index of the section and for the hydrodynamic pitch angle in the slipstream have been used. The error introduced by the use of such expressions is shown in Tables

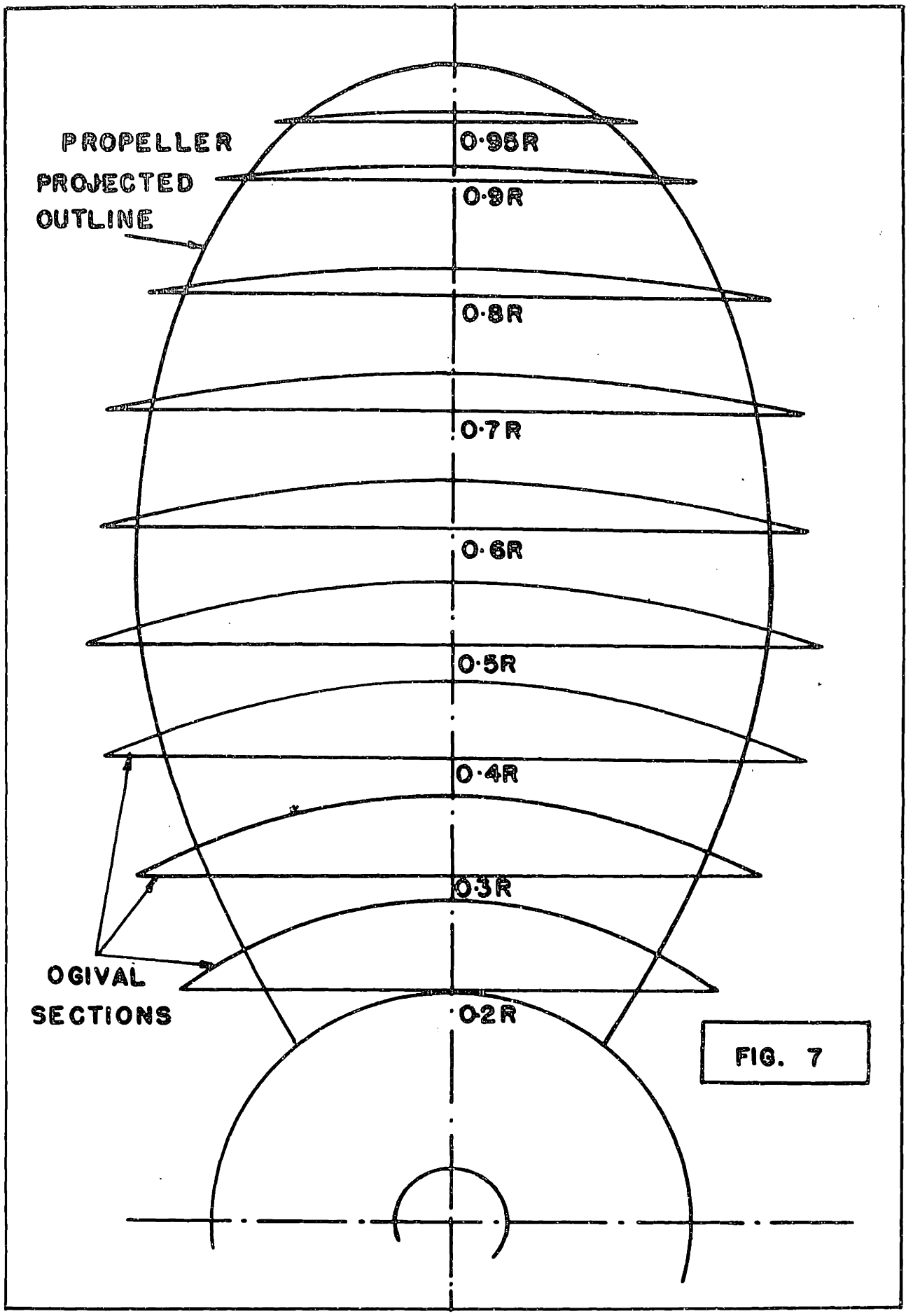
PROPELLER
PROJECTED
OUTLINE
0·95R
0·9R
0·8R
0·7R
0·6R
0·5R
0·4R
0·3R
0·2R
OGIVAL
SECTIONS

FIG. 7

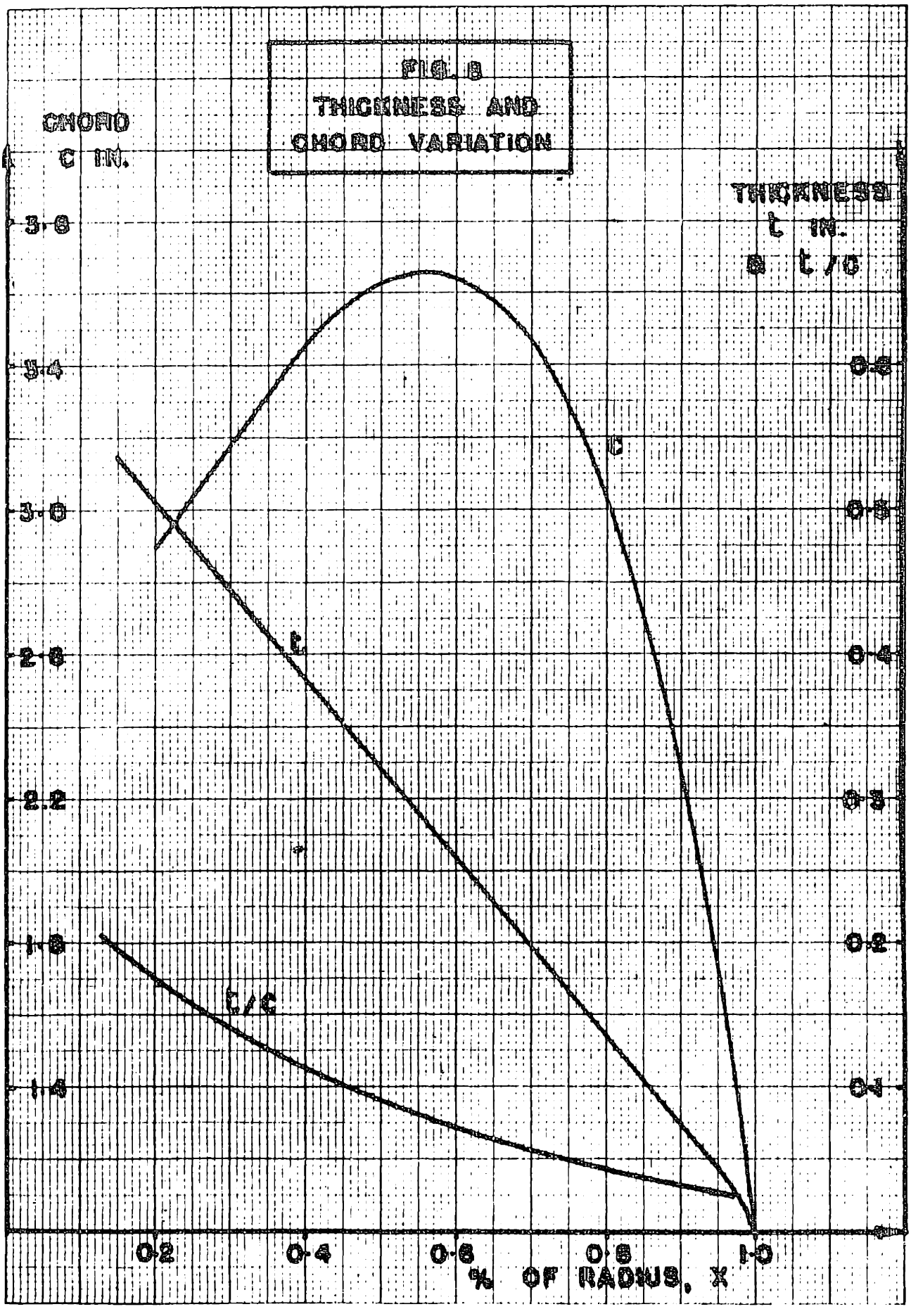
FIG. 8
THICKNESS AND
CHORD VARIATION
CHORD
C IN.
3·6
3·4
3·0
2·6
2·2
1·8
1·4
THICKNESS
t IN.
& t/C
0·6
0·5
0·4
0·3
0·2
0·1
C
t
t/C
0·2
0·4
0·6
0·8
1·0
% OF RADIUS, X

I and II which compare the values derived from the approximate and the correct equations. It is seen that the difference is decreasing towards the tip, a position at which the majority of the thrust and torque is concentrated, and which does not, therefore, warrant a second calculation.

DISCUSSION OF RESULTS.

The calculated results for a propeller having ogival sections are shown in Fig. (9), (10) and (11) where they can be compared with experimental values from tunnel tests. The characteristics having been plotted with constant σ_n values show the range of face cavitation, which starts at the point of increase in slope of the constant cavitation index lines. It will be noticed that when the blade is subjected to back cavitation only, the calculated points are consistent with the experimental values, the error being not more than 6% for the thrust and torque coefficients. Such deviation is reasonable due to the uncertainty in computing the effective increase in chord length which is liable to an error of the same magnitude. The theory, while being based on certain approximations, does give consistent results as borne out by the non-cavitating points which do not have more than 2% variation from the test results.

As the cavitation extends towards the pressure side of the section the difference between experimental and calculated values increases quite considerably. This is to be expected, as during the calculation the effect of face cavitation has not been taken into account. It might be said that this particular propeller operates mainly with negative angles of incidence at high J values, a condition which agravates face cavitation and which is not often encountered in normal operation.

A particular feature of the calculation in the range where face cavitation is present, is the close agreement between experimental and calculated torque coefficients as compared

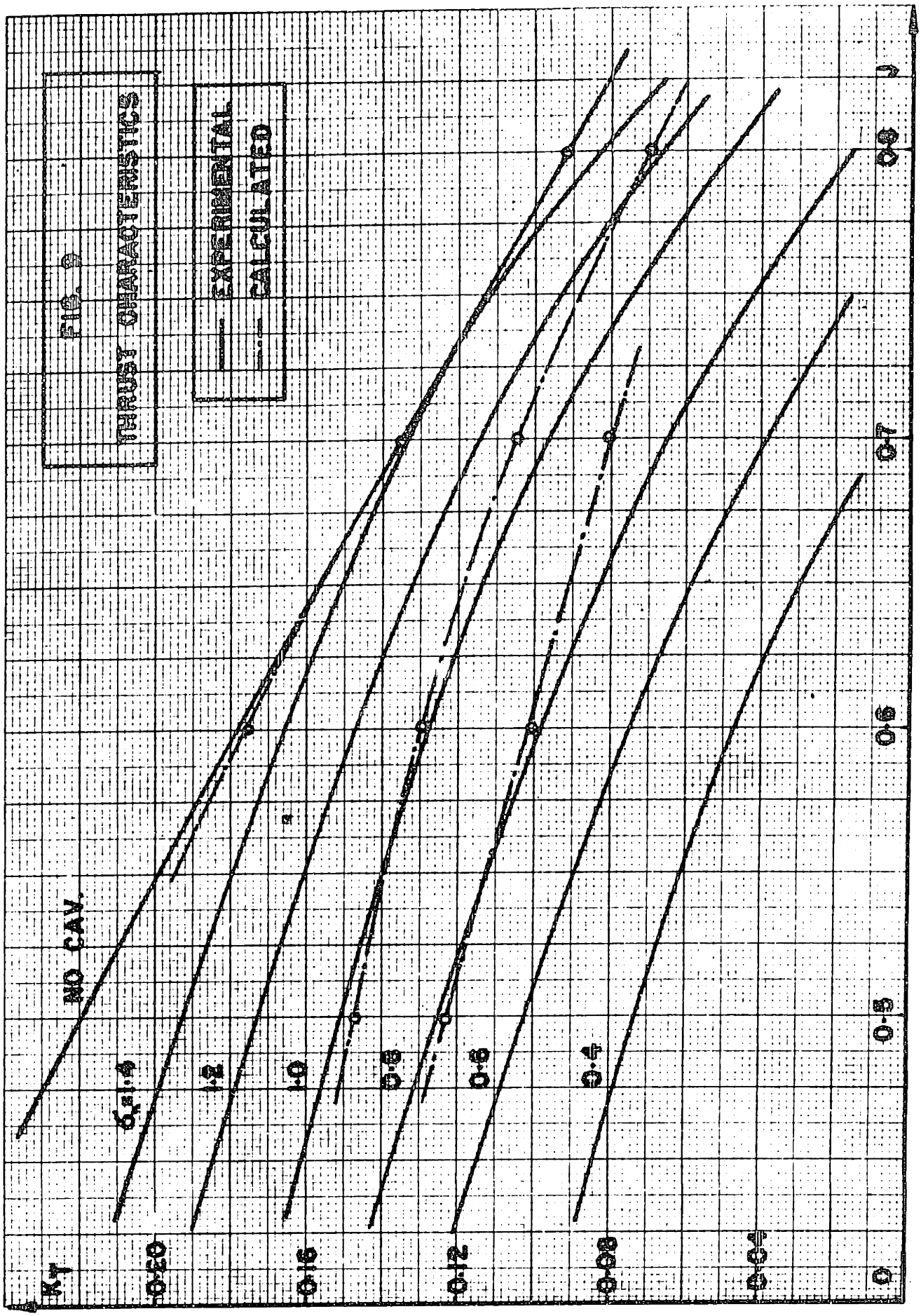
FIG. 9
THRUST CHARACTERISTICS
EXPERIMENTAL
CALCULATED
NO CAV.
K_T
σ_n 1.4
1.2
1.0
0.8
0.6
0.4
0.20
0.16
0.12
0.08
0.04
0
0.5
0.6
0.7
J

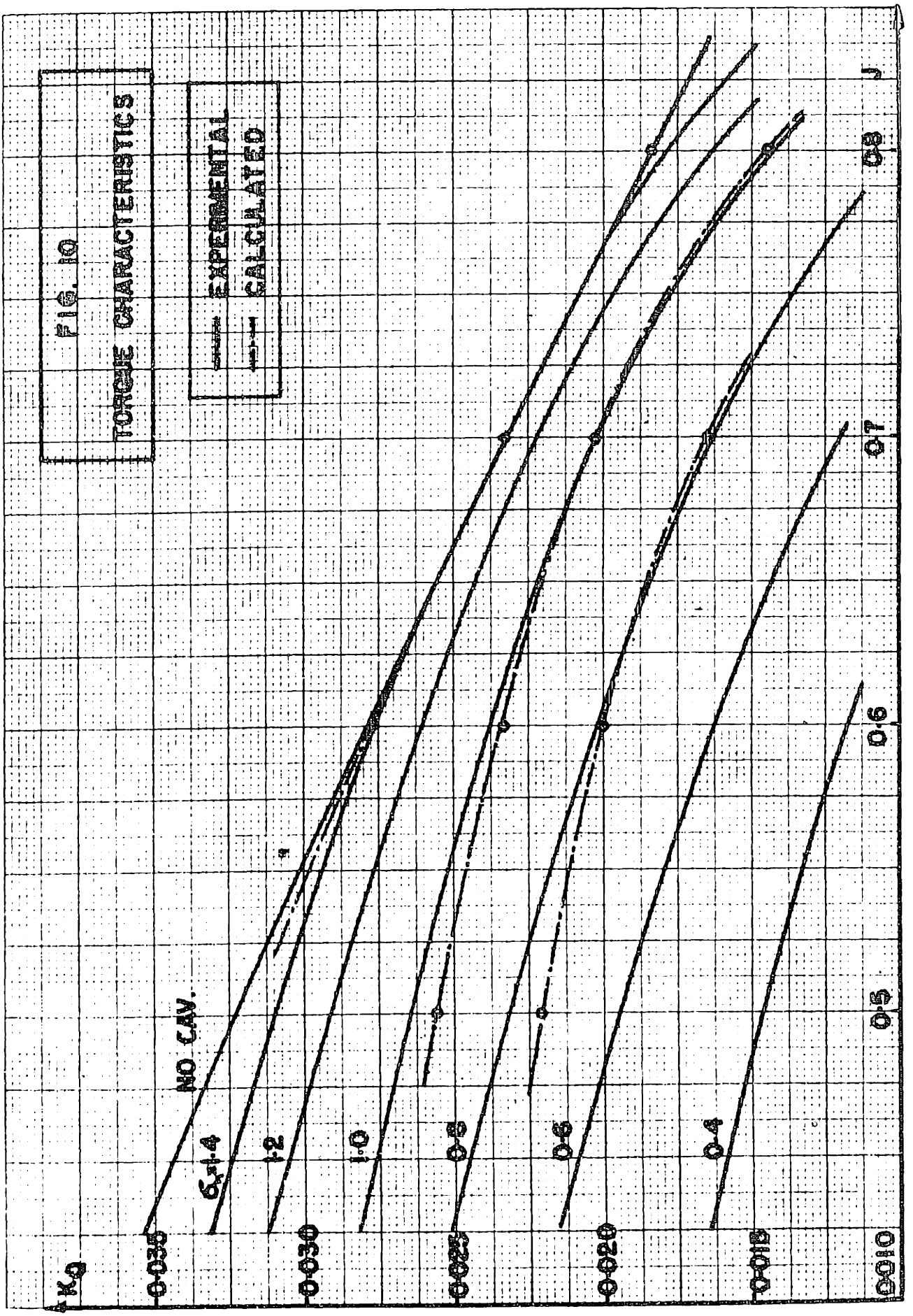
FIG. 10
TORQUE CHARACTERISTICS
EXPERIMENTAL
CALCULATED
K_Q
0·035
0·030
0·025
0·020
0·015
0·010
NO CAV.
σ_c 1·4
1·2
1·0
0·8
0·6
0·4
0·2
0·4
0·5
0·6
0·7
0·8
J

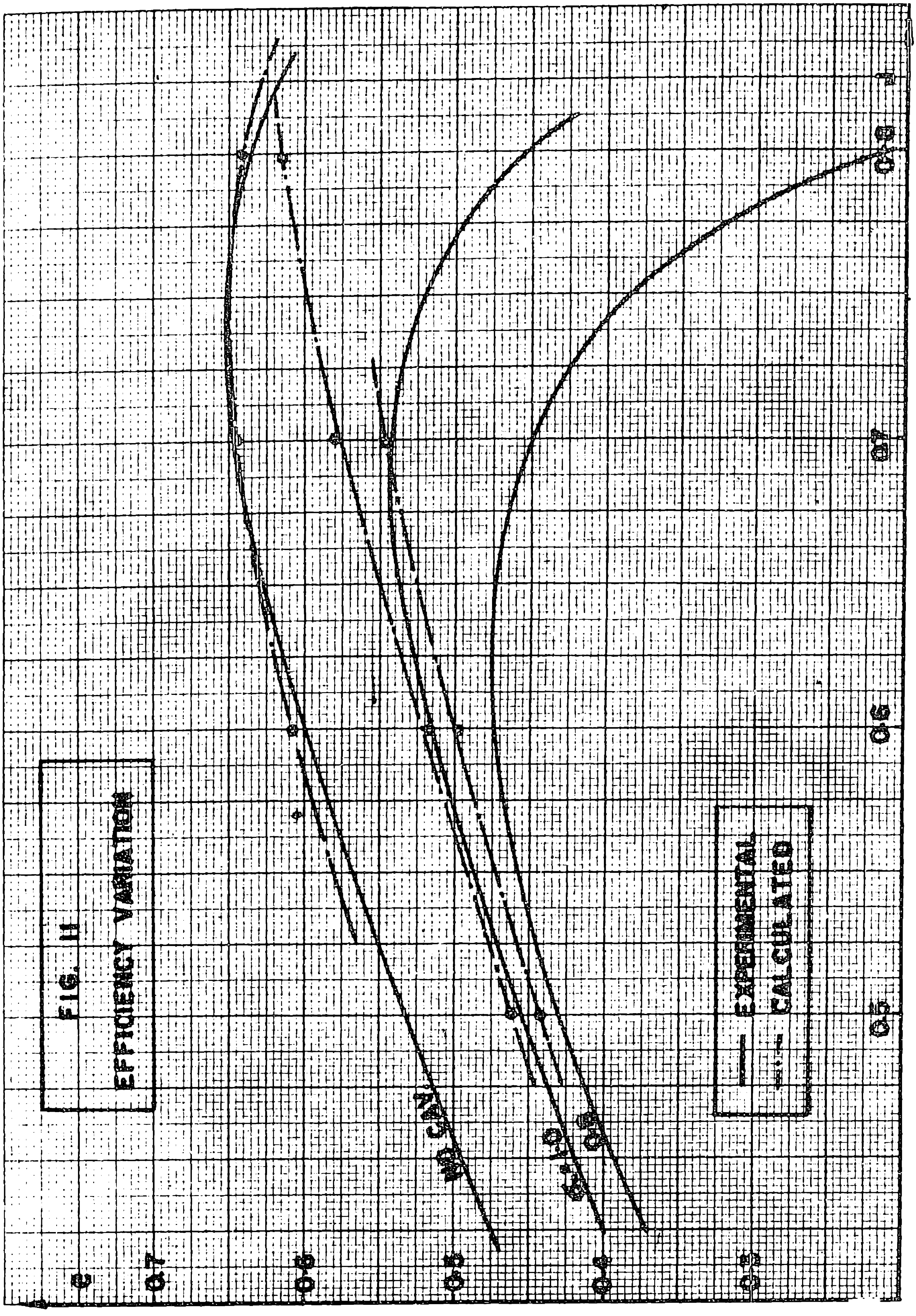
FIG. 11
EFFICIENCY VARIATION
EXPERIMENTAL
CALCULATED
0.7
0.6
0.5
0.4
0.3
0.5
0.6
0.7
0.8

to the thrust coefficients. Such an agreement for the torque is due to two effects which counterbalance each other and which may be regarded in the following way. The effect of face cavitation being neglected during the computation, the effective solidity at that radius is decreased, thus increasing the value of the lift and of the elementary thrust coefficient. This means that when face cavitation is not introduced, γ the ratio of drag to lift coefficient is smaller than what it should be. But as

$$K_{Qx} = \frac{x}{2} \cdot K_{Tx} \cdot \tan(\phi + \gamma)$$

the increment in K_{Tx} is counteracted by the degrement in $\phi + \gamma$ and thus the error of the calculated torque coefficient is decreased. As a result this produces a considerable increase in the value of the efficiency (Fig. (11)).

A correction for the effect of face cavitation cannot be introduced at the present time due to insufficient data on two-dimensional characteristics and the lack of cascade experiments in the cavitating region.

The distribution of thrust and torque for any particular condition of operation is shown by Fig. (36) to Fig. (45). It will be noticed that the effect of cavitation decreases the amount of thrust and torque near the tip of the propeller while the distribution near the hub remains unchanged. The percentage thrust developed by the root of the blade in the cavitating condition increases considerably and it, therefore, becomes important to consider the way the thrust is distributed when approaching the hub. In non-cavitating operation such a consideration is only a minor one and will only slightly affect the total thrust. In this analysis careful consideration has been given as to whether the thrust at the root section should be equal to zero or should have a finite value. Theoretically the thrust will only be zero at the axis of

the screw and there will be a definite amount developed by the root section. It is thought that in the actual case the thrust distribution will be equal to the theoretical up to a section not far from the hub, gradually falling to zero towards the bottom of the blade. As, however, the manner in which this falling off occurs is unknown and undeterminable, the thrust has been carried up to the root section and a discontinuity allowed to form at that point. Such a procedure, while not strictly correct, introduces a small error but may be nearer to the actual thrust distribution due to the presence of fillets which exist near the root and which are not taken into account when the outline of the section is considered.

Error involved in using approximate expressions for cavitation index and hydrodynamic pitch angle in the slipstream.

The calculation has been performed with the expressions giving the first approximation to the cavitation index of the section (equation 12) and to the hydrodynamic pitch angle ϵ in the race of the propeller (equation 10). The values have also been computed from the correct expressions in order to determine whether a second calculation is necessary. It has been found (Table I and II, Appendix F) that the error involved in the overall thrust coefficient amounts to 2%, a value which does not warrant a repetition of the process, as errors of that order are involved in calculating the effective solidity. Equation (12) gives a value of the cavitation index which is lower than that given by the correct expression (11) and which, therefore, tends to yield smaller thrust and torque coefficients. When further two-dimensional experimentation is performed giving more accurate results, it would be of advantage to use the correct expressions in determining

the cavitating index and the pitch angle. At the present time, it is only advisable to perform a check on those values if some boubt exists in the case of unusual propellers.

Effect of cavitation on lift and drag coefficients.

It is well known that during cavitation the lift of a section will be decreased due to the pressure on the suction side reaching the vapor pressure this being accompanied by a diminution in drag due to the formation of a cavity which decreases the frictional resistance. It is generally assumed that such effects are introduced immediately following the onset of cavitation. A consideration, however, of Fig. (1) will show that a discontinuity occurs in the lift curve during the initial stages of cavitation, the trend in the drag being exactly similar. This has also been noticed in propeller testing, where it has been found that some increment of thrust and torque is experienced as soon as the propeller first starts to cavitate. It appears that the amount as well as the position of the jump is dependent on the type of section and the angle of attack at which the section operates. For the same angle of attack such jump is much smaller for aerofoil sections than for ogival ones. Though the mechanism of such phenomenon is unknown the following explanation may be offered as to the reason for such discontinuity.

Regarding the effect from a physical viewpoint, it is reasonable to assume that the formation of a cavity, on say an ogival section, will effectively modify the profile of that section. Such modification is effected in a manner transforming the ogival section into an aerofoil, thus producing a higher lift coefficient, notwithstanding the fact that some suction on the back of the section is lost due to cavitation. This process is a function of the angle of attack

and as it can be seen from Fig. (1) at a small angle, namely 0^{o} or 1^{o}, the discontinuity does not occur. This would indicate that for small angles of attack and for thin sections, ogival profiles have characteristics not very different from aerofoils, a belief which is borne out by two-dimensional experimentation.

If the above concept is true, then it should be possible to test sections in their initial stages of cavitation and determine whether such sections are efficient in normal operation by observing the presence of a discontinuity. If such a discontinuity exists then it should be possible to modify the section in order to give a higher lift coefficient. Such information will only be applicable to one particular angle of attack and one thickness fraction. This would not necessarily mean, however, that the section will have the best drag-lift ratio as it must be remembered that the drag coefficient may also be liable to a discontinuity.

The drag coefficient has also been found to be a function of the Reynolds number for values of σ greater than those at the jump (Ref. 23). It appears that the phenomenon is not a simple one and a number of factors may be involved for a complete consideration, but it seems probable that future experimentation in two-dimensional flow will differentiate such factors.

Effect of scale on cavitation.

It will be noticed that the calculation was done for a model propeller and while in the normal operating case such calculation will not be different from a full size one, the presence of cavitation may introduce a " scale effect ". It is not at all certain that the lift and drag coefficients for any particular cavitating section can be applied to the

full size propeller, as such values of lift and drag have been obtained on sections of model size and if such an effect exists they would have to be modified. It can be said on the basis of a large number of model cavitation tests that have been made in the various propeller tunnels that it is necessary to run the model at a cavitation index which is 0.85 to 0.75 that of the full scale propeller. Although it is known that improvements in the test methods may be expected to give more consistent results it is still an open question whether the step from the model to the full size propeller does not involve some scale effect in cavitation.

In this connection, it is necessary to bear in mind that the known similarity relations do not consider the time during which the fluid particles remain in the low pressure zone. In other words, these considerations assume that the time necessary for the formation and collapse of the vapor pockets is in all cases negligible compared to all other hydraulic phenomena involved. This is in so far as the formation and collapse of the cavities is concerned, as it is known that vaporization and condensation are molecular phenomena depending on molecular velocities that are of a much higher order of magnitude than the hydraulic velocities involved. It seems, however, that this argument does not necessarily include the " growth " of the vapor bubbles after their formation, and it is possible that this effect is opposed by their surface tension. If so, the size of the cavities will not increase proportionally with time but their rate of increase will constantly vary as the surface tension effect must decrease with increase of bubble size. On the other hand, for the same fluid velocities, the increase in the dimensions of the propeller will increase the time element for the fluid particles passing through any particular area of the screw, proportionally to the linear

dimensions. That is to say, in a propeller 20 times the dimensions of the model, fluid particles will remain in the low pressure zone twenty times as long as in the model. If the growth of cavities was proportional to time, similarity would be maintained, but as under the influence of surface tension it may not be constant the cavities on the full scale and model propeller will be dissimilar. In view of the above considerations the increase in solidity as given by Fig. (5) cannot be considered to apply for the full size propeller if such time element is present.

The above may be an explanation of the fact encountered in propeller tunnels, where the cavitation number tested is not equal to the one in actual conditions. It might also be said that the discrepancy varies according to the tunnel, the Taylor Model Basin using a factor of 0.85 while the Haslar Tank using 0.75. This may be due to the magnitude of the fluid velocities which being lower than the full size ones will, at least partly, tend to cancel the time effect.

If the above argument is valid then it must not be assumed that the calculated lift and drag coefficients are those which apply to the full size propeller. The effect of time is, however, rather indeterminate at the present state of knowledge, but this effect seems to warrant careful consideration.

CONCLUSIONS AND RECOMMENDATIONS.

The results derived from the calculation show that the performance characteristics for cavitating propellers can be determined with a close agreement, provided that face cavitation is not present. The method used is limited to ogival sections only, but this limitation can be removed when further experiments are performed on aerofoil profiles in the cavitating region and thus a complete set of two-dimensional data can be plotted. The theory has shown that not withstanding the approximations used for its development the results are consistent with tunnel tests, and the procedure developed for the cavitating cases has indicated that while approximate expressions are used, such expressions yield results well within the error introduced by the two-dimensional data on sections. The knowledge of more accurate values for the lift and drag coefficients of cavitating sections will allow the use of the correct expressions and will produce results having the same magnitude of error as the experimental tests.

The present analysis is valid only for the case of cavitation extending over the suction side of the profile. The presence of face cavitation cannot at the present state of knowledge be corrected, due to the lack of two-dimensional cascade experiments. It has been extremely apparent during this investigation that the fundamentals of cavitation are not known to the desired extent and that basic experiments are needed in order to differentiate the effect of a cavity on the face or the back of a profile when it is introduced in a cascade of sections. While during this analysis a correction factor has been introduced for the cascading effect, such factor has been developed through artificial means by considering the effective increase in chord length and does

not, therefore, take account of face cavitation which produces an increase in thickness. It is essential that experiments in cascading lattices be performed which will yield results of a directly experimental nature, accounting for both face and back cavitation and which can then be introduced in the calculation of a propeller.

Work on fundamental processes occuring in cavitation is just as important in order to determine the effect of factors which have been found to have little or no consequence in the non-cavitating conditions but which may be major parameters when operating under cavitation. Reynolds number may be an important variable for at least a part of the cavitation range and the effect of surface tension and air content may prove to be essential in order to duplicate full scale results by model tests. Though the above factors may eventually be introduced in the calculation of the characteristics, such investigations cannot be done directly on a propeller as it would not be possible to differentiate the results of each effect. They would, therefore, have to be performed on experiments of fundamental nature in two-dimensional flow.

The calculations have shown that it is possible to predict the characteristics of a cavitating propeller provided that sufficient data is available on the individual sections. Though such calculations are rather laborious and will not in any way replace cavitating tests, they are useful in, showing the distribution of lift and drag coefficients, angles of attack and efficiencies along the length of the blade. It is felt that such knowledge may provide a means for improving future designs of propellers which operate in the cavitating region.

BIBLIOGRAPHY.

1. Betz A. " Schraudenpropeller mit geringstem Energieverlust" Gottinger Nachr., 1919.
2. Helmboldt H.B. " Die Betz-Prandtl'sche Wirbeltheorie der Treibschraube " Werft Reederei Hafen, 1926.
3. Glauert H. " Elements of Aerofoil and Airscrew Theory " Cambridge University Press, 1926.
4. Pistolesi E. " Neue Ansatze und Ausfuhrungen zur Theorie der Luftschrauben " Berlin, 1924.
5. Kawada S. " On the Fundamentals of the Vortex Theory of Airscrews " International Congress, Rome, 1928.
6. Burrill L.C. " Calculation of Marine Propeller Performance Characteristics " Trans. North-East Coast Inst. of Engineers and Shipbuilders, Vol. 60, 1944.
7. Hill J.G. " The Design of Propellers " Trans. S.N.A.M.E. November 1949.
8. Edstrand H. " The Effect of the Air Content of Water on the Cavitation Point and upon the Characteristics of Ship Propellers " Publication of the Sweedish State Shipbuilding Tank, 1946.
9. Goldstein S. " The Vortex Theory of Screw Propellers " Proceedings Royal Society, London, 1929.
10. Chartier C. " Sur le Champ Hydrodynamique autour d'une Helice a trois pales " Comptes Rendus, Acad. des Sciences, Paris, 1933, Vol.196.
11. Chartier C. " Champ Hydrodynamique autour d'une Helice Marine Triple Propulsive " Comptes Rendus, Acad. des Sciences, Paris ,1936, Vol.203,
12. Glauert H. " Airscrew Theory " Section L, Aerodynamic Theory, Editor Durand, Berlin, 1935.

13. Lock C.N.H. " An Application of the Prandtl Theory to an Airscrew " Aeron. Research Comm., R. and M. 1521 .

14. Lock C.N.H. " Application of the Goldstein Airscrew Theory to Design " Aeron. Research Comm., R. and M. 1377.

15. Lerbs H.W. " The present state of Research on the Ship Propeller with regard to its Design " Werft Reederei Hafen, 1942.

16. Burrill L.C. " Developments in Propeller Design and Manufacture for Merchant Ships " Trans. Inst. Marine Engineers, Aug. 1943.

17. Walchner O. " Profilmessungen bei Kavitation " Hydromechanische Probleme des Schiffsantriebs, 1932.

18. Ackeret J. " Experimentelle und Theoretische Untersuchung uber Hohlraumbildung " Forschung auf dem Gebiete des Ingenieurwesens, Berlin , Vol. I , 1930.

19. Hinterthan W. " Untersuchungen an Profilkorpern im Kavitationstank " Hamburgishe Schiffbau-Versuchsanstalt, Report 500, 1938.

20. Hinterthan W. " Versuche mit Profilkorper " Hamburgische Schiffbau-Versuchsanstalt, Rep. 441 , 1938.

21. Martyrer E. " Kraftmessungen an Widerstandskorpern und Flugelprofilen im Wasserstrom bei Kavitation " Hydromechanische Probleme des Schiffsantriebs, 1932.

22. Pottinger H. " Untersuchungen uber Kavitation und Korrosion bei Turbinen, Turbopumpen und Propellern " Hydraulische Probleme, 1926.

23. Konstantinov V.A. " Influence of Reynolds Number on the Cavitation Flow " T.M.B. Trans. 233, 1950.

APPENDICES.

A. Supplementary Introduction .

1. Nomenclature
2. Definition of Angles
3. Propeller with a finite number of blades

B. Development of Theory.

C. Data of Propeller.
Characteristics of ogival sections in cavitation.

D. Procedure for Calculation and Sample Calculation.

E. Cavitation Photographs.

F. Table of Results.

APPENDIX A.

SUPPLEMENTARY INTRODUCTION.

1. Nomenclature.

d	Diameter of propeller
R	Radius of propeller
r	Radius of section
$x = r/R$	Fraction of blade length
p	Pitch of propeller at x
t	Thickness of section
c	Chord length at x
Z	Number of blades
τ	Circulation
V	Velocity of advance
W	Resultant velocity at x
Ω	Angular velocity
n	Revolutions per second
$J = V/n.d$	Advance ratio
$s = Z.c/\pi.d.x$	Solidity
s_e	Effective solidity
α	Angle of attack
$\theta = \tan^{-1}(p/\pi.d.x)$	Pitch angle at x
$\psi = \tan^{-1}(J/\pi.x)$	Advance angle at x
$\phi = \theta - \alpha$	Hydrodynamic pitch angle at propeller plane
ϵ	Hydrodynamic pitch angle in slipstream
$\beta = \phi - \psi$	Hydrodynamic inflow angle

k_ϕ	Goldstein factor corresponding to angle ϕ
k_ϵ	Goldstein factor corresponding to angle ϵ
C_L	Lift coefficient
C_D	Drag coefficient
$\delta = \tan^{-1}(C_D/C_L)$	Lift-drag ratio
a	Axial inflow factor
a'	Rotational inflow factor
K_T	Thrust coefficient
K_Q	Torque coefficient
$K_{Tx} = \frac{dK_T}{dx}$	Element of thrust coefficient
$K_{Qx} = \frac{dK_Q}{dx}$	Element of torque coefficient
η	Efficiency of propeller
η_x	Efficiency of blade section
p	Static pressure on blade
p_v	Vapor pressure
ρ	Density
$\sigma_v = \frac{p - p_v}{\frac{1}{2}\rho V^2}$	Cavitation index based on velocity
$\sigma_n = \frac{p - p_v}{\frac{1}{2}\rho n^2 d^2}$	Cavitation index based on revolutions
$\sigma_x = \frac{p - p_v}{\frac{1}{2}\rho W^2}$	Cavitation index for section

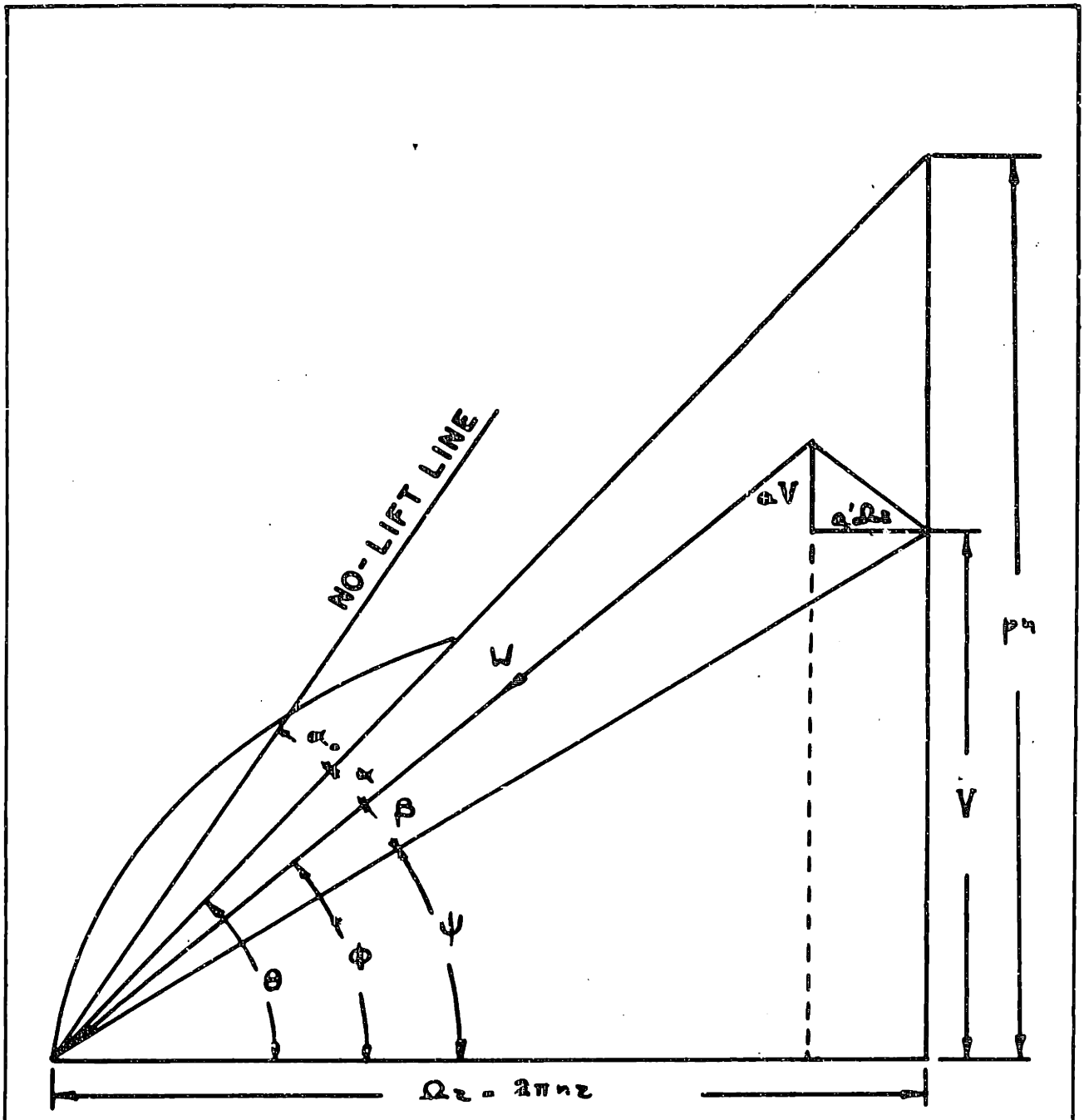

FIG. 12 .— DIAGRAM OF ANGLES AT PROPELLER PLANE

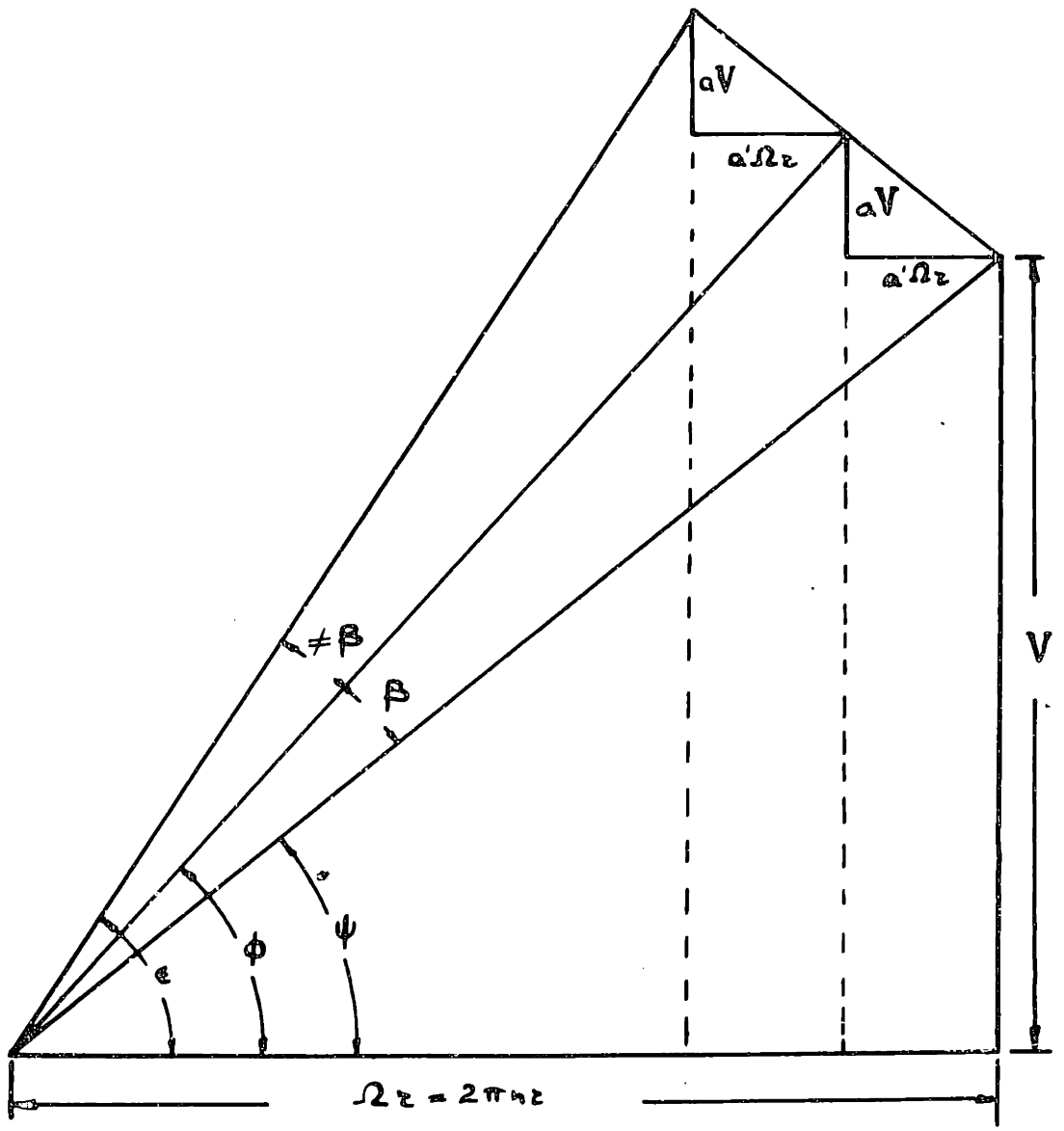

FIG. 13 .- DIAGRAM OF ANGLES IN PROPELLER SLIPSTREAM

2. Definition of angles.

Fig (12) shows the various angles of the blade element which are refered to in the text. The angle θ corresponds to the face pitch angle of the blade at a radius r and is defined as $\tan^{-1}(\text{pitch}/2\pi.r)$. As the propeller is considered advancing with a uniform velocity V and having a uniform rotation Ω, the advance angle ψ will be equal to $\tan^{-1}(V/\Omega.r)$.

The hydrodynamic pitch angle is denoted by ϕ, where :

$$\tan\phi = \frac{V}{\Omega.r}\left(\frac{1+a}{1-a'}\right)$$

$$= \tan\psi \left(\frac{1+a}{1-a'}\right)$$

the values a and a' being the axial and rotational inflow factors.

The angle of attack, denoted by α, is measured from the face, while β, the hydrodynamic inflow angle is equal to $\phi - \psi$.

The no-lift angle α_o is measured from the face of the section, and as all other angles pertaining to the face are measured counter-clockwise, α_o is a negative angle with respect to the remaining.

The angles at infinity behind the screw are given by Fig. (13). The angle of the vortex sheets at a radius r behind the propeller is given by ϵ and the total hydrodynamic inflow angle is approximated to 2β as shown in Appendix B.

3. Propeller with a finite number of blades.

As it can be shown from the vortex theory there is an increase in velocity while the water passes through the plane of the propeller, this increment being due to the formation of trailing vortices in the slipstream and being equal to one half of that at the propeller plane. In addition a system of radial dound vortices exists at the propeller, but owing to their symmetrical disposition, these have no influence on the axial induced velocities in the slipstream. They do, however, contribute to the induced angular velocities which are one half of those at infinity behind.

The above theory is based for its development on the assumption of a propeller with an infinite number of blades, and a correction must be introduced when dealing with an actual propeller. In this case, the trailing vortex sheets are separated from each other, resulting in a radial velocity which decreases the mean induced velocity. Betz (Ref. 1) has shown that a propeller will operate in its optimum condition when the trailing vortices in the ultimate wake lie on a regular screw surface. In that case the induced velocities of the slipstream are calculated by assuming that the vortex sheets forms a rigid membrane which moves backwards with constant axial velocity. It is known that this is not true for an actual propeller and that the vortex sheet, while formed uniformely at the blade, will tend to " curl " towards its ends and form two cylinders which travel down the slipstream. According to Betz's analysis the velocity imparted to the water in the interior of the slipstream will have important axial and rotational components. Near the boundary of the slipstream, however, the water will tend

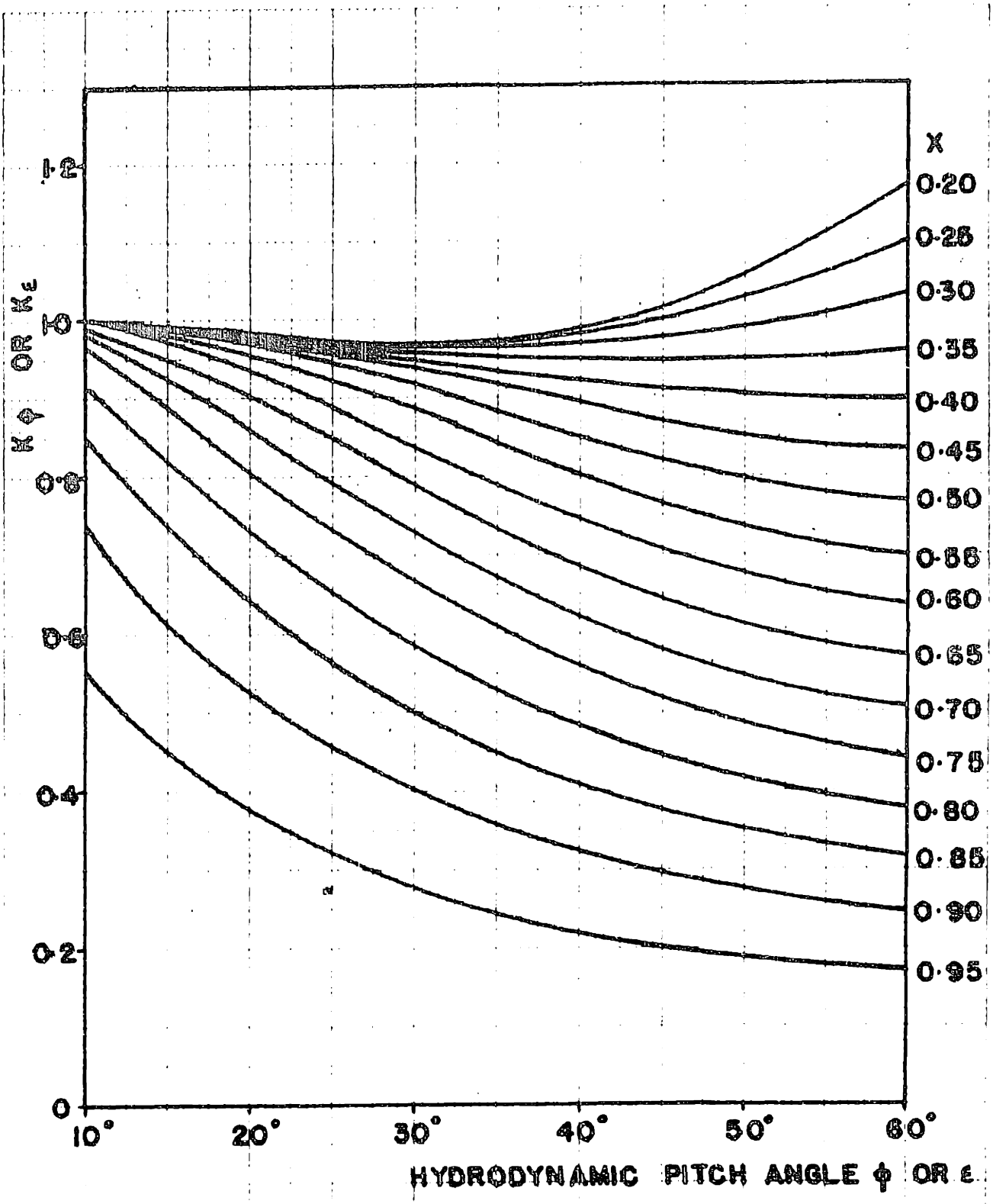

FIG. 14 .— GOLDSTEIN CORRECTION FACTOR FOR 3-BLADED PROPELLER

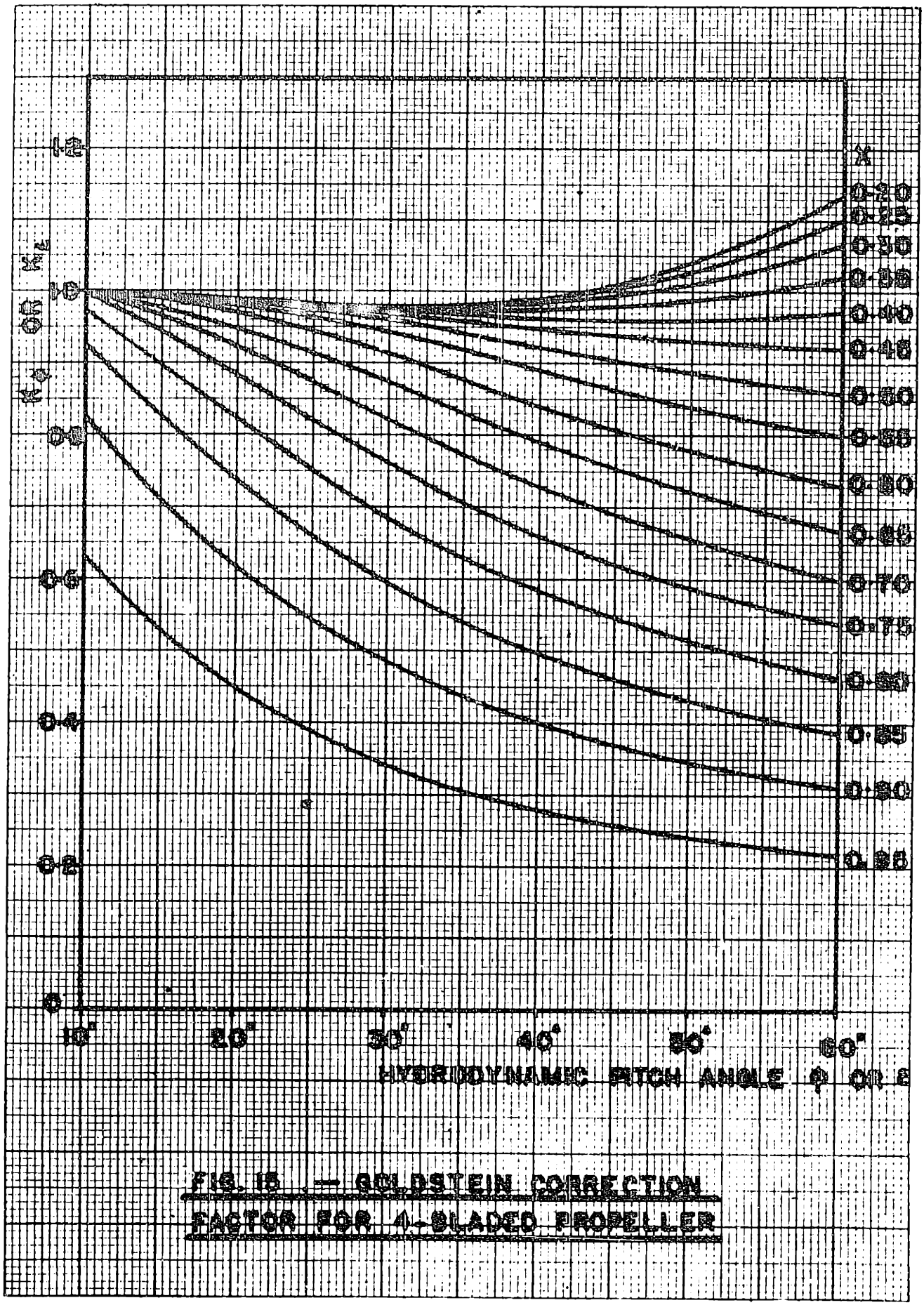

FIG. 15 — GOLDSTEIN CORRECTION FACTOR FOR 4-BLADED PROPELLER

to flow over the edges of the vortex sheets thus acquiring a considerable radial velocity.

This effect was first investigated by Prandtl in an appendix to Betz's paper (Ref. 1) and is given in the form of a correction factor to the velocity, by :

$$\text{Correction factor} = \frac{2}{\pi}.\arccos e^{-f}$$

$$\text{where} \quad f = \frac{Z}{2}.\frac{R - r}{R}.\frac{(\pi^2 + J^2)^{\frac{1}{2}}}{J}$$

the expression being obtained from considerations of flow past a system of parallel lines. A more accurate analysis has been developed by Goldstein (Ref. 9) who investigated the flow past a series of truly helicoidal surfaces of infinite length and obtained an expression for the ratio between the mean circulation taken round an annulus at a radius r and the circulation at the helicoidal surfaces. Goldstein's solution is a rigorous representation of Betz's optimum condition but refers only to lightly loaded propellers since it ignores the contraction of the slipstream.

The above defect, which in the case of cavitating propellers may be important, can be included by considering the hydrodynamic pitch angle of the vortex sheets in the slipstream. Goldstein's results are given in terms of the percentage radius and the pitch angle of the surfaces. As an approximation, therefore, it is possible to use the hydrodynamic pitch angle of the sheets, thus allowing for the contraction of the slipstream. Further, as the Goldstein factor has been calculated to correct the circulation, it may instead be considered as a correction to the velocity. The above may be substantiated by considering the lift at any section. By the Kutta-Joukowski theorem , we have that :

$$\text{Lift} = \rho.\Gamma.V$$

When the Goldstein correction factor k is introduced,

the lift of a section in the propeller will be diminished and will be given by :

$$\text{Lift} = \rho . \Gamma . k . V$$

It is possible to regard this diminution of lift not as occuring due to a reduction in circulation, but as being formed due to a reduction in velocity. In this case the resultant velocity in which the section is operating will be k.V instead of V, and as the ratio of the axial and rotational induced velocities is constant if the hydrodynamic pitch angle is fixed, the Goldstein correction factor may be regarded as diminishing the induced velocities as it is itself a function of the pitch angle. The above treatment is somewhat substantiated by Chartier's diagrams (Ref. 10 and 11) which give a velocity exploration around the propeller.

Another viewpoint which has been suggested by Glauert (Ref. 12) is that the propeller may be regarded as having an infinite number of blades but a smaller diameter. This effective diameter can be calculated in terms of the gap between the vortex sheets, but it is obvious that such a method has a disadvantage for calculation purposes owing to the variation of the gap for different advance ratios. It would, therefore, be necessary to calculate such an effective diameter for every value of the advance coefficient J.

In view of the above considerations, it is thougnt that an easier as well as a more accurate method would be to use the Goldstein correction factor directly as given in Fig. (14) and (15) (taken from Ref. 6) for three and four bladed propellers and apply it as a correction to the induced velocities of the section.

APPENDIX B.

DEVELOPMENT OF THEORY.

Considering an element of a propeller at a radial distance r from the axis of rotation (Fig. 12), the effective velocity on this blade element will be the component W. This component is the resultant of an induced axial velocity added to the axial velocity passing through the screw and an induced rotational velocity substracted from the rotational velocity of the blade element. If ϕ is the hydrodynamic pitch angle of the section considered, the velocities can be expressed in the following manner

$$W.\sin\phi = V\,(1 + a)$$
$$W.\cos\phi = \Omega.r\,(1 - a')$$

where a and a' are the axial and rotational inflow factors. The corresponding advance ratio J of the blade element is then obtained as

$$J = \frac{V^*}{n.2r} = \pi.\frac{(1 - a')}{(1 + a)}.\tan\phi \qquad \ldots\ldots\ldots(13)$$

The determination of the elements of thrust and torque acting on the section can be obtained by consideration of the lift and drag forces. The element will experience a lift force normal to the direction of the resultant velocity W, and a drag force parallel to this direction. Expressing these forces in terms of the usual lift and drag coefficients, C_L and C_D, and considering Z sections with a chord length c, we can obtain :

$$dT = \tfrac{1}{2}.\rho.Z.c.W^2\,(C_L.\cos\phi - C_D.\sin\phi)\,dr$$
$$dQ = \tfrac{1}{2}.\rho.Z.c.W^2\,(C_L.\sin\phi + C_D.\cos\phi)\,r.dr$$

The introduction of a non dimensional parameter s, where

$$s = \text{solidity} = Z.c/2\pi.r$$

will yield :

$$dT = \pi.r.s.\rho.V^2(1+a)^2(C_L.\cos\phi - C_D.\sin\phi)\frac{dr}{\sin^2\phi} \quad \ldots\ldots(14)$$

$$dQ = \pi.r.s.\rho.V^2(1+a)^2(C_L.\sin\phi + C_D.\cos\phi)\frac{r.dr}{\sin^2\phi} \quad \ldots\ldots(15)$$

while the efficiency of the section, e_x, becomes :

$$e_x = \frac{V.dT}{\Omega.dQ} = \frac{V}{\Omega.r} \cdot \frac{(C_L.\cos\phi - C_D.\sin\phi)}{(C_L.\sin\phi + C_D.\cos\phi)}$$

and if we write $C_D / C_L = \tan\gamma$
this becomes :

$$e_x = \frac{\tan\psi}{\tan(\phi+\gamma)} \quad \ldots\ldots\ldots\ldots\ldots\ldots\ldots\ldots(16)$$

(See Appendix A for definition of angles)

The above expressions express the characteristics of the blade element in terms of the flow to which they are subjected. It will be noticed, that the efficiency of the section may actually be considered as the product of two efficiencies. It may be written as :

$$e_x = \frac{\tan\psi}{\tan\phi} \cdot \frac{\tan\phi}{\tan(\phi+\gamma)}$$

The first ratio would signify an efficiency which is not directly dependent on the blade element but which results from the flow through the entire propeller. This term which may conveniently be known as a hydrodynamic efficiency, is a function of the inflow factors a and a', and hence of the overall performance of the screw. The second term, on the other hand, is effectively a blade efficiency and determinable from the two dimensional flow characteristics of the section. It is this second term which it is usual to improve in

order to increase the overall performance of the propeller without affecting the thrust and torque characteristics.

It will be seen that the above equations are sufficient to enable the thrust, torque and efficiency of any propeller to be determined, provided the values of C_L and C_D are known. In order, therefore, to solve these equations it is necessary to obtain two more equations which can be equated to dT and dQ. Such equations can be obtained on the basis of the simple momentum theory, due allowance being made for a propeller having a finite number of blades.

Correcting for the contraction of the slipstream, i.e. for the variation of the hydrodynamic pitch angle in the ultimate wake, we have the following velocity distribution.

V = Velocity at infinity ahead

$V.(1 + k_\phi.a)$ = Velocity at propeller plane

$V.(1 + 2k_\epsilon.a)$ = Velocity at infinity behind

If M = Mass of water passing through an annulus between the radii r and r+dr

$= 2\pi.r.\rho.V(1 + k_\phi.a)dr$

$$\therefore \quad dT = M\left\{ V(1 + 2k_\epsilon.a) - V \right\}$$

$$= 4\pi.r.\rho.V^2(1 + k_\phi.a).k_\epsilon.a.dr \qquad \ldots\ldots\ldots\ldots (17)$$

and $$dQ = M (2k_\epsilon.a'.\Omega.r^2)$$

$$= 4\pi.r^3.\rho.V.\Omega.(1 + k_\phi.a).k_\epsilon.a'.dr \qquad \ldots\ldots\ldots (18)$$

It may be argued that the Goldstein factors have not been introduced in the expressions (14) and (15), but it must be borne in mind that these have been derived considering one blade element only, and in that case a correction from an infinite to a finite number of blades is unnecessary. In the case of equations (17) and (18), however, the initial theory has been formulated for the case of an infinite number of blades and a correction must, therefore, be applied when dealing with actual propellers.

It is now possible to equate equations (17) and (14) as well as (18) and (15), in order to determine the axial and rotational inflow factors a and a'.

From (14)

$$\frac{dT}{dr} = \pi.r.s.\rho.V^2(1+a)^2.C_L \frac{\cos(\phi+\gamma)}{\cos\gamma.\sin^2\phi}$$

and equating to (17), we obtain :

$$\frac{a}{(1+a)}.\frac{(1+k_\phi.a)}{(1+a)} = \frac{C_L.s}{4k_\epsilon}.\frac{\cos(\phi+\gamma)}{\cos\gamma.\sin^2\phi} \quad \ldots\ldots(19)$$

From (15)

$$\frac{dQ}{dr} = \pi.r^2.s.\rho.V^2(1+a)^2.C_L \frac{\sin(\phi+\gamma)}{\cos\gamma.\sin^2\phi}$$

Equating to (18), and using the expression

$$\frac{V}{\Omega.r} = \tan\phi.\frac{(1-a')}{(1+a)}$$

we obtain :

$$\frac{a'}{(1-a')}.\frac{(1+k_\phi.a)}{(1+a)} = \frac{C_L.s}{2k_\epsilon}.\frac{\sin(\phi+\gamma)}{\cos\gamma.\sin 2\phi} \quad \ldots\ldots(20)$$

From equations (19) and (20)

$$\frac{a}{(1+a)}.\frac{2\cos\gamma.\sin^2\phi}{\cos(\phi+\gamma)} = \frac{a'}{(1-a')}.\frac{\cos\gamma.\sin 2\phi}{\sin(\phi+\gamma)}$$

$$\therefore \frac{a}{(1+a)} = \frac{a'}{(1-a')}.\frac{1}{\tan\phi.\tan(\phi+\gamma)}$$

By definition $\tan\psi = \tan\phi.(1-a')/(1+a)$

$$\therefore \quad a'/a = \tan\psi.\tan(\phi+\gamma)$$

and

$$a = (1-a').\frac{\tan\phi}{\tan\psi} - 1 \quad \ldots\ldots(21)$$

$$= \frac{\tan\phi}{\tan\psi} - \frac{a.\tan\psi.\tan(\phi+\gamma).\tan\phi}{\tan\psi} - 1$$

$$\therefore \quad a = \frac{\tan\phi - \tan\psi}{\tan\psi\{1+\tan\phi.\tan(\phi+\gamma)\}} \quad \ldots\ldots(22)$$

and $$a' = \frac{(\tan\phi - \tan\psi).\tan(\phi+\gamma)}{1+\tan\phi.\tan(\phi+\gamma)} \quad \ldots\ldots(23)$$

The hydrodynamic pitch angle in the slipstream is given by :

$$\tan \epsilon = \tan \psi \frac{(1 + 2a)}{(1 - 2a')}$$

Substituting the value of a from (21)

$$\tan \epsilon = \frac{1}{(1 - 2a')} \left\{ \tan \psi + 2(1 - a').\tan\phi - 2\tan \psi \right\}$$

$$= \frac{1}{(1 - 2a')} \left\{ 2(1 - a').\tan \phi - \tan \psi \right\} \quad \ldots\ldots(24)$$

or if a' is substituted from (23)

$$\tan \epsilon = \frac{2\tan \phi - \tan \psi + \tan \psi.\tan \phi.\tan(\phi + \gamma)}{1 + 2\tan \psi.\tan(\phi + \gamma) - \tan \phi.\tan(\phi + \gamma)} \quad \ldots\ldots(25)$$

If γ is neglected in comparison with ϕ, equation (25) becomes :

$$\tan \epsilon = \frac{2\tan \phi - \tan \psi + \tan \psi.\tan^2 \phi}{1 + 2\tan \psi.\tan \phi - \tan^2 \phi}$$

$$= \frac{\tan \phi + \dfrac{\tan \phi - \tan \psi}{1 + \tan \phi.\tan \psi}}{1 - \tan \phi \dfrac{\tan \phi - \tan \psi}{1 + \tan \phi.\tan \psi}}$$

$$= \frac{\tan \phi + \tan(\phi - \psi)}{1 - \tan \phi.\tan(\phi - \psi)}$$

$$= \frac{\tan \phi + \tan \beta}{1 - \tan \phi.\tan \beta}$$

$$= \tan(\phi + \beta)$$

$$\therefore \quad \epsilon = \phi + \beta \quad \ldots\ldots\ldots\ldots(26)$$

In order to determine the value of the lift coefficient we can consider the expression already developed

$$\frac{a}{(1 + a)} \cdot \frac{(1 + k_\phi.a)}{(1 + a)} = \frac{C_L.s}{4k_\epsilon} \cdot \frac{\cos(\phi + \gamma)}{\cos \gamma.\sin^2 \phi} \quad \ldots\ldots\ldots(19)$$

From (22)

$$\frac{a}{(1 + a)} = \frac{\tan \phi - \tan \psi}{\tan \psi[1 + \tan \phi.\tan(\phi + \gamma)] + \tan \phi - \tan \psi}$$

$$= \frac{\tan \phi - \tan \psi}{\tan \phi[1 + \tan \psi.\tan(\phi + \gamma)]}$$

Also if we substitute the value of a in the expression $\dfrac{(1 + k_\phi.a)}{(1 + a)}$ and neglect γ in comparison with ϕ

$$Y = \frac{(1 + k_\phi.a)}{(1 + a)} = 1 - \frac{\tan \beta}{\tan \phi}(1 - k_\phi) \quad \ldots\ldots\ldots(27)$$

$$\therefore \quad \frac{C_L \cdot s}{2Y \cdot k_\epsilon} \cdot \frac{\cos(\phi + \gamma)}{2\cos\gamma \cdot \sin^2\phi} = \frac{\tan\phi - \tan\psi}{\tan\phi\left[1 + \tan\psi \cdot \tan(\phi + \gamma)\right]}$$

$$\frac{C_L \cdot s}{2Y \cdot k_\epsilon} = \frac{(\tan\phi - \tan\psi) \cdot 2\sin\phi \cdot \cos\phi \cdot \cos\gamma}{\cos(\phi + \gamma) + \tan\psi \cdot \sin(\phi + \gamma)}$$

$$= \frac{(\tan\phi - \tan\psi) \cdot 2\sin\phi \cdot \cos\phi \cdot \cos\gamma}{\cos\phi \cdot \cos\gamma - \sin\phi \cdot \sin\gamma + \tan\psi \cdot \sin\phi \cdot \cos\gamma + \tan\psi \cdot \cos\phi \cdot \sin\gamma}$$

$$= 2\sin\phi \; \frac{1}{\frac{1 + \tan\psi \cdot \tan\phi}{\tan\phi - \tan\psi} - \tan\gamma}$$

$$= 2\sin\phi \; \frac{\tan\beta}{1 - \tan\beta \cdot \tan\gamma}$$

where $\beta = \phi - \psi$

$$\therefore \quad C_L = \frac{2Y}{s} \cdot k_\epsilon \cdot 2\sin\phi \cdot \tan\beta \cdot (1 + \delta C_L)$$

where $$\delta C_L = \frac{\tan\beta \cdot \tan\gamma}{1 - \tan\beta \cdot \tan\gamma} \qquad \ldots(28)$$

Neglecting δC_L for the moment,

$$C_L = \frac{4}{s} \cdot k_\epsilon \cdot \sin\phi \cdot \tan\beta \cdot \frac{(1 + k_\phi \cdot a)}{(1 + a)}$$

$$= \frac{4}{s} \cdot k_\epsilon \cdot \sin\phi \cdot \tan\beta \cdot \left\{1 - \frac{\tan\beta}{\tan\phi} \cdot (1 - k_\phi)\right\} \qquad \ldots\ldots(29)$$

The elementary thrust coefficient will be given by :

$$dK_T = \frac{dT}{\rho \cdot n^2 \cdot d^4}$$

Substituting for dT from (14)

$$dK_T = \frac{\rho \cdot s \cdot \pi \cdot r \cdot dr}{\rho \cdot 16R^4 \cdot \frac{\Omega^2}{4\pi^2}} (1 + a)^2 \cdot V^2 \cdot C_L \frac{\cos(\phi + \gamma)}{\cos\gamma \cdot \sin^2\phi}$$

$$= \frac{s \cdot \pi^3 \cdot x^3 \cdot dx}{4} (1 + a)^2 \cdot \tan^2\psi \cdot C_L \frac{\cos(\phi + \gamma)}{\cos\gamma \cdot \sin^2\phi}$$

where $x = r/R$

$$K_{Tx} = \frac{dK_T}{dx} = \frac{s \cdot \pi^3 \cdot x^3}{4} (1 - a')^2 \cdot C_L \cdot \frac{\tan^2\phi}{\sin^2\phi} \cdot \frac{\cos(\phi + \gamma)}{\cos\gamma}$$

$$K_{Tx} = \frac{s \cdot \pi^3 \cdot x^3}{4} (1 - a')^2 \cdot C_L \cdot (1 + \tan^2\phi) \frac{\cos(\phi + \gamma)}{\cos\gamma} \qquad \ldots(30)$$

Similarly

$$dK_Q = \frac{dQ}{\rho . n^2 . d^5}$$

$$dQ = \frac{\rho . s . \pi . r^2 . dr}{\rho . 32R^5 . \frac{\Omega^2}{4\pi^2}} (1 + a)^2 . V^2 . C_L \frac{\sin(\phi + \gamma)}{\cos\gamma . \sin^2\phi}$$

$$= \frac{s . \pi^3 . x^4 . dx}{8} (1 + a)^2 . \tan^2\psi . C_L \frac{\sin(\phi + \gamma)}{\cos\gamma . \sin^2\phi}$$

$$K_{Qx} = \frac{dK_Q}{dx}$$

$$K_{Qx} = \frac{s . \pi^3 . x^4}{8} (1 - a')^2 . C_L . (1 + \tan^2\phi) \frac{\sin(\phi + \gamma)}{\cos\gamma} \quad \ldots(31)$$

or $$K_{Qx} = \frac{x}{2} . \tan(\phi + \gamma) . K_{Tx} \quad \ldots\ldots\ldots\ldots\ldots(32)$$

For the efficiency

$$e_x = \frac{J}{2\pi} . \frac{K_{Tx}}{K_{Qx}} \quad \ldots\ldots\ldots\ldots\ldots(33)$$

The cavitation index will be given by :

$$\sigma_v = \frac{p - p_v}{\frac{1}{2} . \rho . V^2} \quad \text{and} \quad \sigma_n = \frac{p - p_v}{\frac{1}{2} . \rho . n^2 . d^2} = J^2 . \sigma_v$$

where p = pressure at propeller axis

$= p_a + i . \rho . g$

p_a = Atmospheric pressure , lbs/sq.ft.

p_v = Vapor pressure , lbs/sq.ft.

i = Depth of immersion of axis , ft. H_2O

ρ = Density , slugs/c.ft.

V = Velocity of advance , ft/sec.

n = Revolutions per second

at x% of the radius

$$\sigma_x = \frac{p_x - p_v}{\frac{1}{2} . \rho . W^2}$$

but $$W^2 = V^2 . (1 + a)^2 + (\pi . x . n . d)^2 (1 - a')^2$$

$$= V^2 . (1 - a')^2 \left\{ \frac{(1 + a)^2}{(1 - a')^2} + \frac{(\pi . x)^2}{J^2} \right\}$$

and $\tan\psi = \tan\phi \left(\frac{1 - a'}{1 + a} \right)$

$$\therefore \quad W^2 = V^2 . (1 - a')^2 \left\{ \frac{\tan^2\phi}{\tan^2\psi} + \frac{(\pi . x)^2}{J^2} \right\}$$

$$\sigma_x = \frac{p_x - p_v}{\frac{1}{2} . \rho . V^2 (1 - a')^2 \left\{ \frac{\tan^2\phi}{\tan^2\psi} + \frac{(\pi . x)^2}{J^2} \right\}}$$

If we assume that $p_x = p$, i.e. neglect the decrease of immersion when the section is in its uppermost position

$$\sigma_x = \frac{\sigma_v}{(1 - a')^2 \left\{ \frac{\tan^2\phi}{\tan^2\psi} + \frac{(\pi . x)^2}{J^2} \right\}} \quad \ldots\ldots (34)$$

Assuming that the inflow velocities are neglected, equation (34) becomes

$$\sigma_x \doteq \frac{\sigma_v}{\left\{ 1 + \frac{(\pi . x)^2}{J^2} \right\}} \quad \ldots\ldots\ldots\ldots\ldots\ldots (35)$$

APPENDIX C.

DATA OF PROPELLER.

The model propeller used for the calculation is a merchant type propeller, having the following particulars :

Propeller		No. 62, M.I.T.	
Number of blades		= 4	
Diameter	d	= 12.00"	
Pitch	p	= 10.80"	constant
Pitch ratio	p/d	= 0.90	constant
B.Th.F.		= 0.05	
M.W.R.		= 0.25	
Projected area ratio		= 0.474	
Developed area ratio		= 0.509	
Hub diameter		= 0.2 d	
		= 2.4"	
Type of sections		= Ogival	
Rake		= None	
Skewback		= None	
Blade outline		= Elliptical	

Fig. (7) shows the outline of the propeller blade and Fig. (8) shows the variation of thickness t , chord c and thickness fraction t/c along the blade length.

CHARACTERISTICS OF OGIVAL SECTIONS

IN CAVITATION.

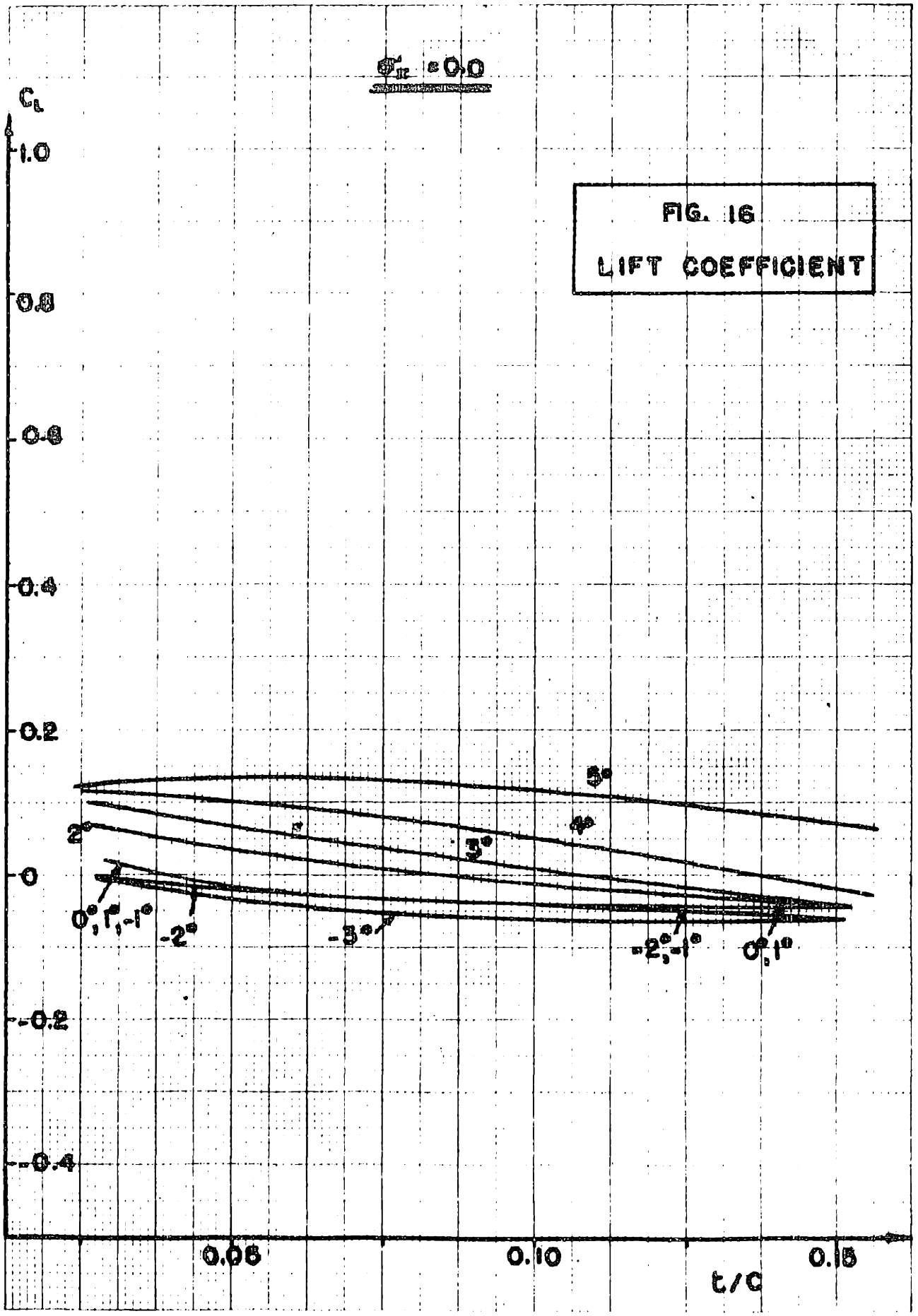

FIG. 16
LIFT COEFFICIENT

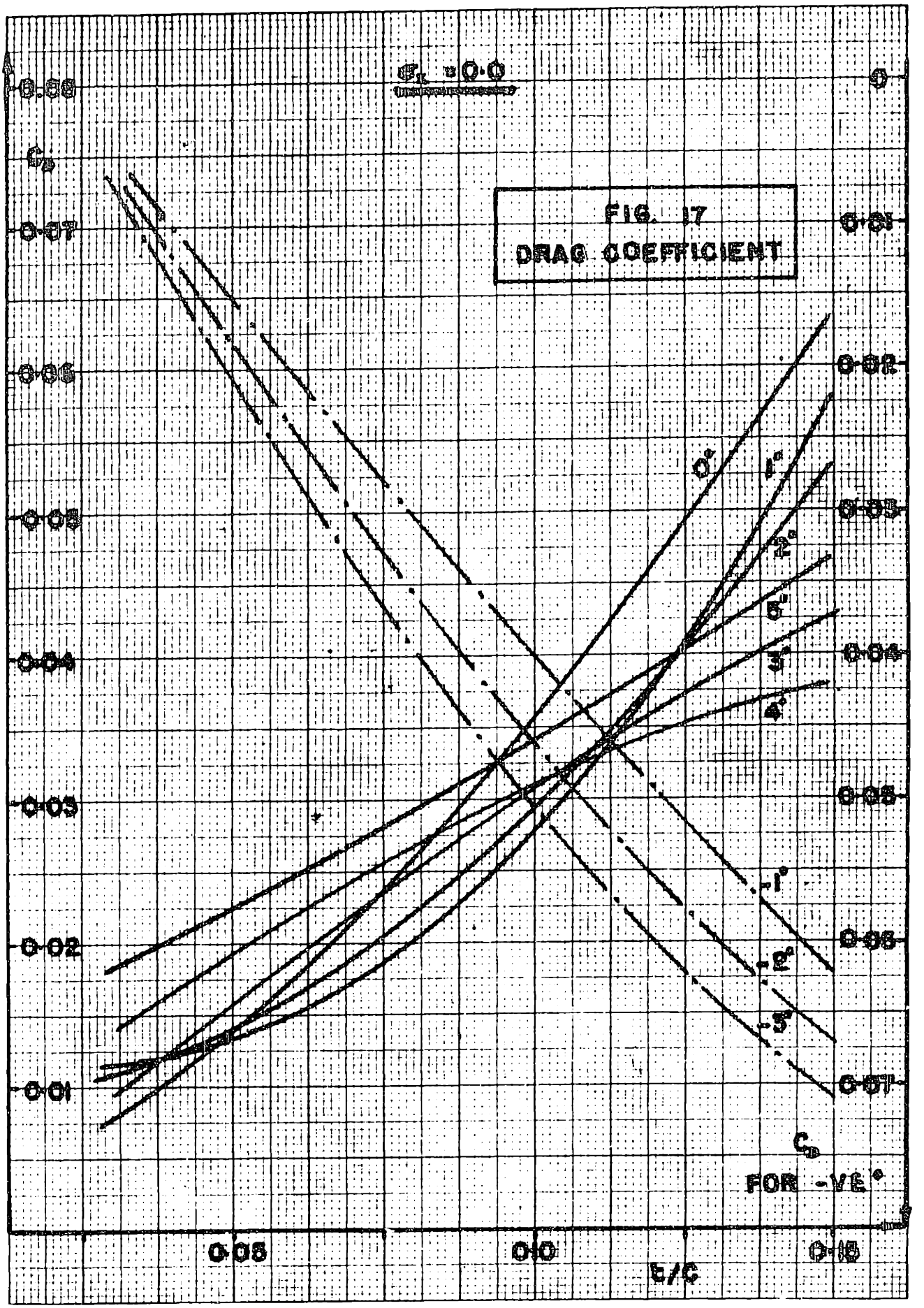
FIG. 17
DRAG COEFFICIENT
C_L = 0·0
C_D
0·08
0·07
0·06
0·05
0·04
0·03
0·02
0·01
0
0·01
0·02
0·03
0·04
0·05
0·06
0·07
0·08
0·10
0·12
t/c
0°
1°
2°
5°
3°
4°
-1°
-2°
-3°
C_D FOR -VE°

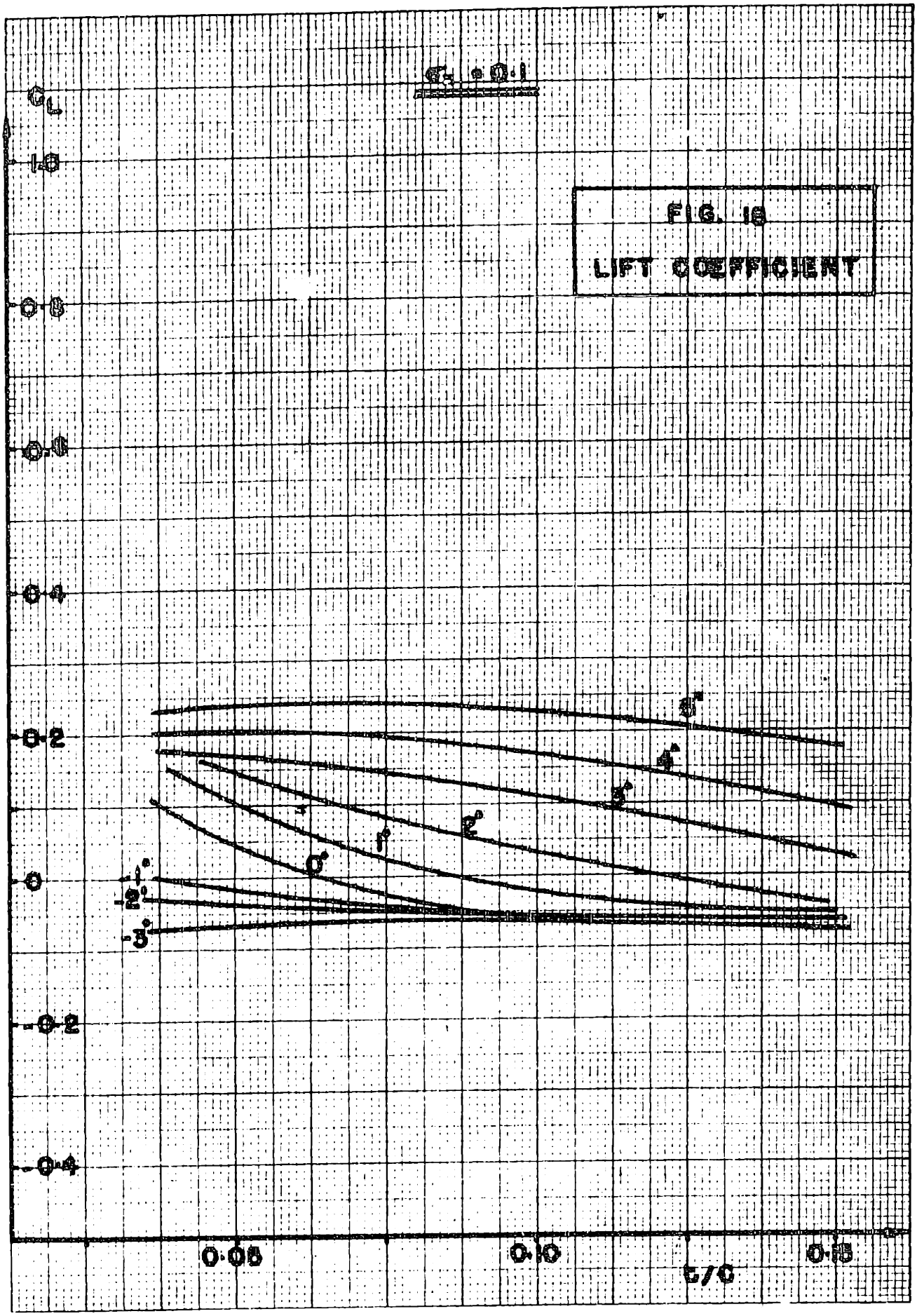

FIG. 18
LIFT COEFFICIENT

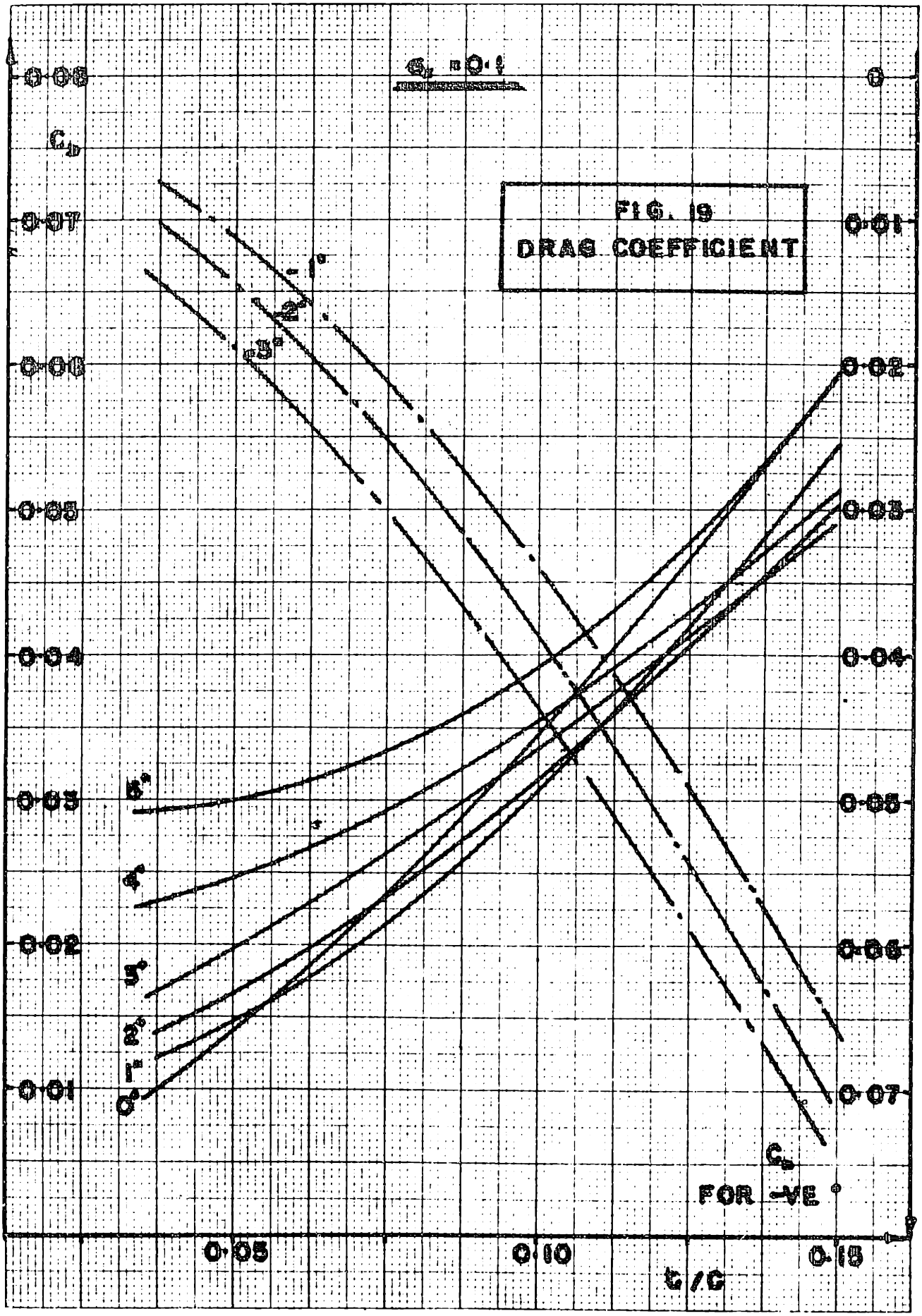

FIG. 19
DRAG COEFFICIENT

$\sigma_L = 0.2$

FIG. 20
LIFT COEFFICIENT

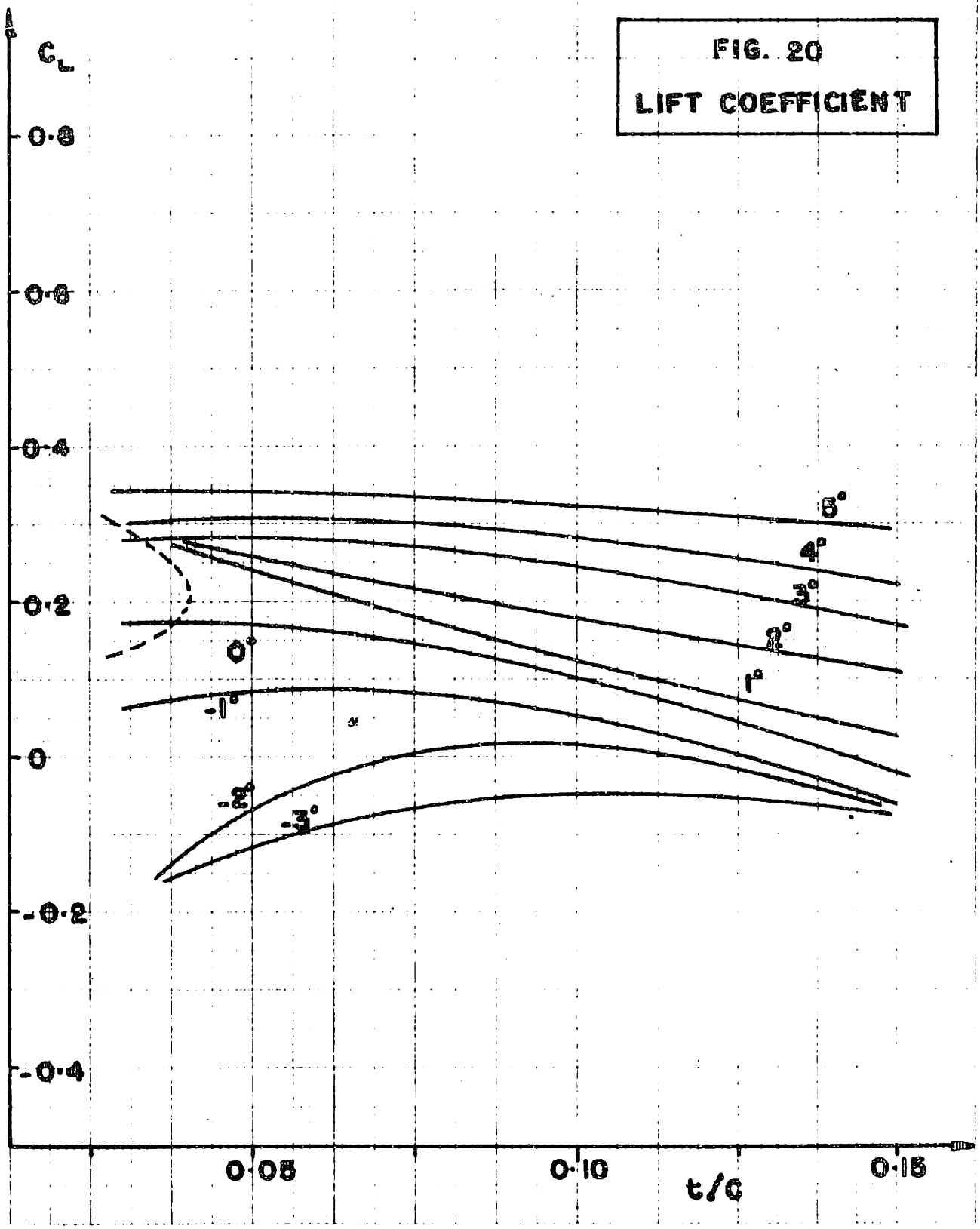

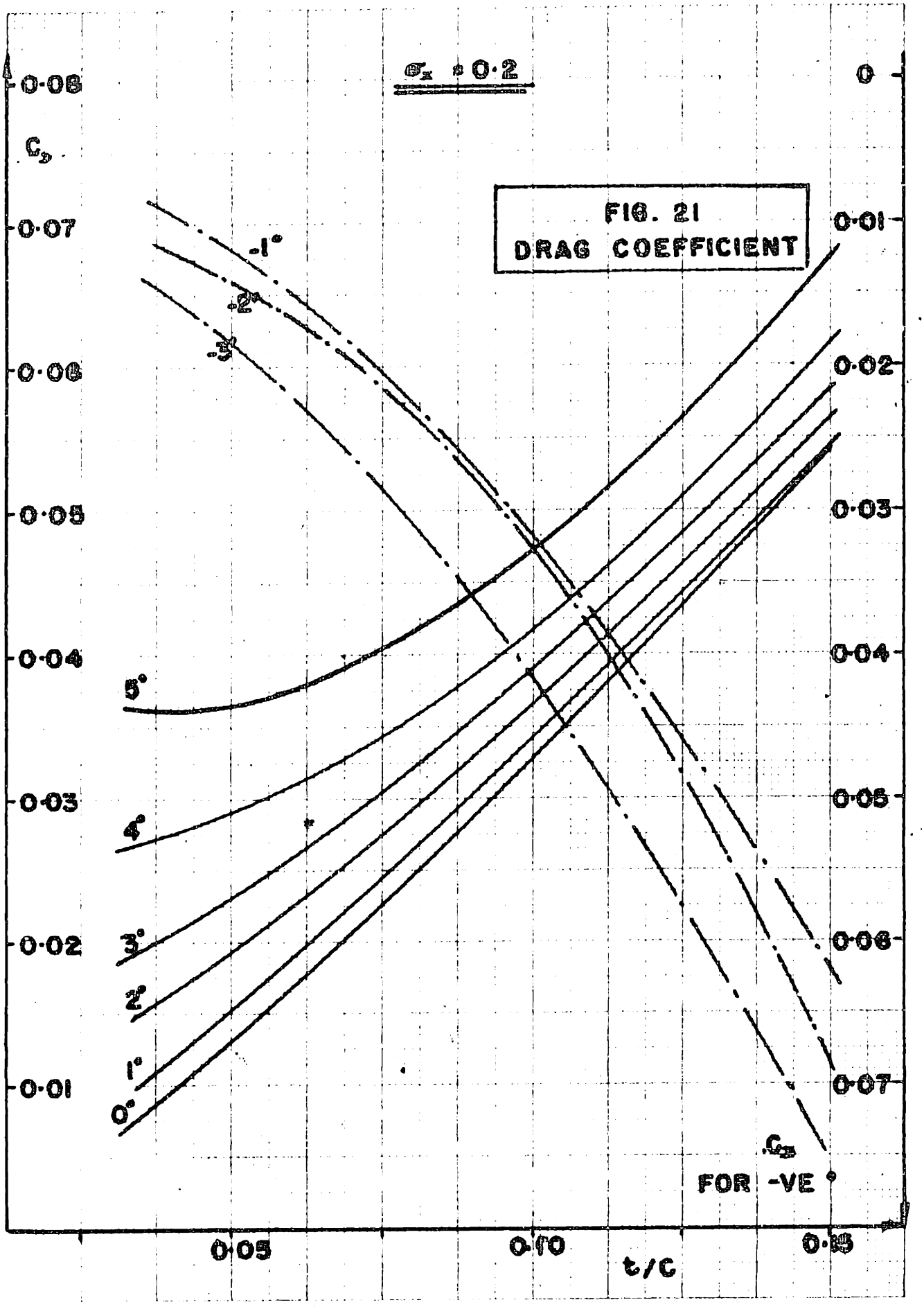
σ_x = 0·2
FIG. 21
DRAG COEFFICIENT
C_D
0·08
0·07
0·06
0·05
0·04
0·03
0·02
0·01
0
0·01
0·02
0·03
0·04
0·05
0·06
0·07
-1°
-2°
-3°
5°
4°
3°
2°
1°
0°
C_{D_0}
FOR -VE °
0·05
0·10
0·15
t/C

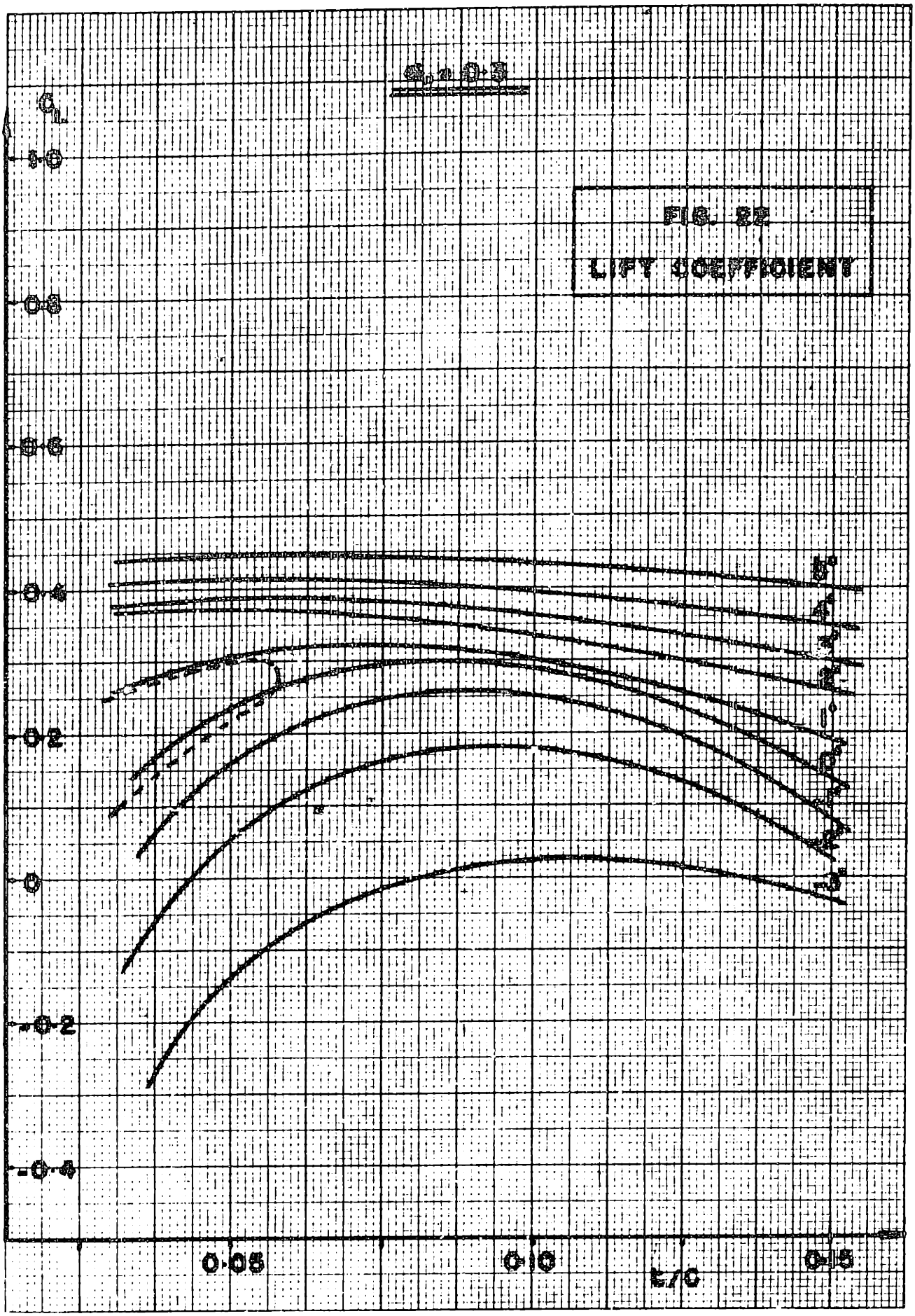

FIG. 22
LIFT COEFFICIENT

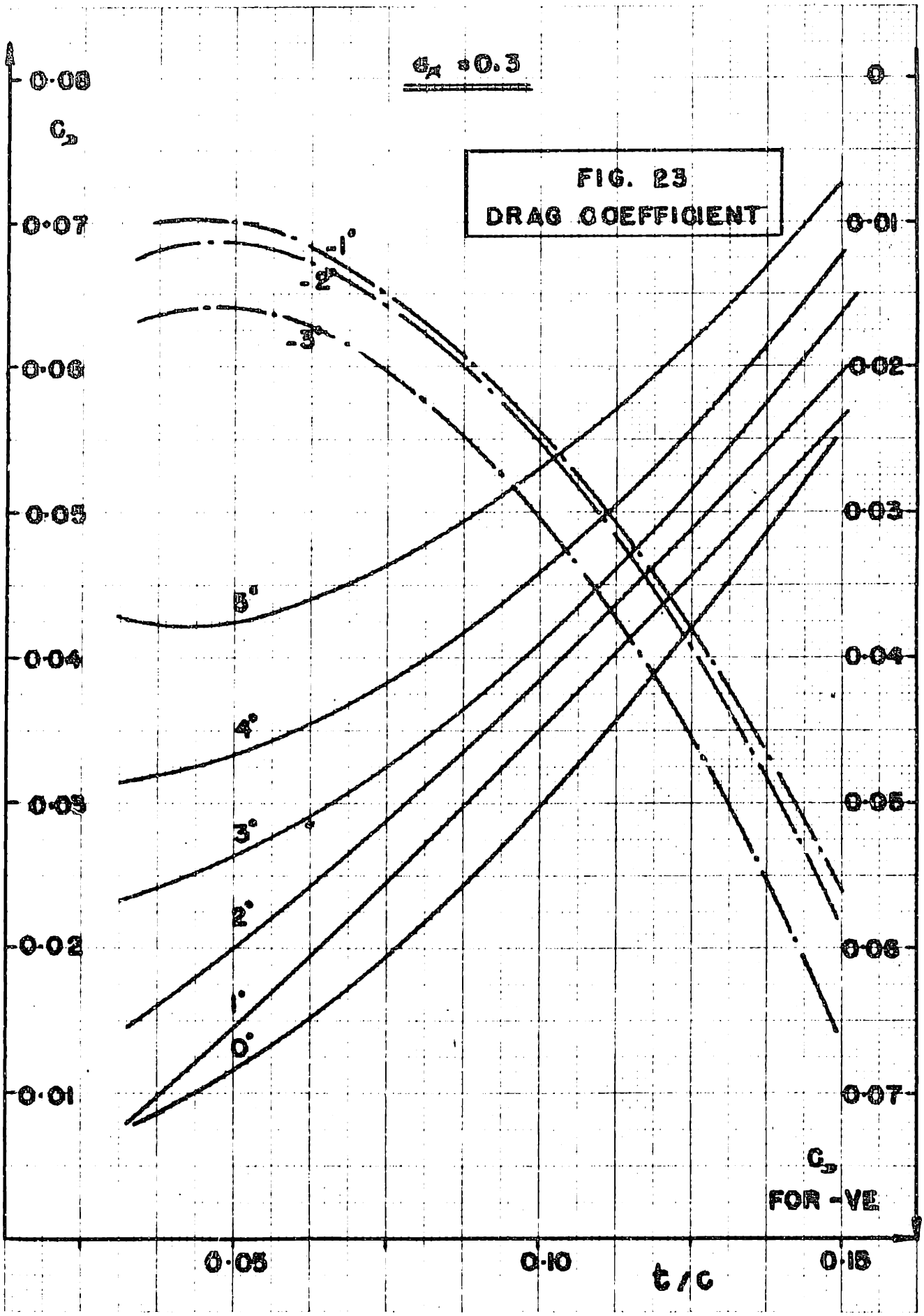
C_{L_d} = 0.3
FIG. 23
DRAG COEFFICIENT
0·08
0·07
0·06
0·05
0·04
0·03
0·02
0·01
C_D
0
0·01
0·02
0·03
0·04
0·05
0·06
0·07
C_D FOR -VE
-1°
-2°
-3°
5°
4°
3°
2°
1°
0°
0·05
0·10
0·15
t/c

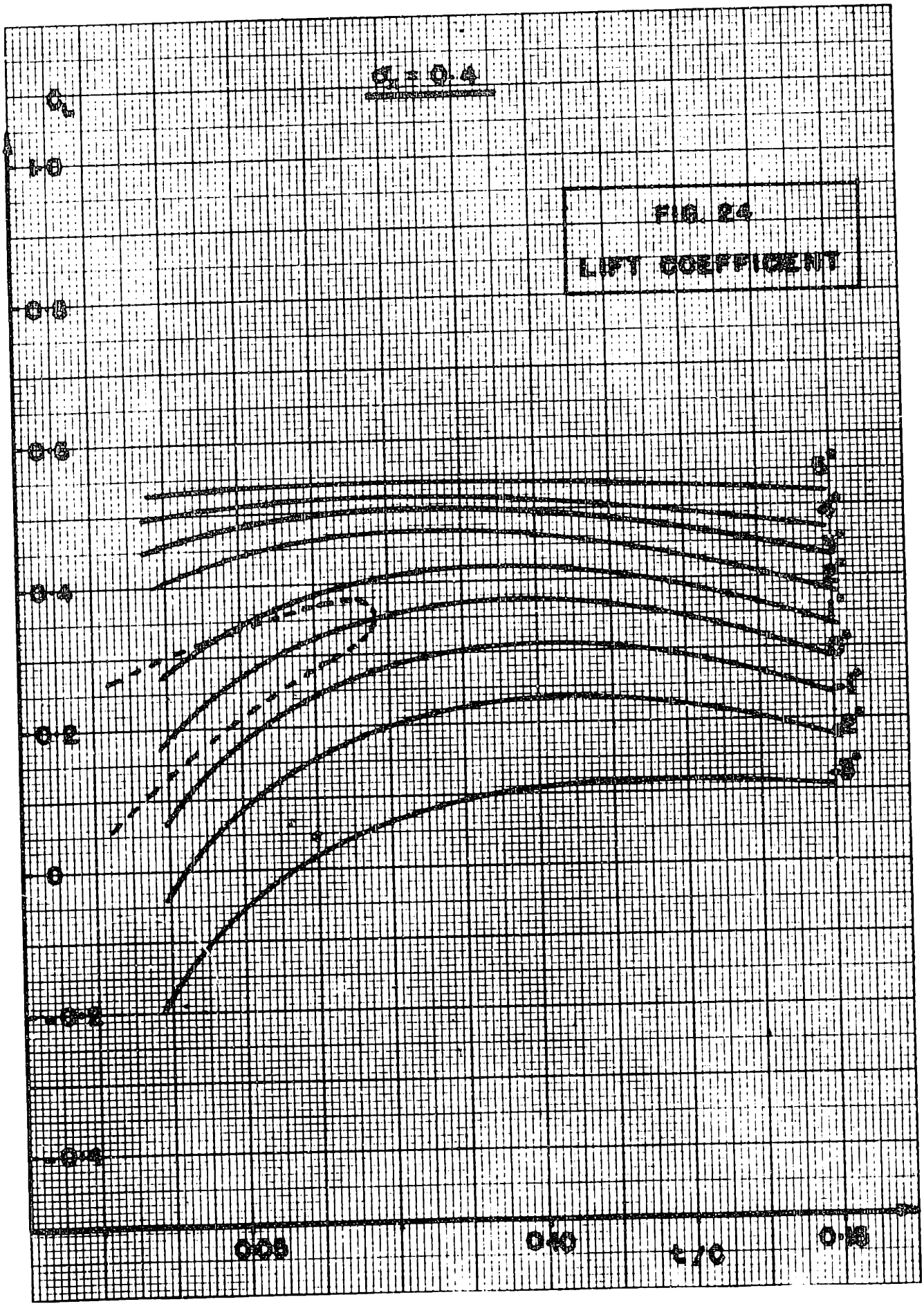

FIG. 24
LIFT COEFFICIENT

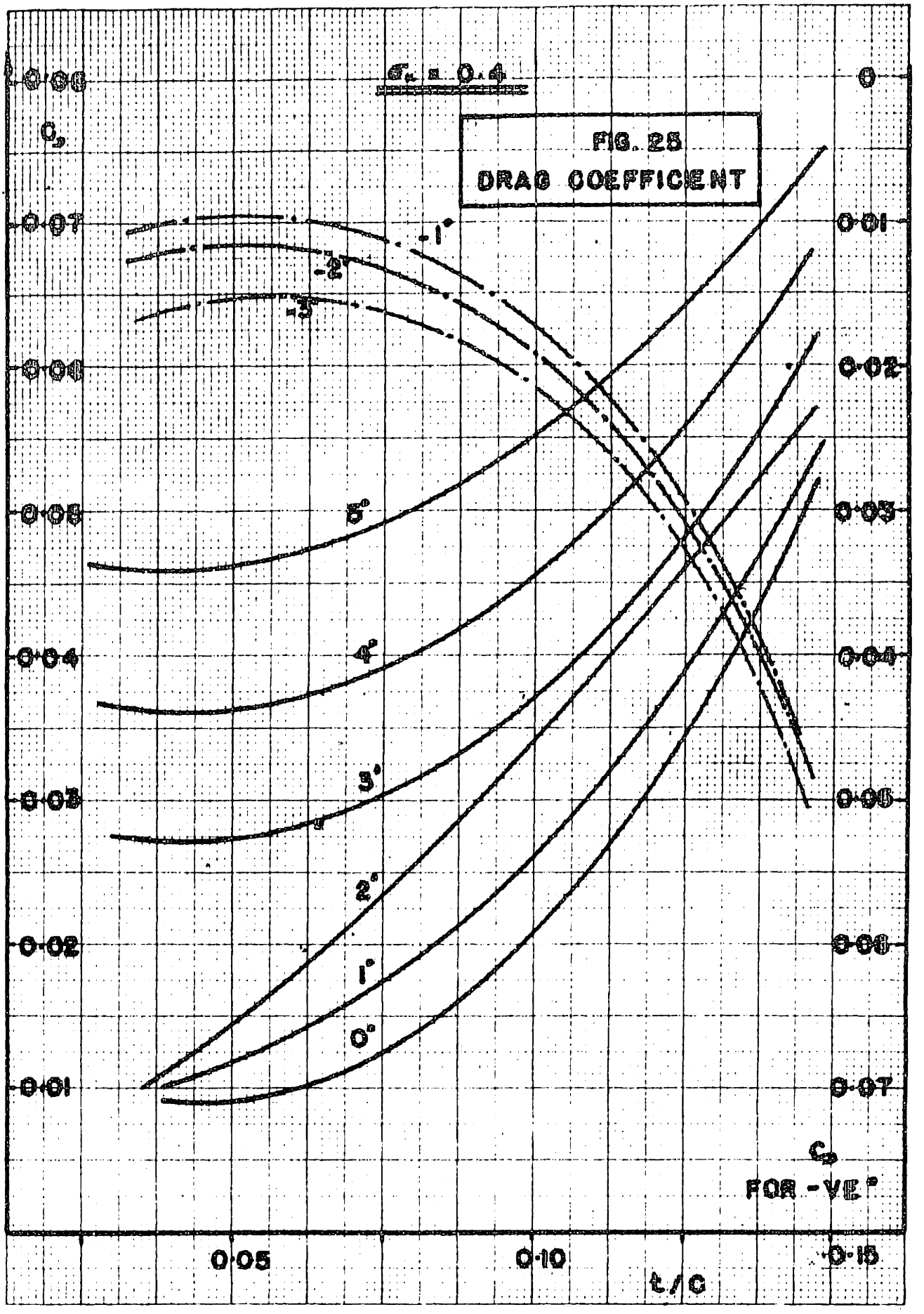
$\sigma_c = 0.4$
FIG. 25
DRAG COEFFICIENT
C_D
0·08
0·07
0·06
0·05
0·04
0·03
0·02
0·01
0
0·01
0·02
0·03
0·04
0·05
0·06
0·07
-1°
-2°
-3°
5°
4°
3°
2°
1°
0°
C_D FOR -VE σ
0·05
0·10
0·15
t/c

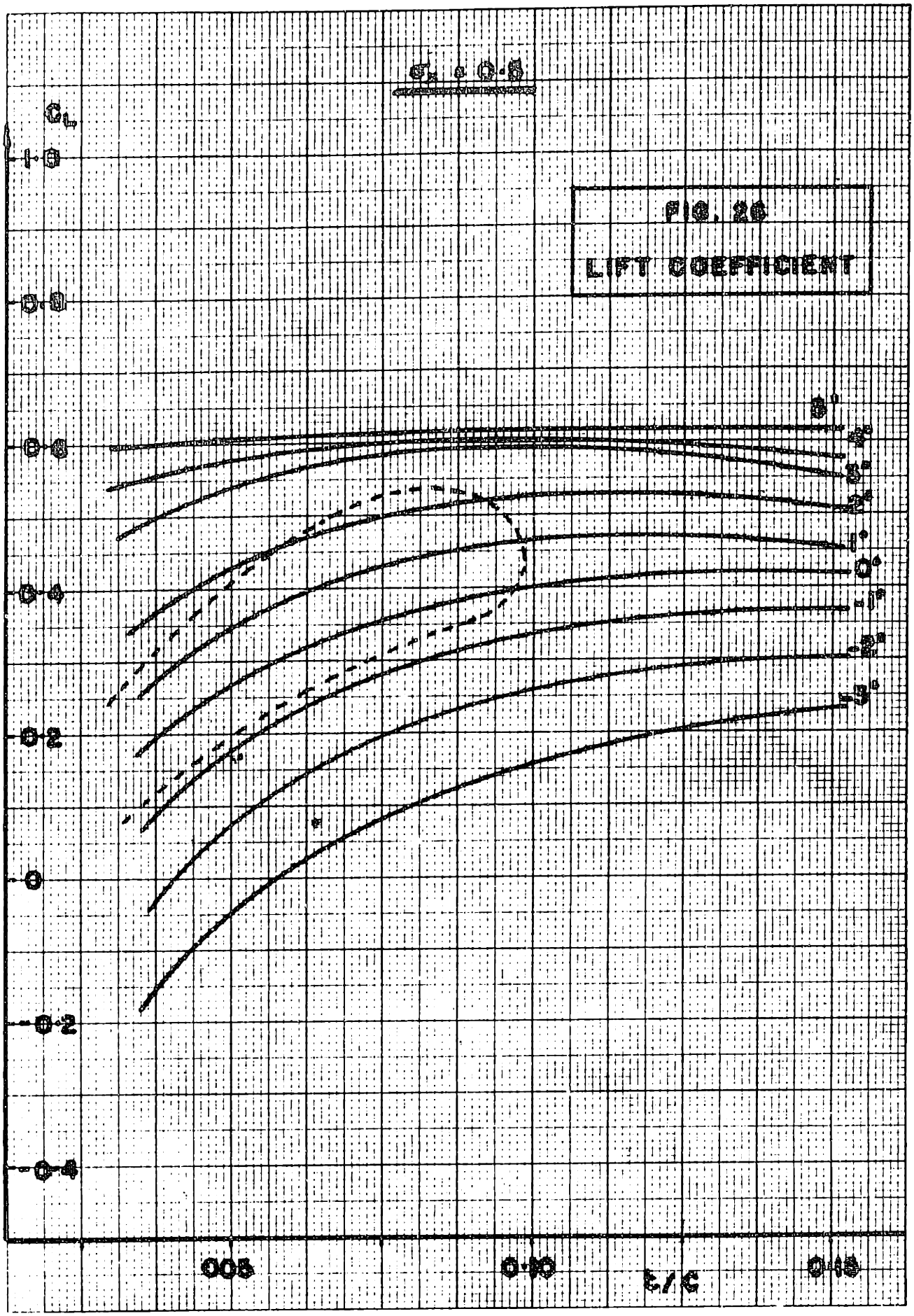

FIG. 26
LIFT COEFFICIENT

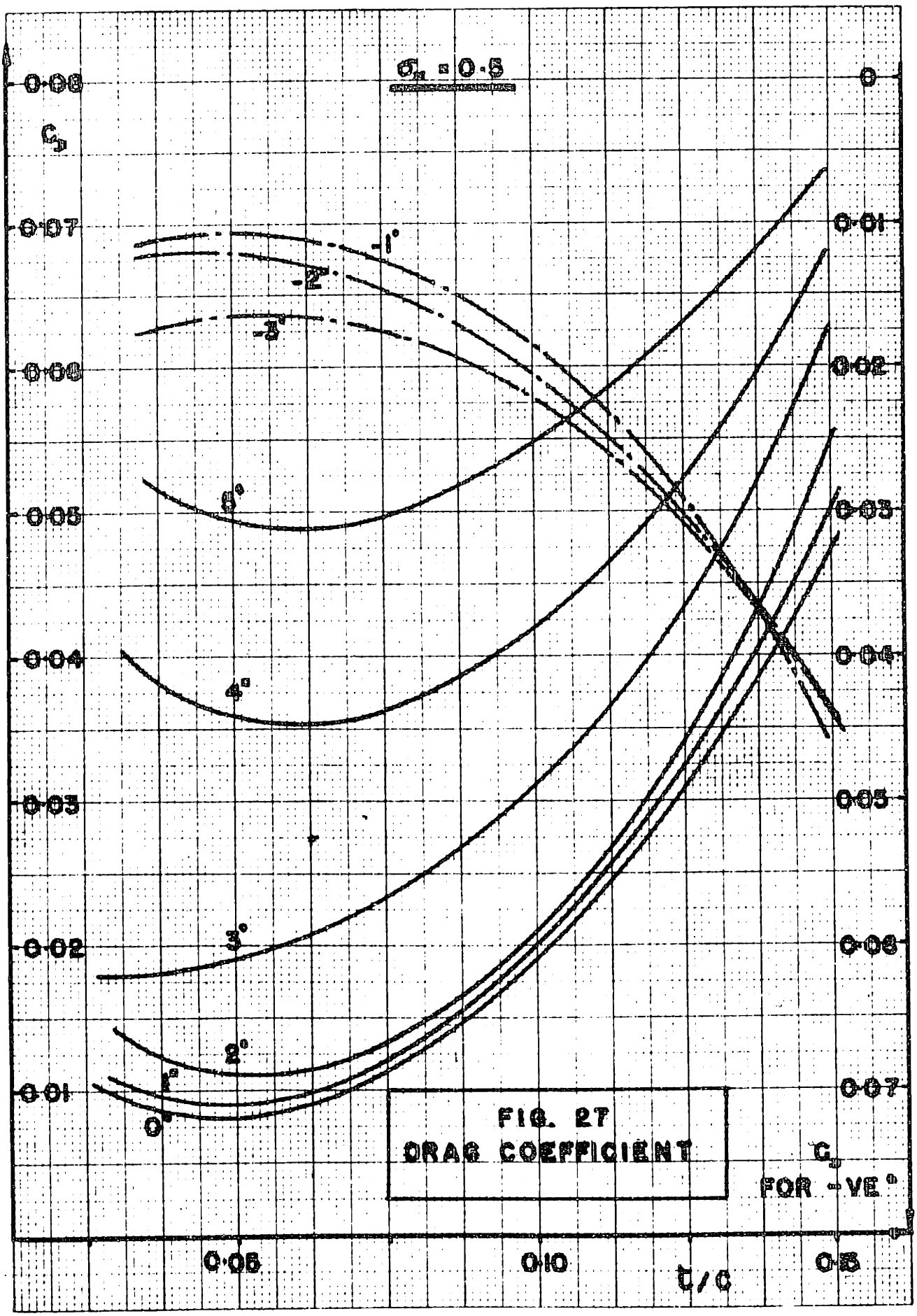

FIG. 27
DRAG COEFFICIENT

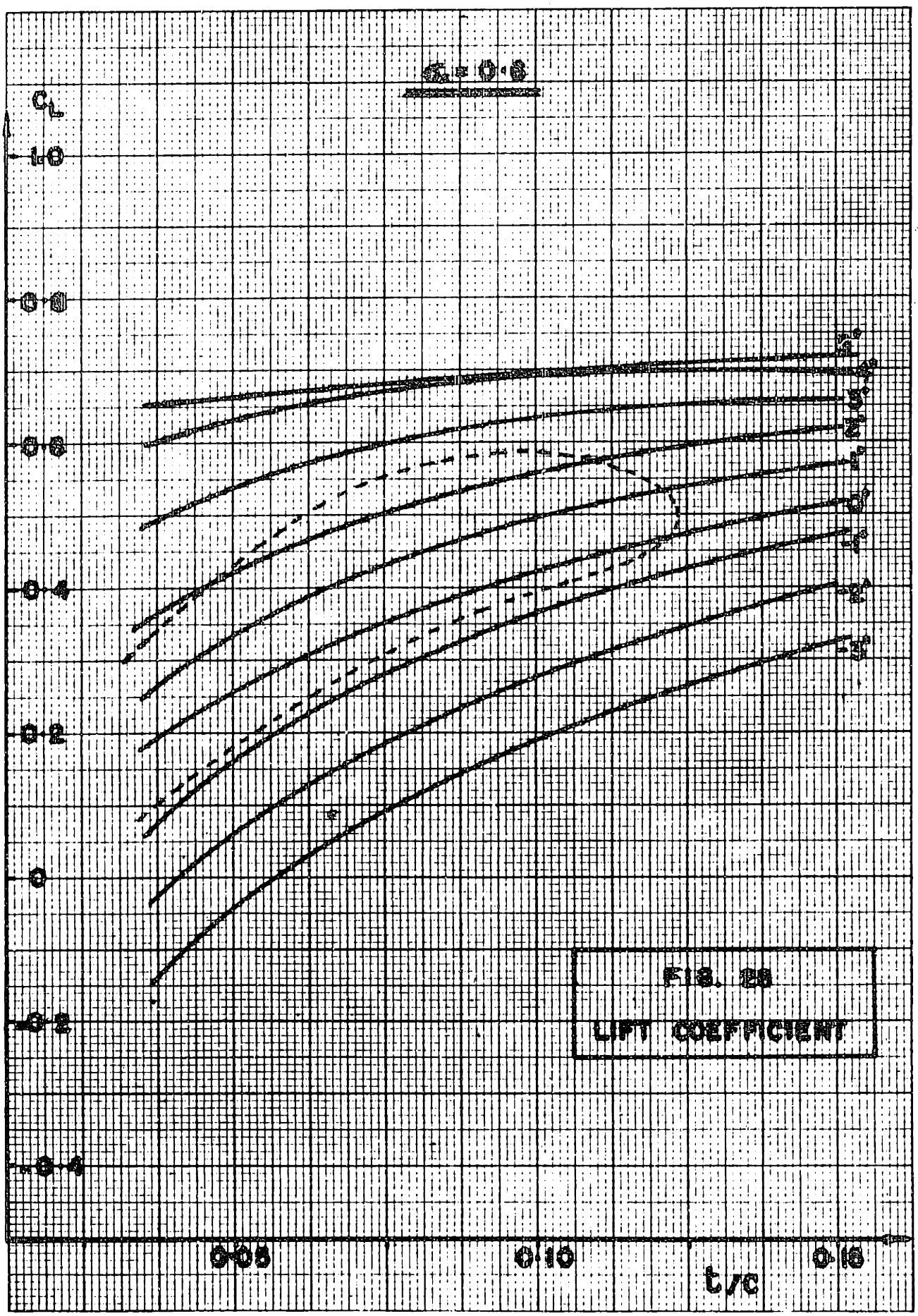

FIG. 28
LIFT COEFFICIENT

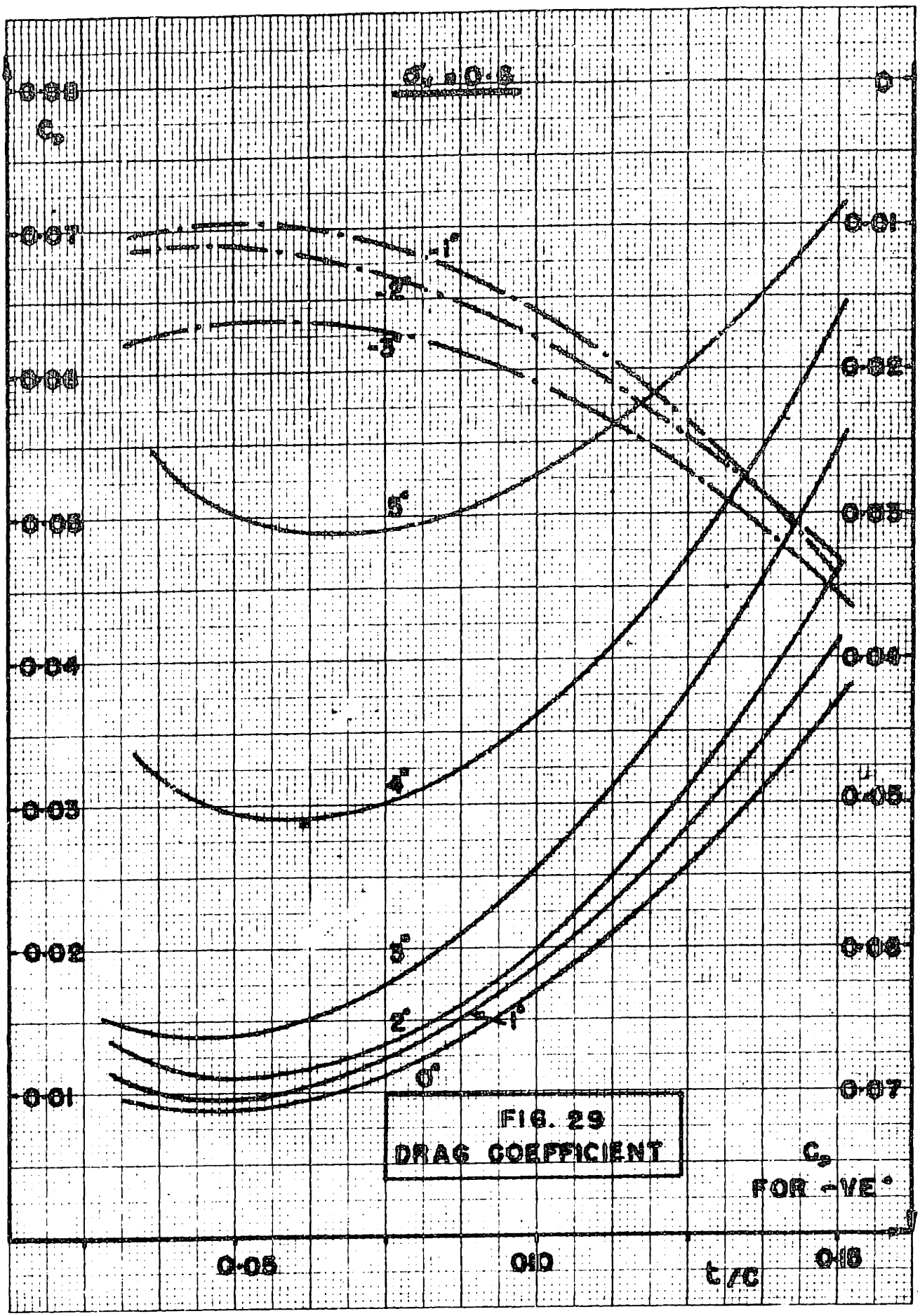

FIG. 29
DRAG COEFFICIENT

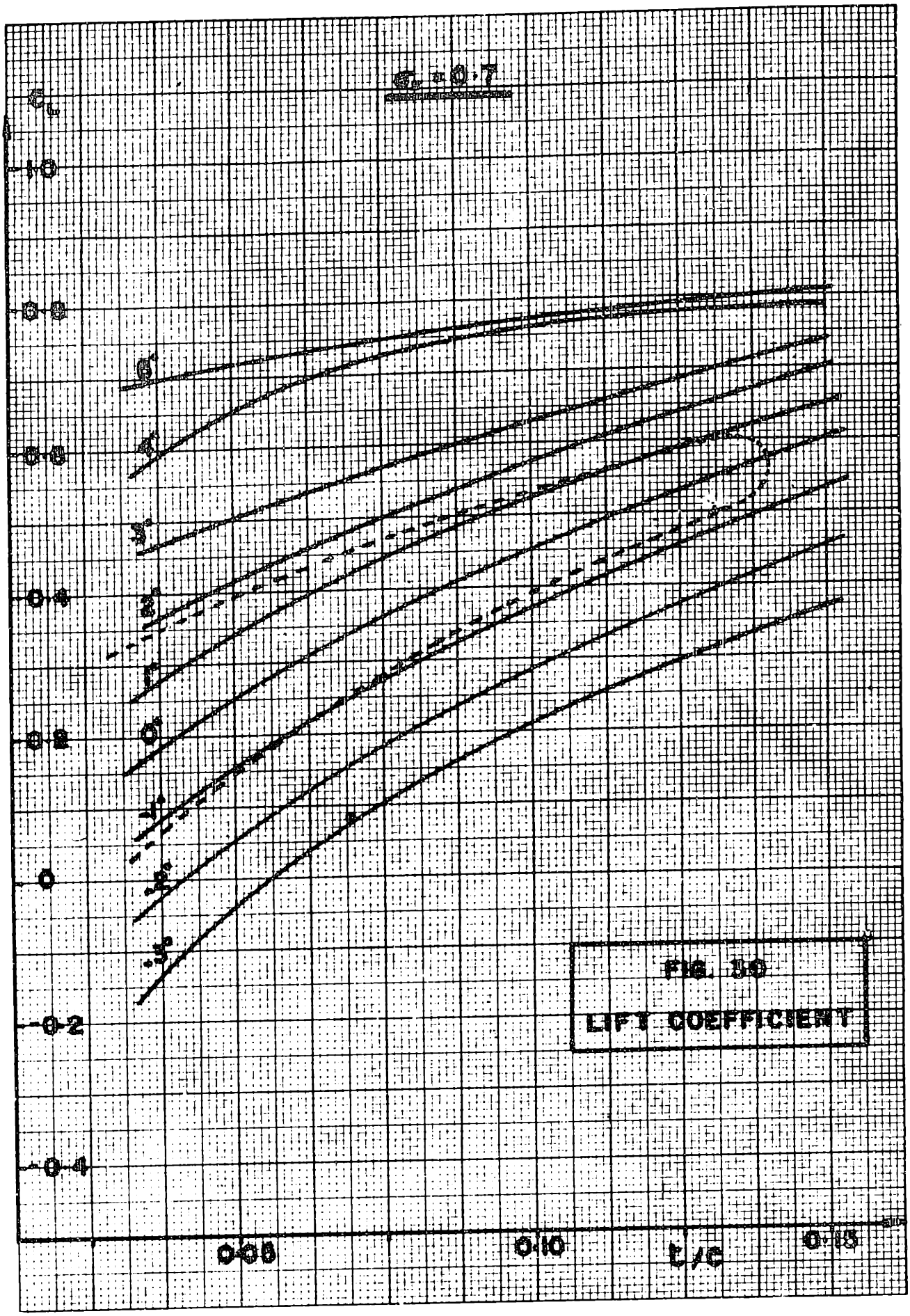

FIG. 10

LIFT COEFFICIENT

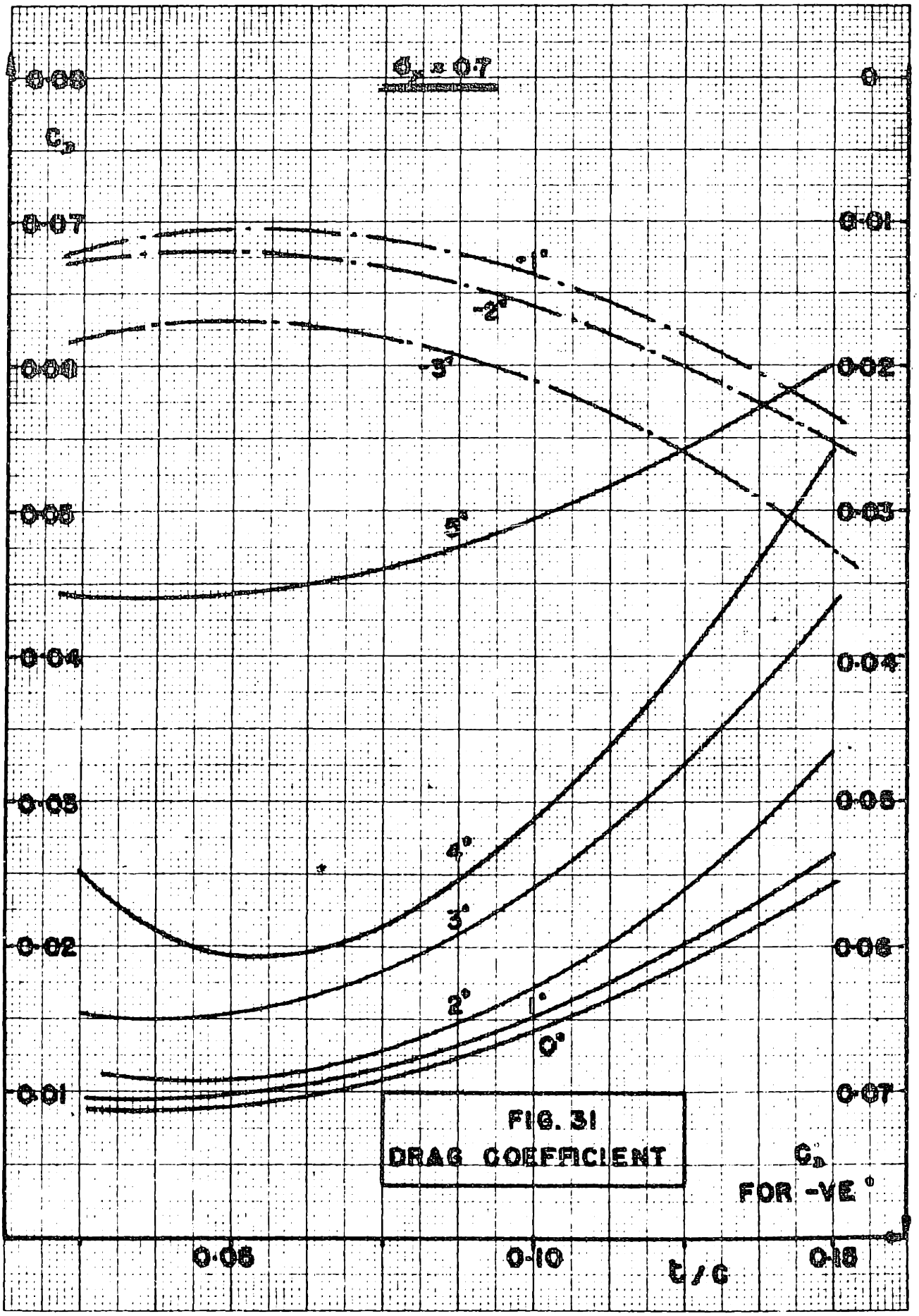

FIG. 31
DRAG COEFFICIENT

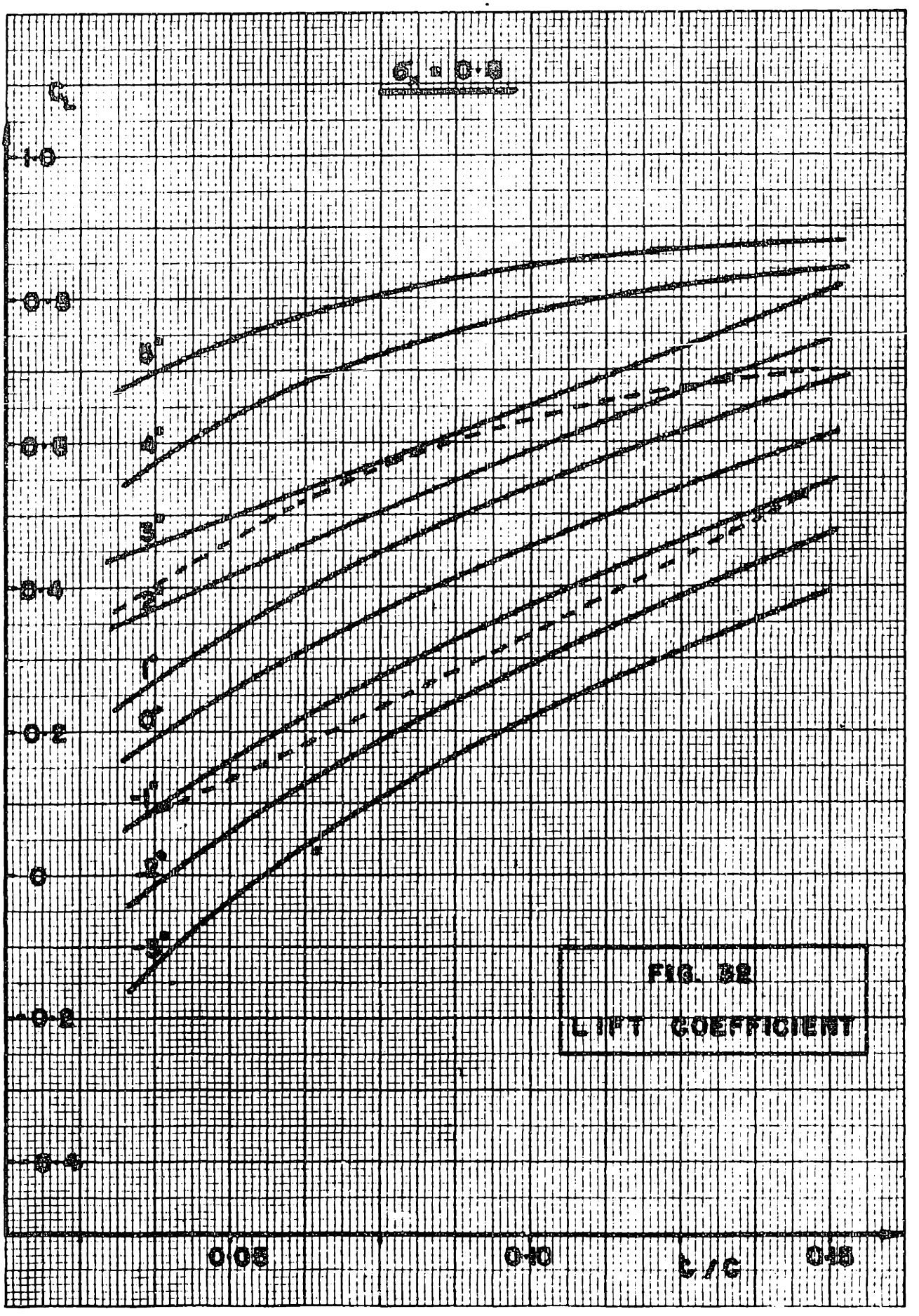

FIG. 52
LIFT COEFFICIENT

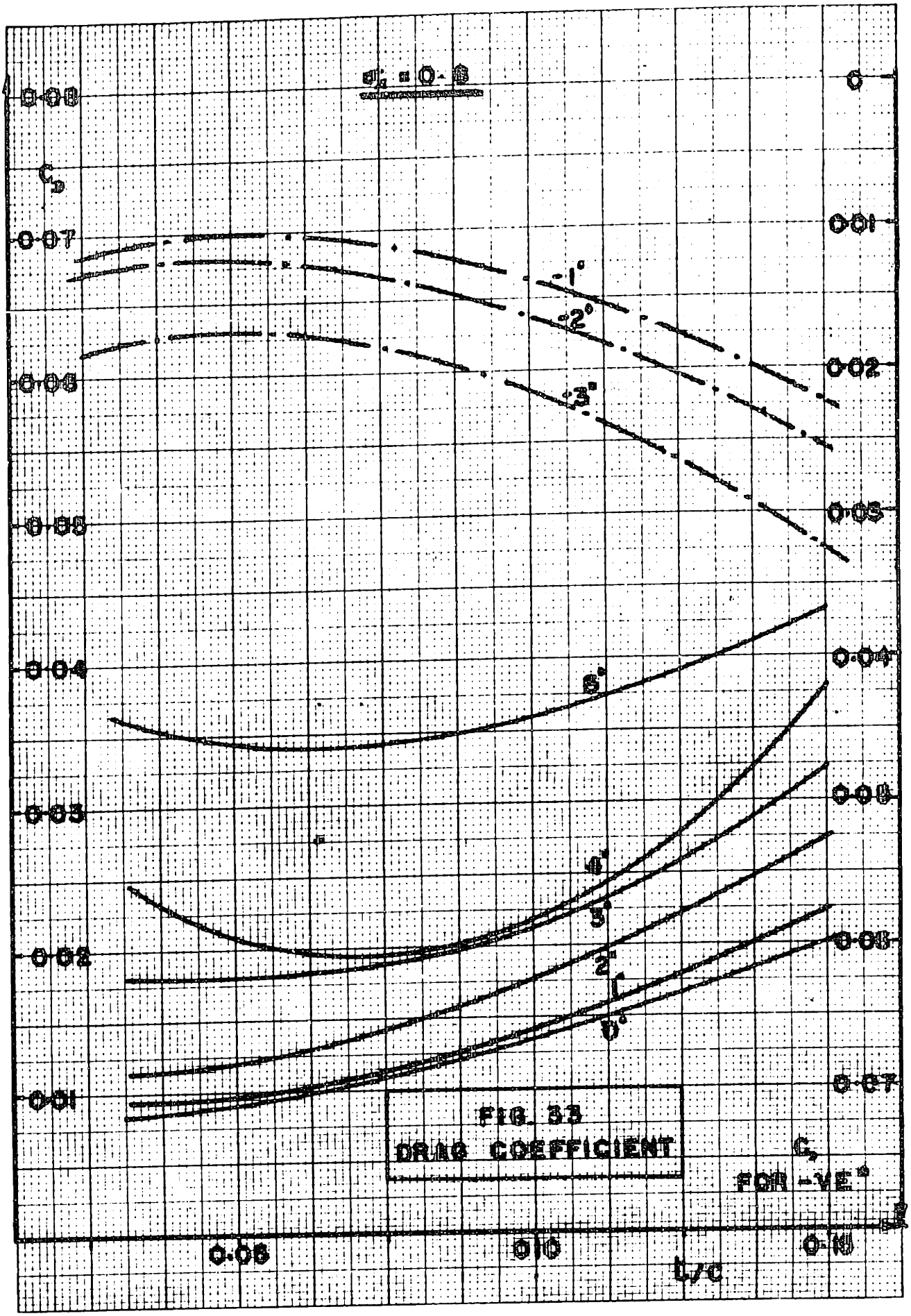

FIG. 33
DRAG COEFFICIENT C_D FOR -VE α

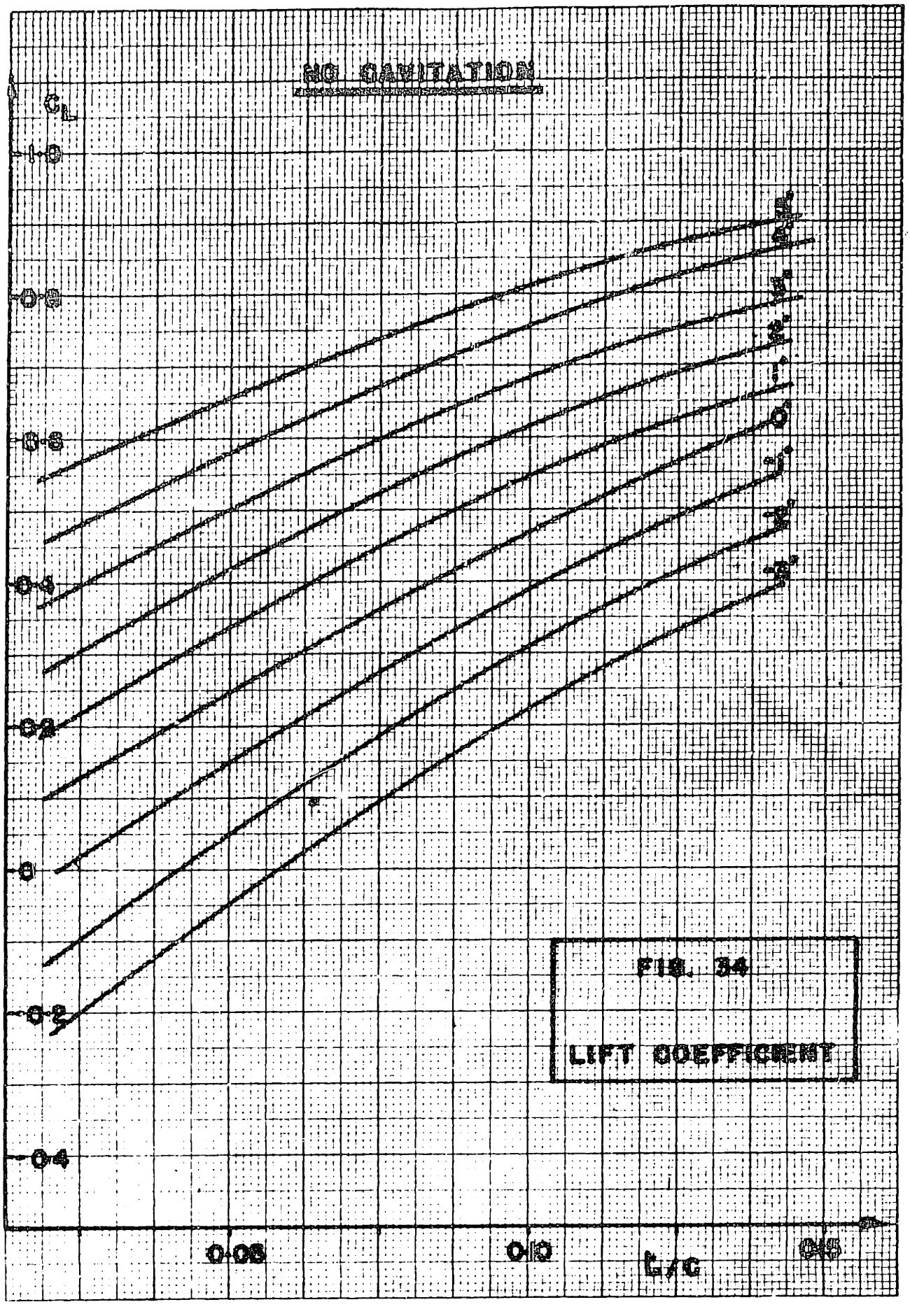

FIG. 34

LIFT COEFFICIENT

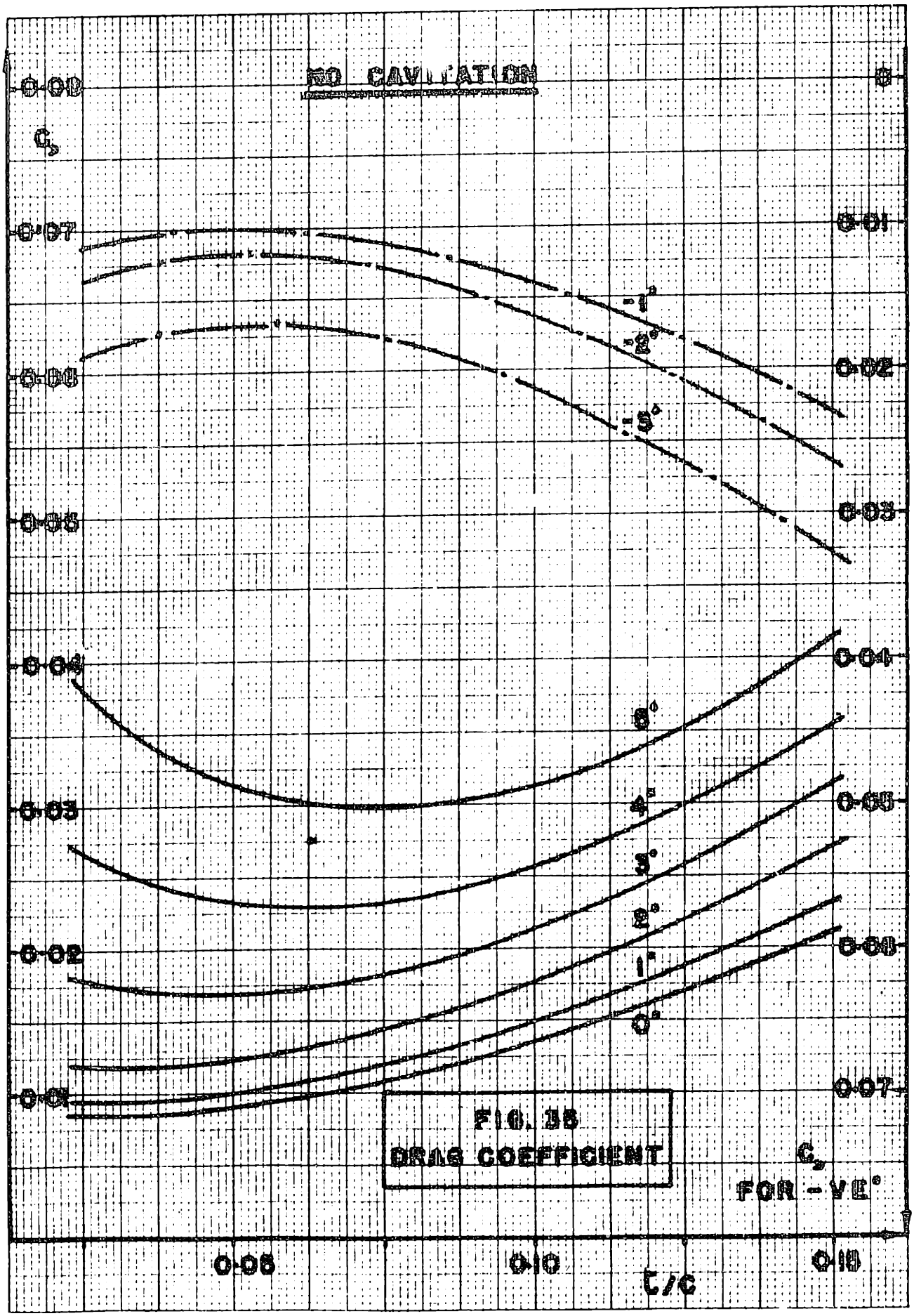

FIG. 35
DRAG COEFFICIENT C_D
FOR -VE°

APPENDIX D.

PROCEDURE FOR CALCULATION AND SAMPLE CALCULATION.

The procedure described is the one used in order to determine the thrust, torque and efficiency for a given propeller when the design features are known.

Considering the x = 0.7 section for a model 4-bladed propeller having the following particulars at that radius :

Diameter = d = 1.0 ft.

Pitch = p = 0.9 ft.

Thickness of section = t = 0.200 in.

Chord of section = c = 3.47 in.

It is required to compute the thrust and torque coefficients as well as the efficiency for J = 0.6 and $\sigma_v = 2.22$.

The cavitation index for the section is given by equation (12)

$$\sigma_x = \frac{\sigma_v}{1 + \frac{(\pi . x)^2}{J^2}}$$

and in this case $\sigma_x = 0.154$ (See sample calculation form).

The value of the pitch angle θ, the advance angle ψ and the solidity s can be computed from the features of the section and the propeller. The no-lift angle α_o is obtained from Fig. (2) .

It is now required to assume an angle of attack. As a first try α is assumed at 2.00 deg. Entering Fig. (16)

through Fig. (35) with the appropriate σ_x and t/c we can obtain the lift coefficient corresponding to that angle of attack in two dimensional flow, the value geing 0.186. The hydrodynamic pitch angle ϕ can now be found :

$$\phi = \theta - \alpha = 22.32 - 2.00 = 20.32$$

$$\beta = \phi - \psi = 20.32 - 15.28 = 5.04$$

and the pitch angle in the slipstream is given by :

$$\epsilon = \phi + \beta = 20.32 + 5.04 = 25.26$$

From Fig. (15) the Goldstein correction factor can be obtained and C_L computed by equation (6). It is found that $C_L = 0.195$, hence a second value of α has to be assumed.

When $\alpha = 2.05$ deg., both the curves and the computation give a C_L of 0.193 . The effective solidity can now be obtained from Fig. (5).

$$s_e = 1.18 \times 0.526 = 0.621$$

Entering Fig. (6) the cascade correction factor k_g is determined and the drag coefficient obtained from the two dimensional curves, no cascade correction being applied to the drag.

Hence

$$\tan \gamma = \frac{C_D}{C_L \cdot k_g} = \frac{0.0206}{0.193 \times 0.705} = 0.1518$$

The value of C_L is computed by equation (28), Appendix B and added to C_L.

The rotational inflow factor a' can then be determined and the values of K_{Tx}, K_{Qx} and e_x computed by equations (30) (32) and (33).

The same procedure is repeated for a number of sections along the length of the blade and the result integrated by Simpson's Rule as shown in the following table.

SAMPLE CALCULATION.

Calculation of thrust, torque and efficiency.

$x = r/R = 0.7$ $\quad J = V/n.d = 0.6$ $\quad \sigma_v = 2.22$ $\quad \sigma_n = 0.8$

$d = 1.0$ ft.	$t = 0.200$ in.
$p = 0.9$ ft.	$c = 3.47$ in.
$p/d = 0.9$	$t/c = 0.0576$

$$\frac{\pi.x}{J} = \frac{3.14 \times 0.7}{0.6} = 3.66$$

$$\sigma_x = \frac{2.22}{1 + 3.66^2} = 0.154$$

Assumed	2.00	2.05
C_L (from curves)	0.186	0.193
$\phi = \theta - \alpha$	20.32	20.27
$\beta = \phi - \psi$	5.04	4.99
$\epsilon = \phi + \beta$	25.36	25.26
k_ϵ	0.86	0.86
$\sin\phi$	0.347	0.347
$\tan\beta$	.0878	.0870
$C_L' = \frac{4k_\epsilon}{s}\sin\phi.\tan\beta$	0.199	0.197
$\tan\phi$	0.370	0.369
k_ϕ	0.92	0.92
$C_L'' = C_L' \frac{\tan\beta}{\tan\phi}(1-k_\phi)$	0.004	0.004
$C_L = C_L' - C_L''$	0.195	0.193
$k_g.C_L$		0.136

$s = Z.c/\pi.d.x = 0.526$ $\quad \alpha_o = -1.30$

$\tan\theta = p/\pi.d.x = 0.41$ $\quad \theta = 22.32$

$\tan\psi = J/\pi.x = 0.273$ $\quad \psi = 15.28$

$k_\theta = 0.621$ $\quad k_g = 0.708$

$C_D = 0.0206$

$\tan\gamma = C_D/k_g.C_L = 0.1518$

$\gamma = 8.64$

$\phi + \gamma = 28.91$

$$\delta C_L = C_L.k_g \frac{\tan\beta\tan\gamma}{1 - \tan\beta.\tan\gamma} = \frac{0.00179}{1 - 0.0132} = 0.002$$

$k_g.C_L + \delta C_L = 0.138$

$$a' = \frac{[\tan\phi - \tan\psi]\tan(\phi+\gamma)}{1 + \tan\phi.\tan(\phi+\gamma)} = \frac{0.096 \times 0.551}{1 + 0.369 \times 0.551} = 0.0440$$

$$K_{Tx} = \frac{s}{4}.\pi^3.x^3(1 - a')^2(1 + \tan^2\phi).C_L.\frac{\cos(\phi+\gamma)}{\cos\gamma}$$

$$= \frac{0.526}{4}\pi^3 0.343 \times 0.914 \times 1.136 \times 0.138 \times \frac{0.875}{0.983} = 0.177$$

$$K_{Qx} = \frac{x}{2}.\tan(\phi+\gamma).K_{Tx} = 0.35 \times 0.551 \times 0.177 = 0.0342$$

$$e_x = \frac{J.K_{Tx}}{2\pi.K_{Qx}} = 0.495 \qquad \text{Check } e_x = \frac{\tan\psi}{\tan(\phi+\gamma)} = 0.495$$

Integration of Thrust and Torque.

x	K_{Tx}	S.M.	$f(K_{Tx})$	K_{Qx}	$f(K_{Qx})$
0.20	0.028	1	0.028	0.0040	0.0040
0.25	0.046	4	0.176	0.0085	0.0340
0.30	0.065	2	0.130	0.0113	0.0226
0.35	0.082	4	0.168	0.0150	0.0600
0.40	0.100	2	0.200	0.0187	0.0374
0.45	0.114	4	0.456	0.0219	0.0876
0.50	0.130	2	0.260	0.0249	0.0498
0.55	0.140	4	0.560	0.0278	0.1112
0.60	0.153	2	0.306	0.0297	0.0594
0.65	0.165	4	0.660	0.0325	0.1288
0.70	0.177	2	0.354	0.0342	0.0684
0.75	0.179	4	0.716	0.0350	0.1400
0.80	0.180	2	0.360	0.0346	0.0692
0.85	0.180	4	0.720	0.0340	0.1360
0.90	0.181	2	0.362	0.0326	0.0652
0.95	0.163	4	0.652	0.0300	0.1200
1.00	0.000	1	0.000	0.0000	0.0000
			$\Sigma f(K_{Tx}) = 6.208$		$\Sigma f(K_{Qx}) = 1.1956$

$$\therefore \quad K_T = 6.208 \frac{0.05}{3} = 0.1034$$

$$K_Q = 1.1956 \frac{0.05}{3} = 0.0199$$

The following results are then obtained :

	Calculated	Experimental	Difference
K_T	0.1034	0.100	+ 3.4%
K_Q	0.0199	0.0202	- 1.5%
e	49.7%	47.3%	+ 2.4%

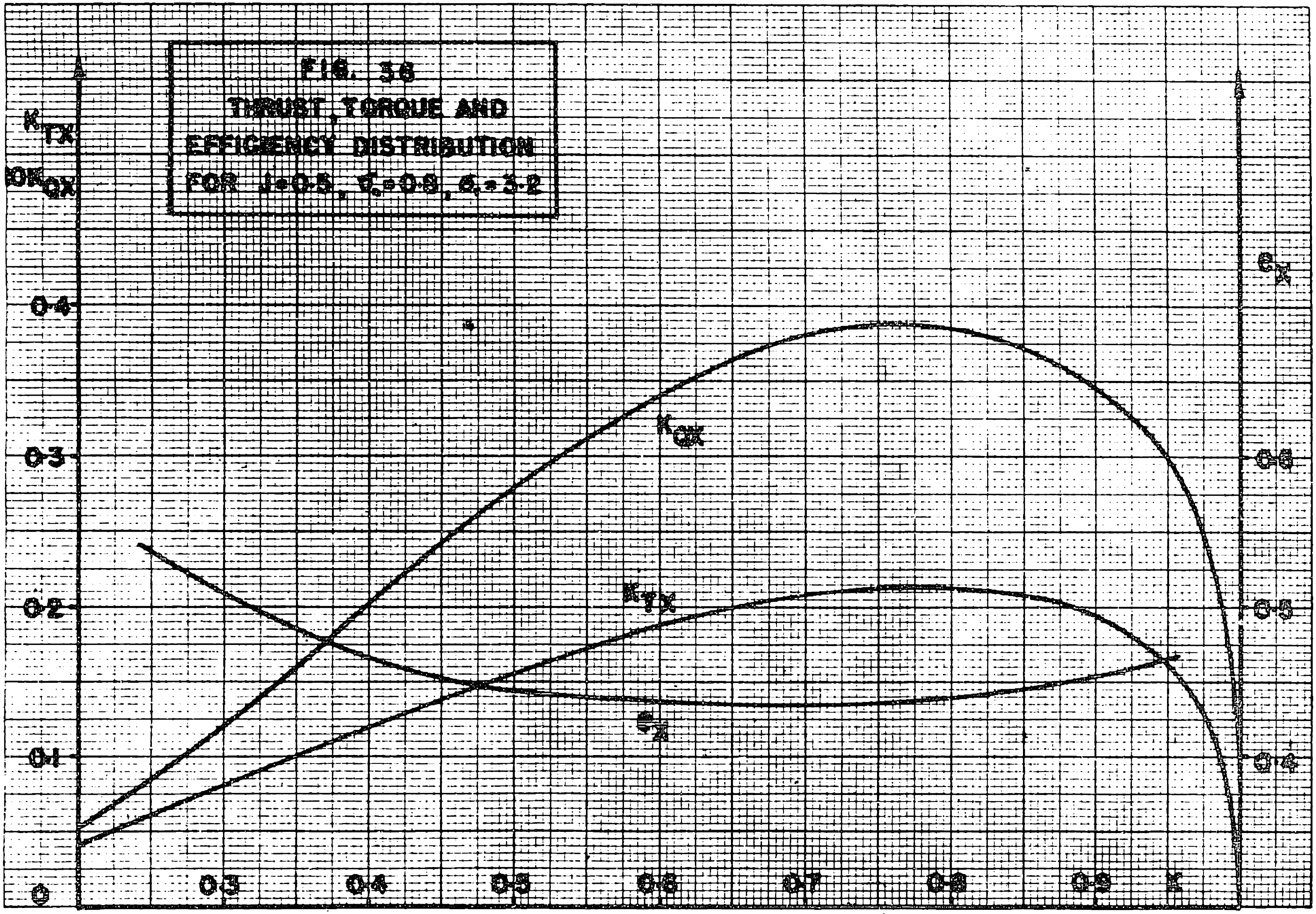

FIG. 36
THRUST, TORQUE AND
EFFICIENCY DISTRIBUTION
FOR $J = 0\cdot5$, $\sigma_o = 0\cdot9$, $\theta_o = 3\cdot2$

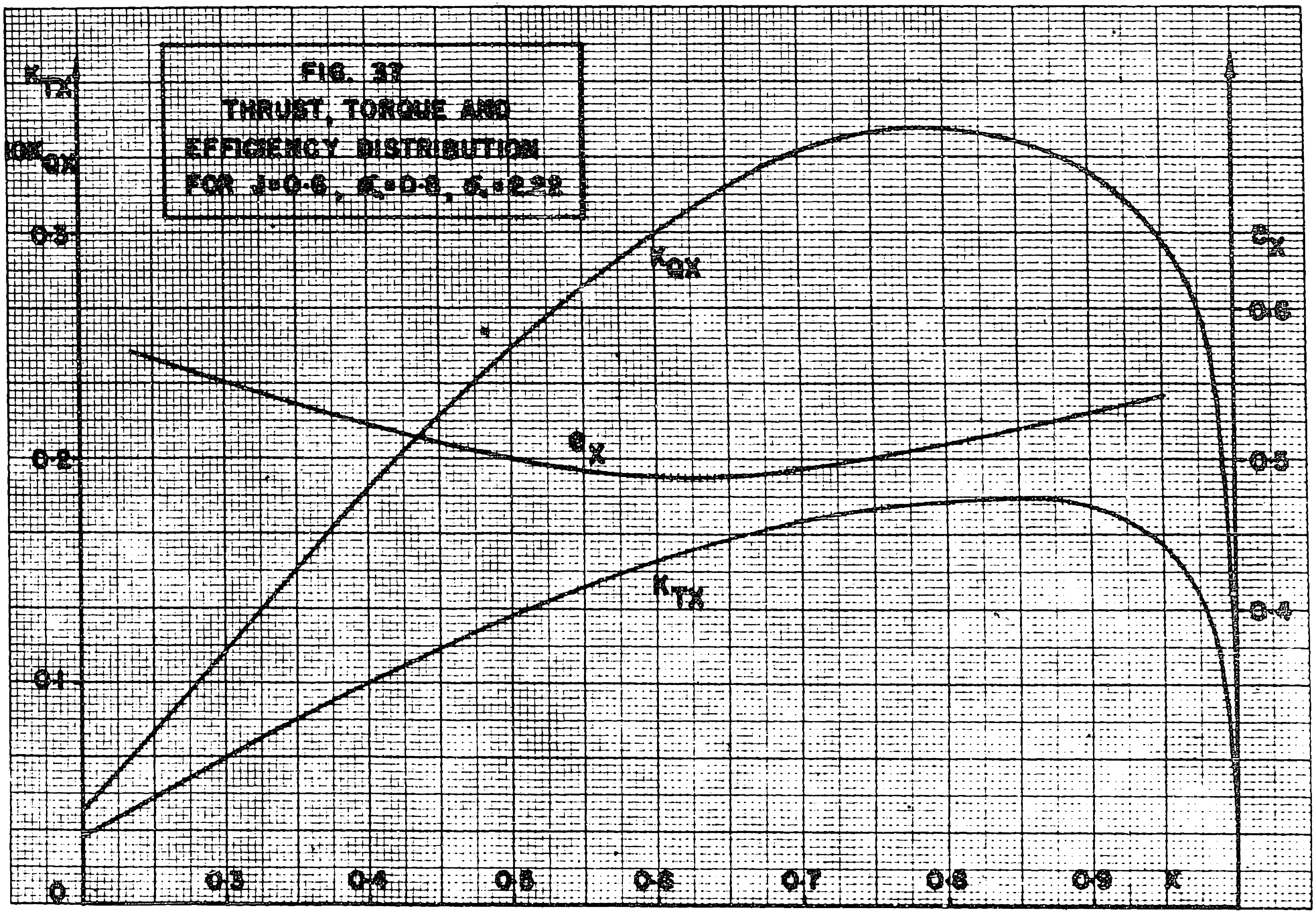

FIG. 37
THRUST, TORQUE AND
EFFICIENCY DISTRIBUTION
FOR J=0·6, σ_r=0·8, σ_t=2·22

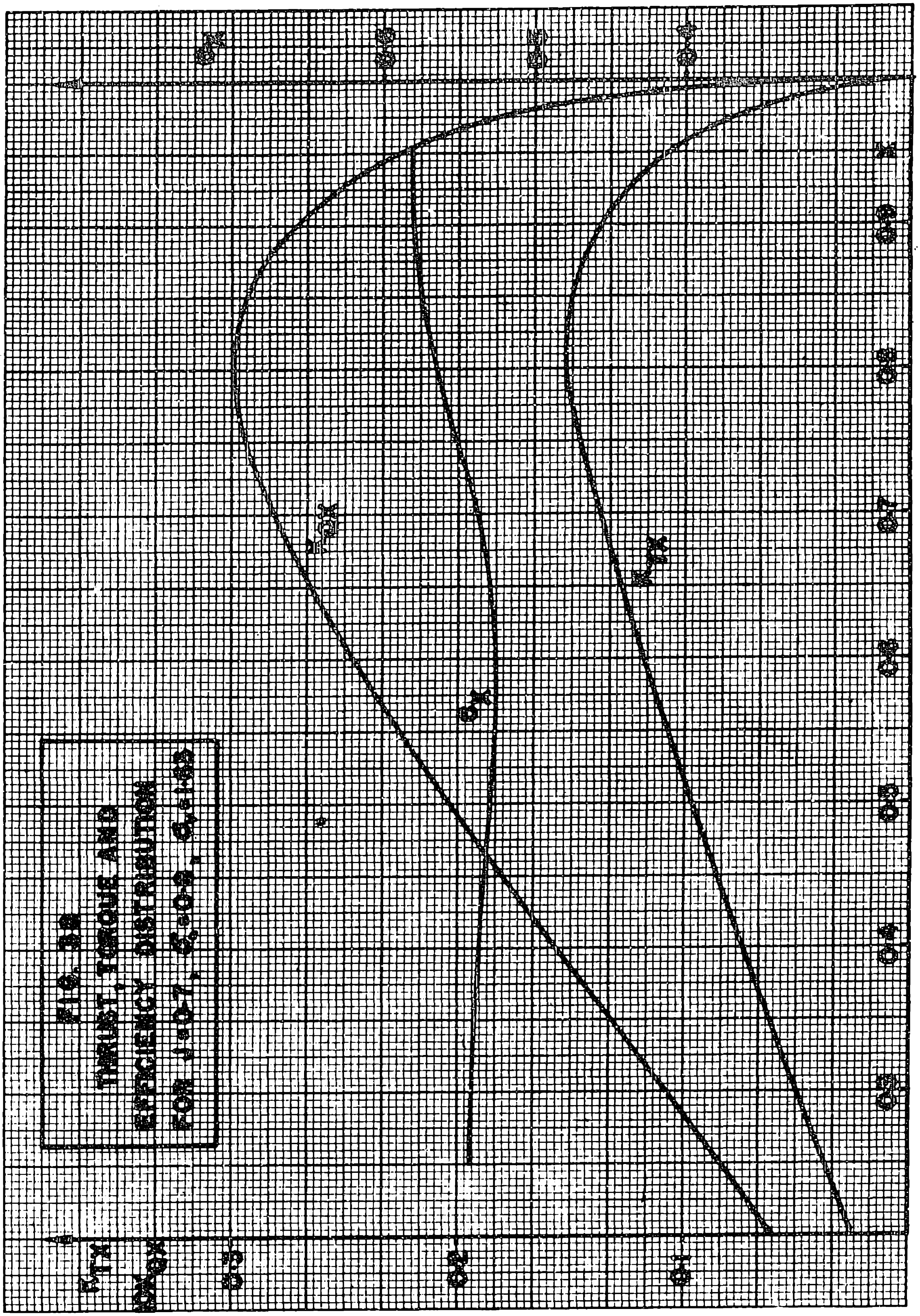
FIG.
THRUST, TORQUE AND
EFFICIENCY DISTRIBUTION
FOR J=0·7, C_L=0·9, C_D=1·63
K_{TX}
$10K_{QX}$
0·3
0·2
0·1
0·3
0·4
0·5
0·6
0·7
0·8
0·9
X
η_X
0·6
0·5
0·4
K_{QX}
η_X
K_{TX}

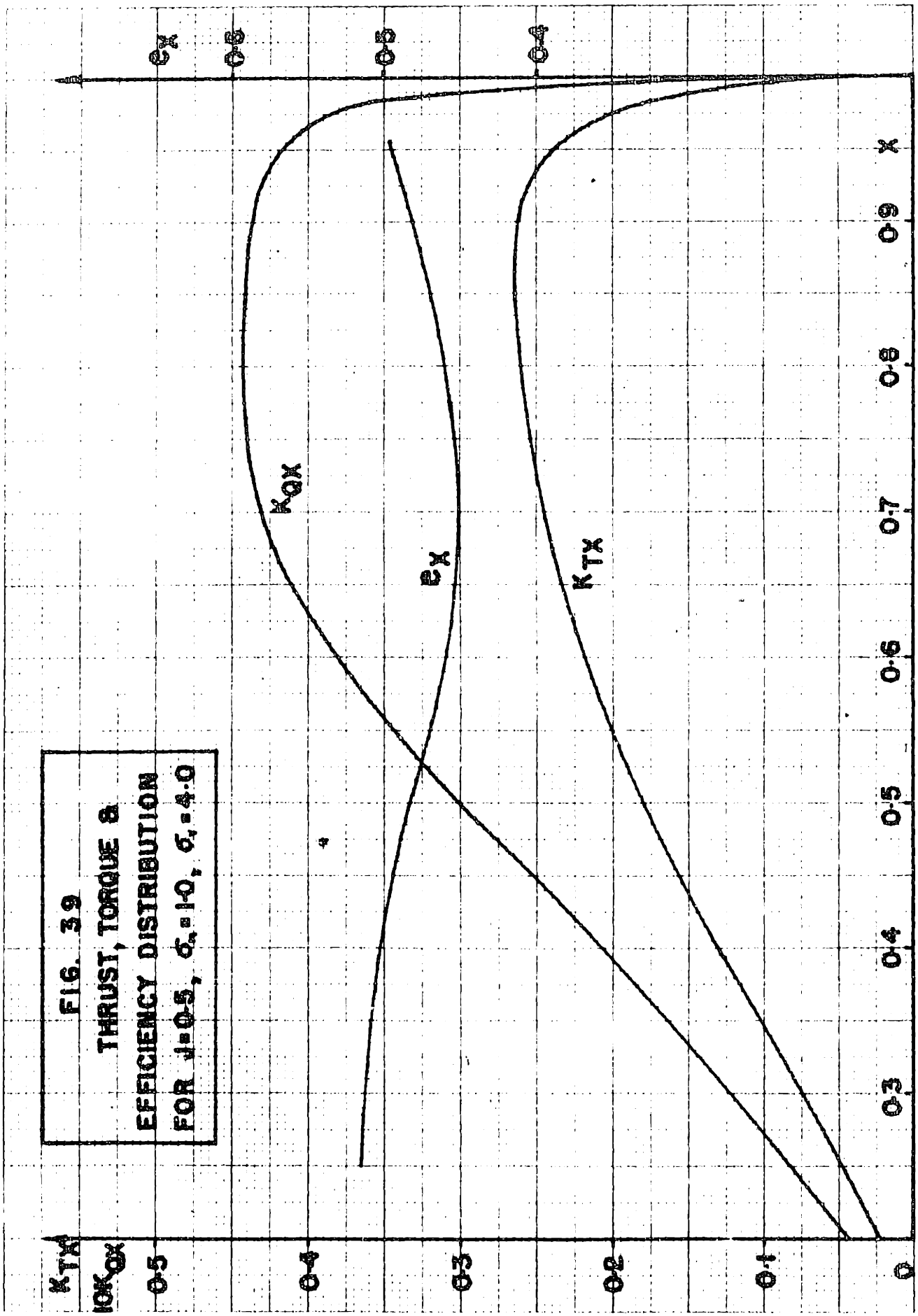

FIG. 39
THRUST, TORQUE & EFFICIENCY DISTRIBUTION FOR $J=0.5$, $\sigma_c=1.0$, $\sigma_t=4.0$

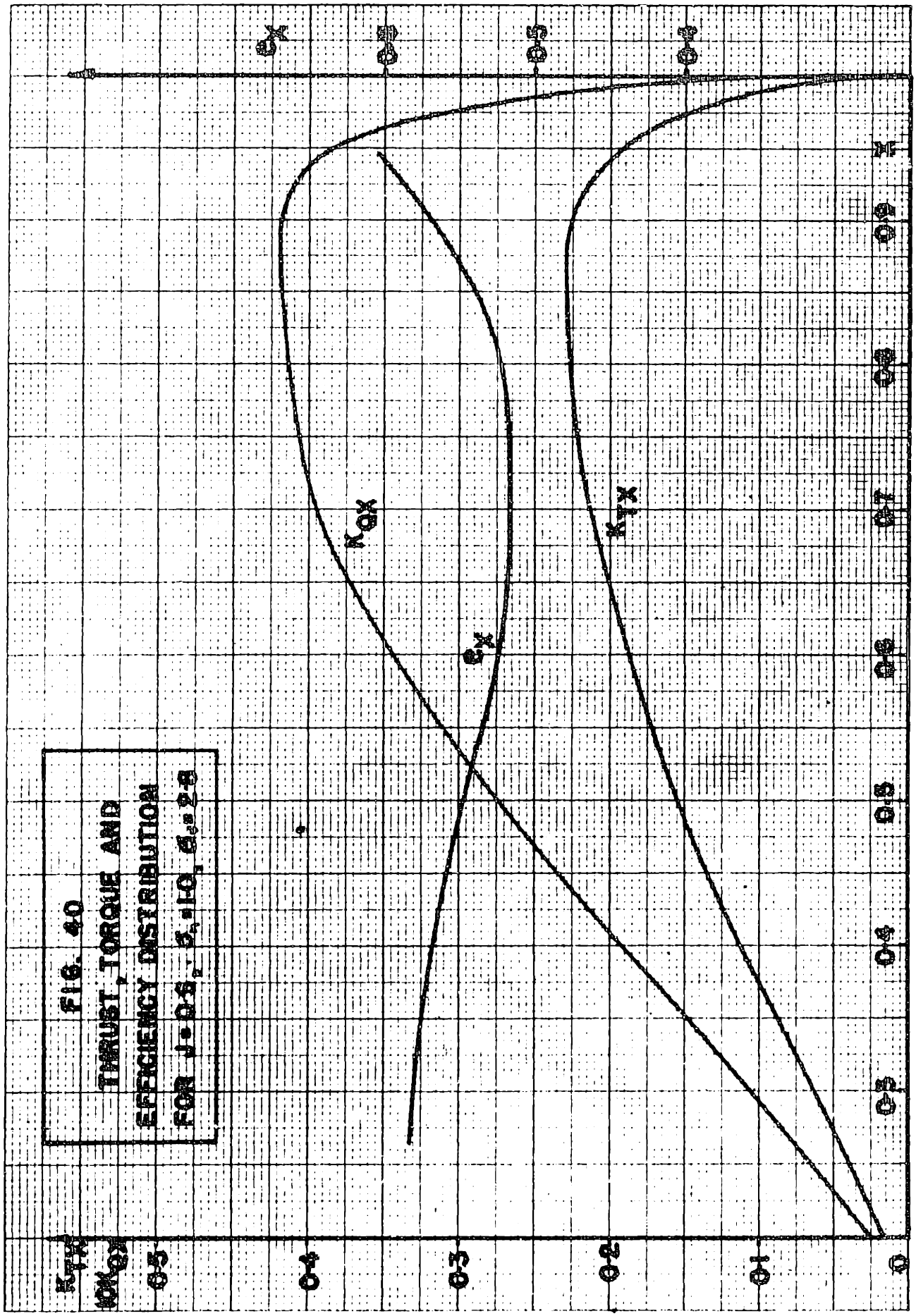
FIG. 40
THRUST, TORQUE AND
EFFICIENCY DISTRIBUTION
FOR J = 0.6 , Z = 4 , Ho/D = 2.0
K_{TX}
$10K_{QX}$
η_x
K_{QX}
K_{TX}
e_x
0
0.1
0.2
0.3
0.4
0.5
0.6
0.7
0.8
0.9
1.0
x

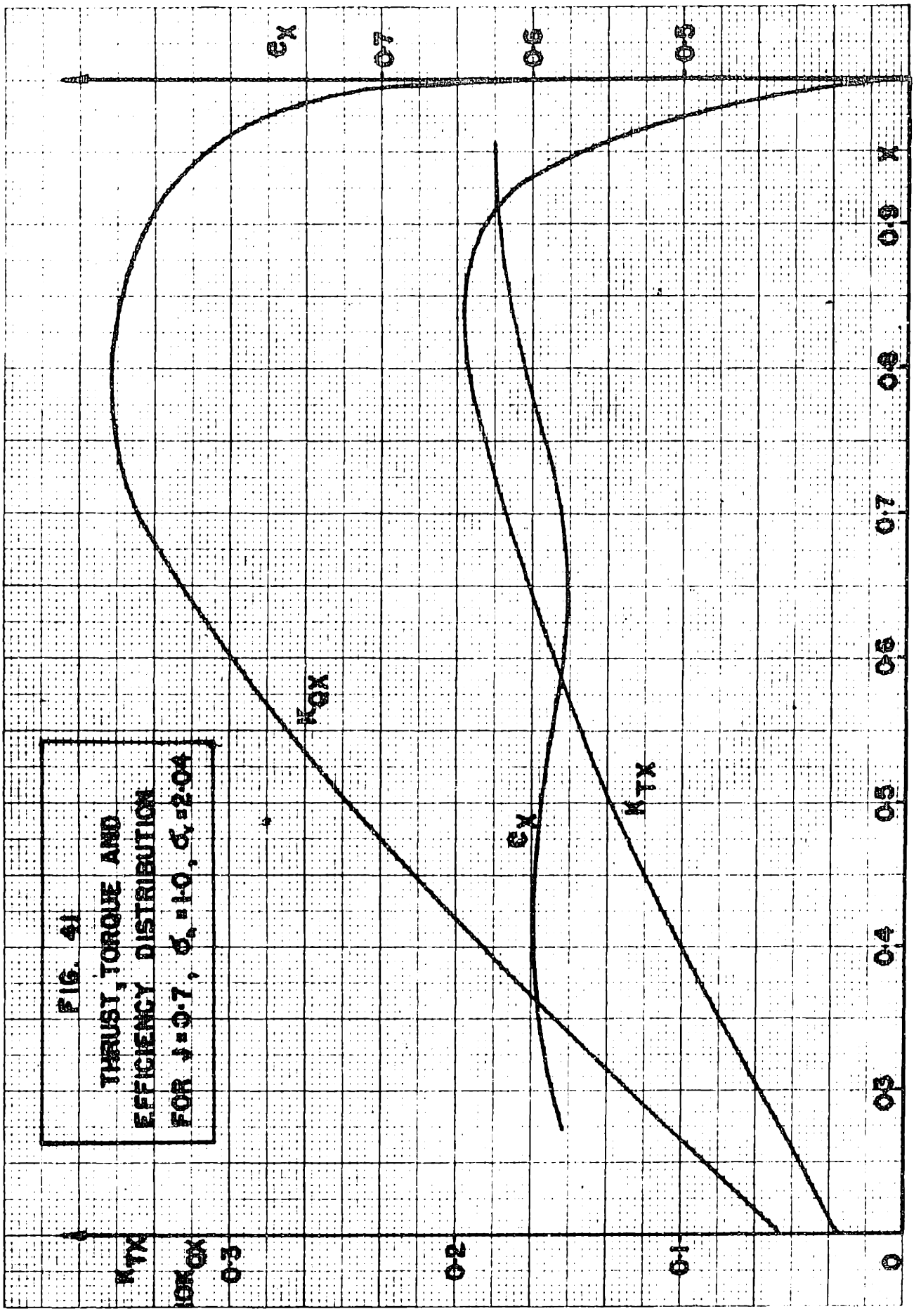

FIG. 41
THRUST, TORQUE AND EFFICIENCY DISTRIBUTION FOR $J=0.7$, $\phi_0=1.0$, $\phi_1=2.04$

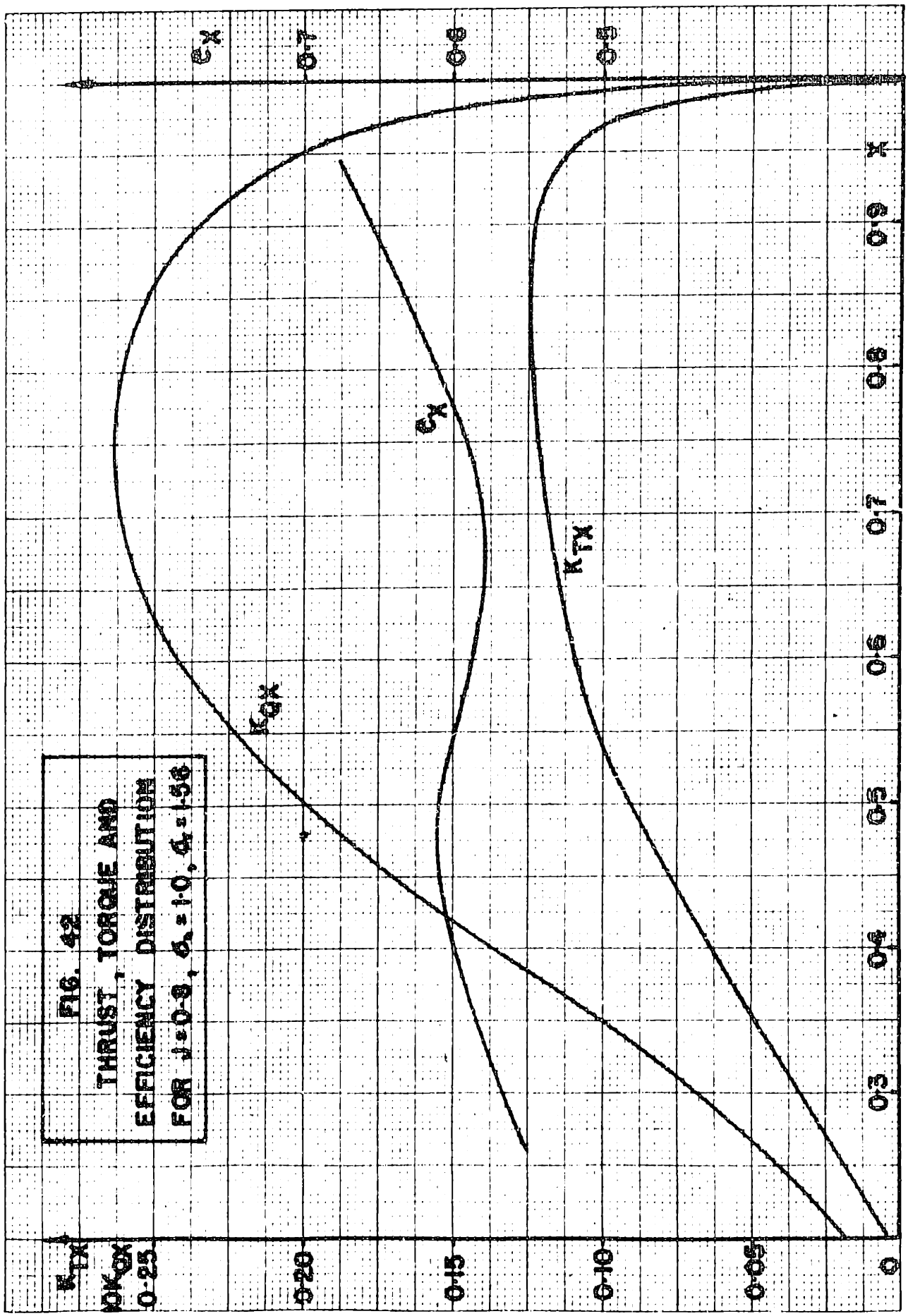

FIG. 42
THRUST, TORQUE AND EFFICIENCY DISTRIBUTION FOR $J = 0{\cdot}8,\ \phi_0 = 1{\cdot}0,\ \phi_1 = 1{\cdot}56$

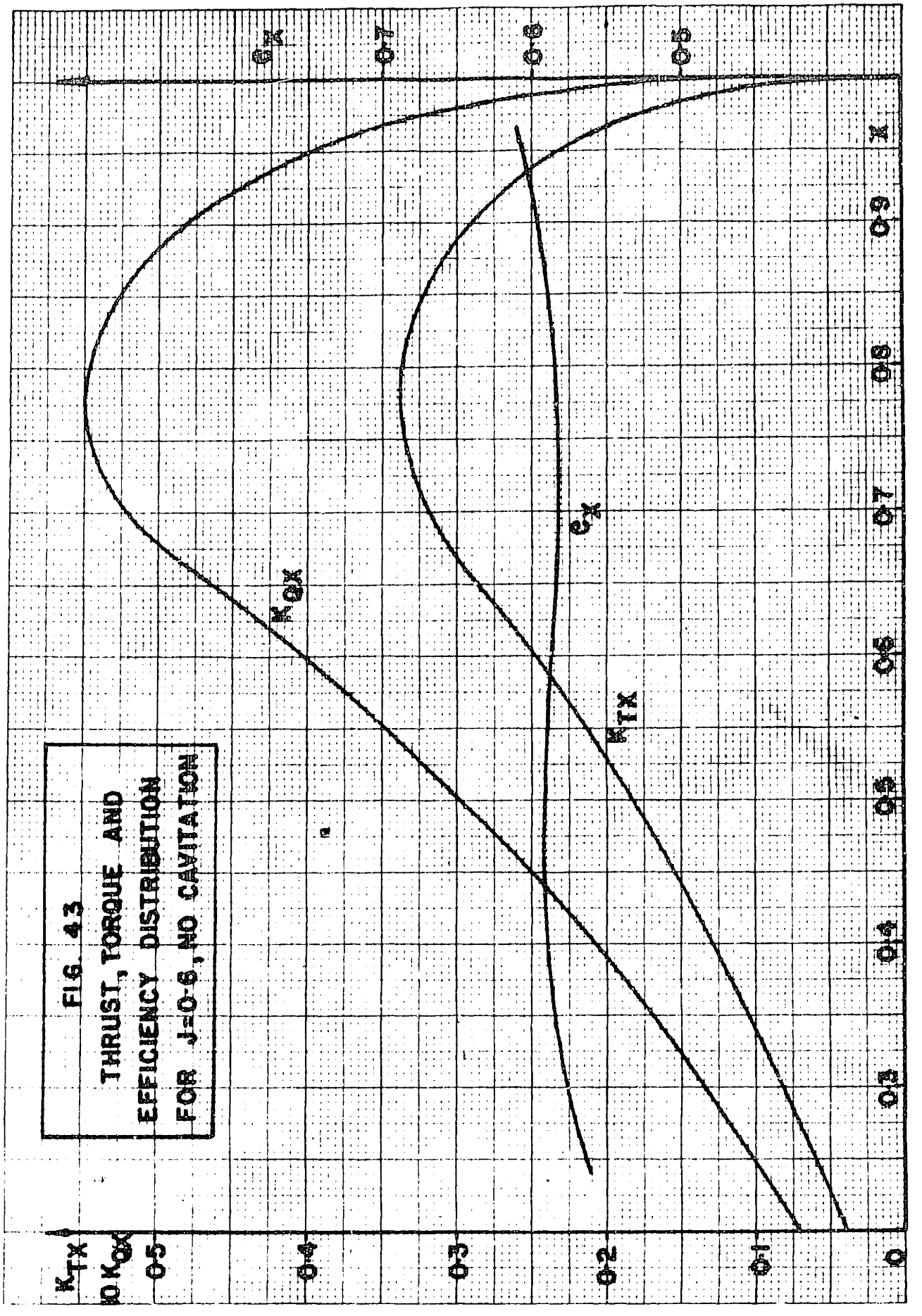
FIG. 43
THRUST, TORQUE AND
EFFICIENCY DISTRIBUTION
FOR J=0·6, NO CAVITATION
K_{TX}
10 K_{QX}
K_{QX}
e_X
K_{TX}
0·5
0·4
0·3
0·2
0·1
0
0·3
0·4
0·5
0·6
0·7
0·8
0·9
X
e_X
0·5
0·6
0·7

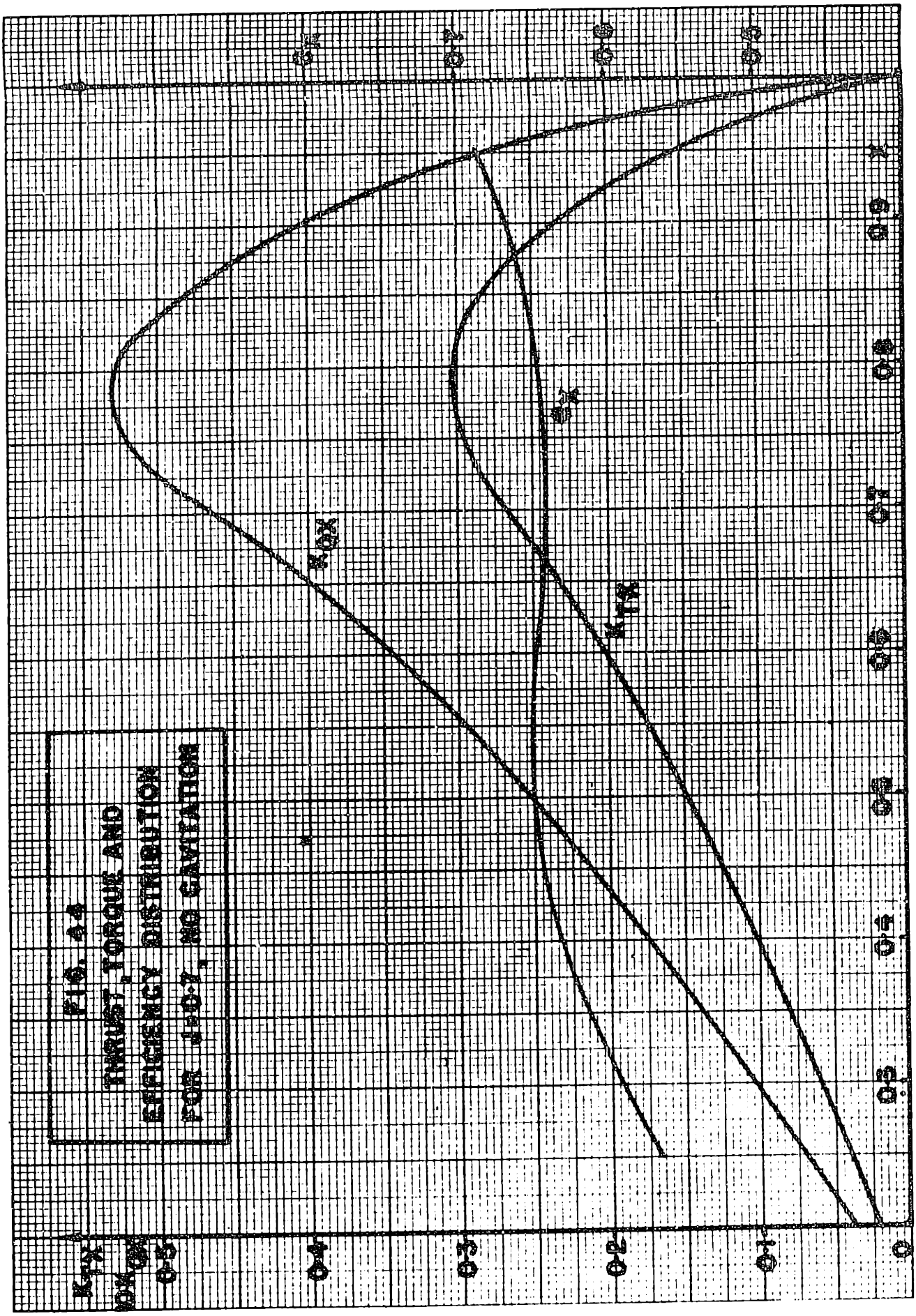
FIG. 6.4
THRUST, TORQUE AND
EFFICIENCY DISTRIBUTION
FOR J=0.7, NO CAVITATION
K_T, K_Q, η_0
K_T
K_Q
η_0
0
0.1
0.2
0.3
0.4
0.5
0.6
0.7
0.8
0.9
1.0
x

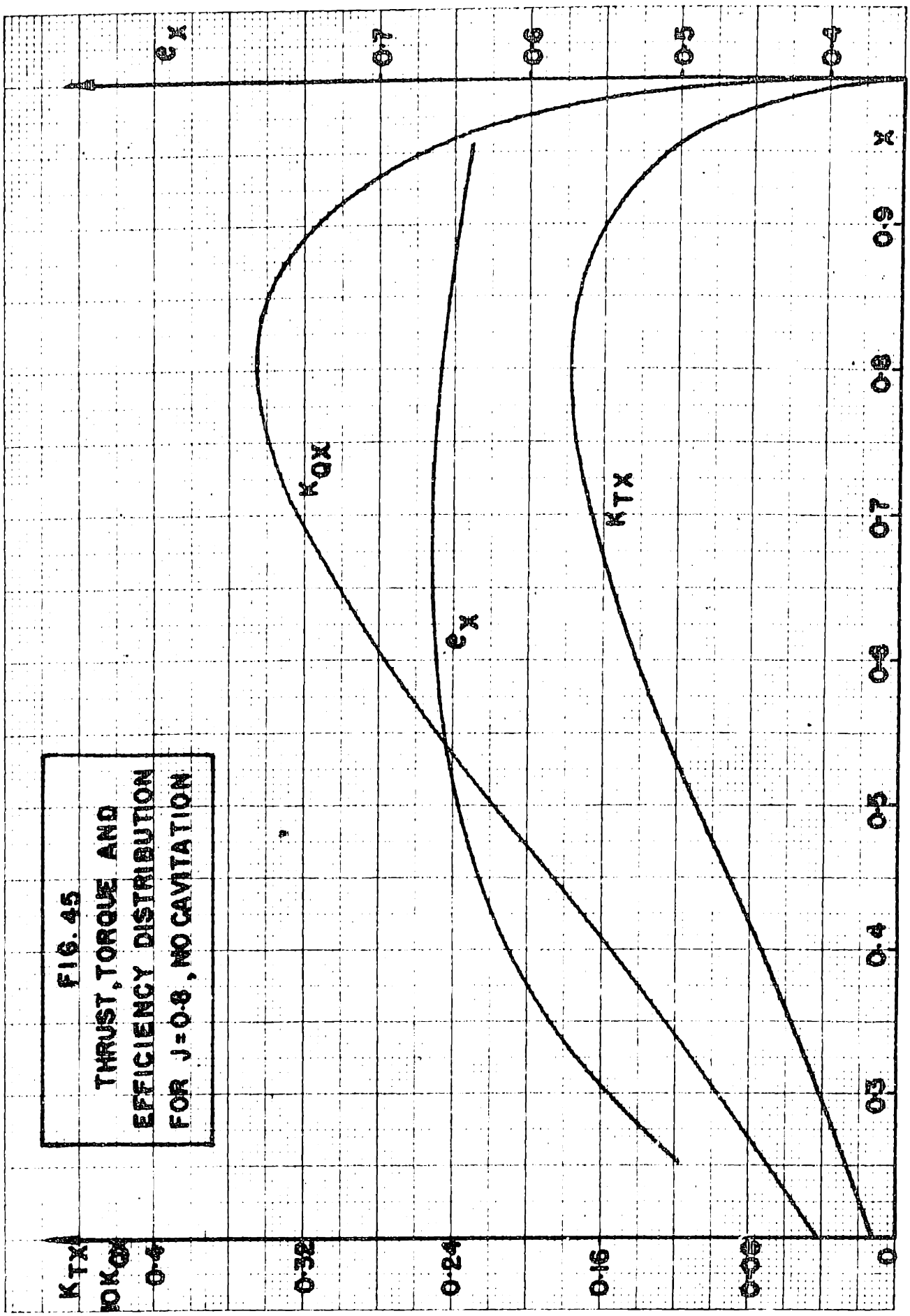

FIG. 45
THRUST, TORQUE AND EFFICIENCY DISTRIBUTION FOR J=0·8, NO CAVITATION

APPENDIX E.

CAVITATION PHOTOGRAPHS.

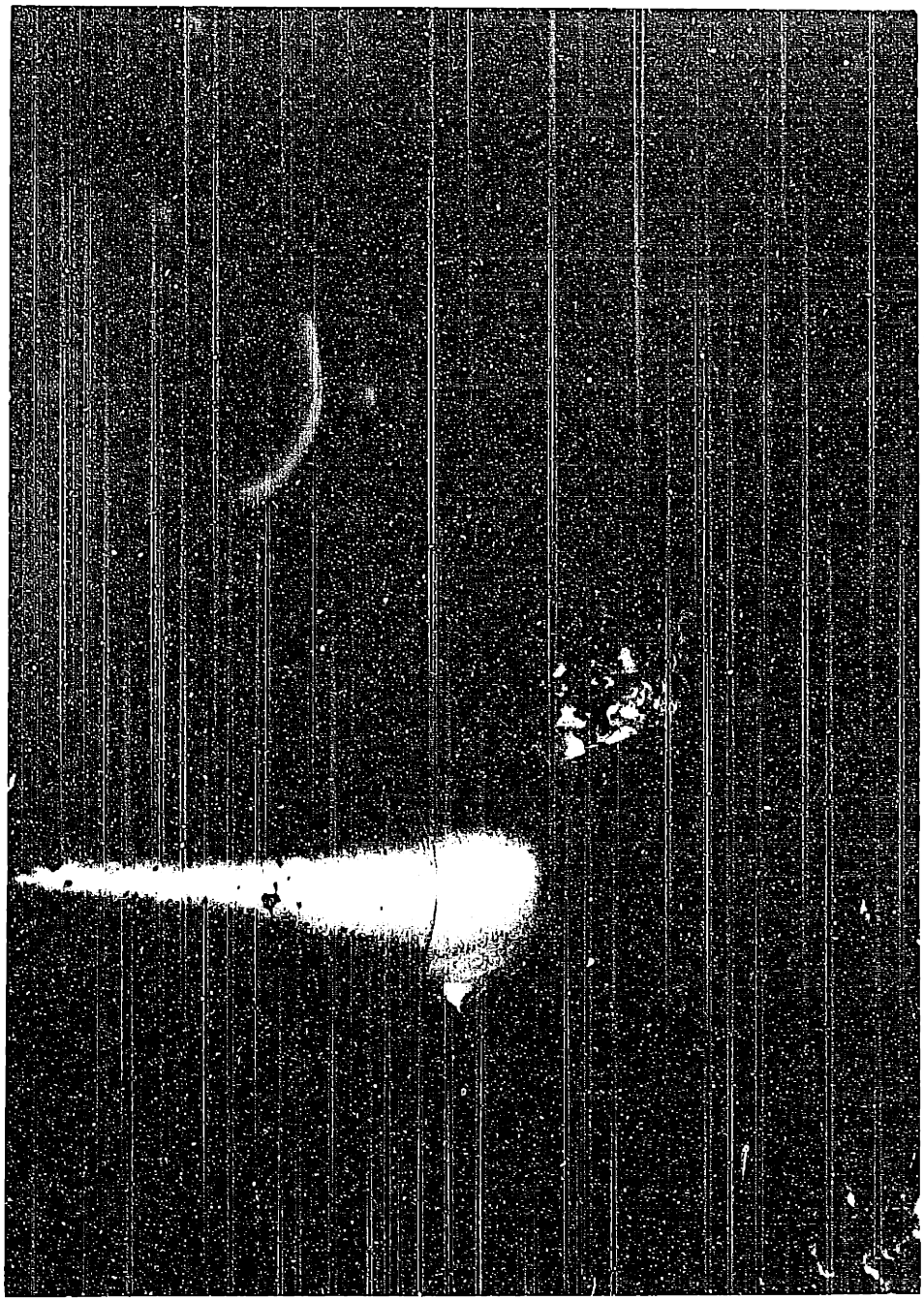

Phot. (1). - Cavitation at $\sigma_n = 0.8$, $J = 0.5$

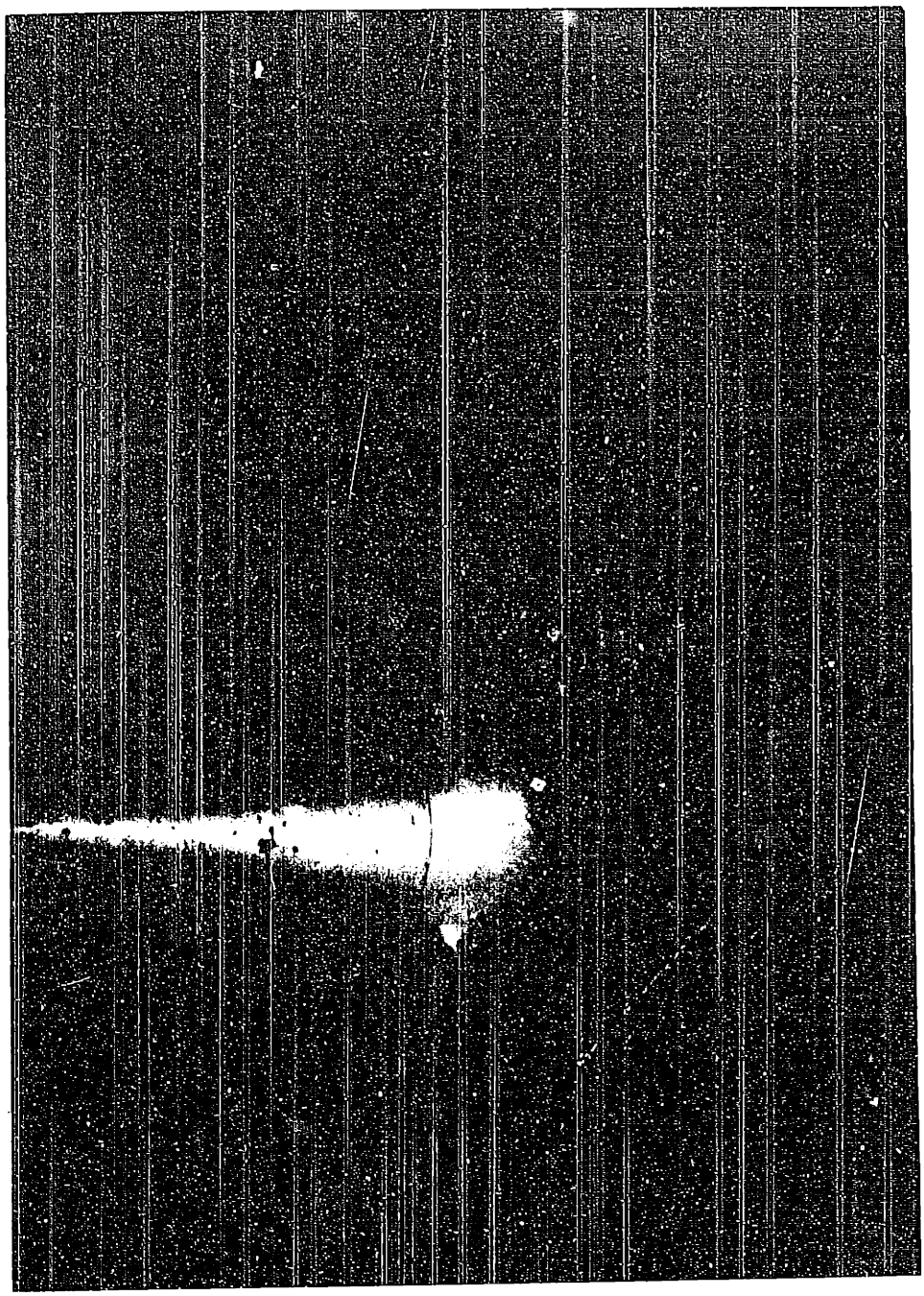

Phot. (2). - Cavitation at $\sigma_n = 0.8$, $J = 0.6$

EXPOSING FOR LIGHT POINT

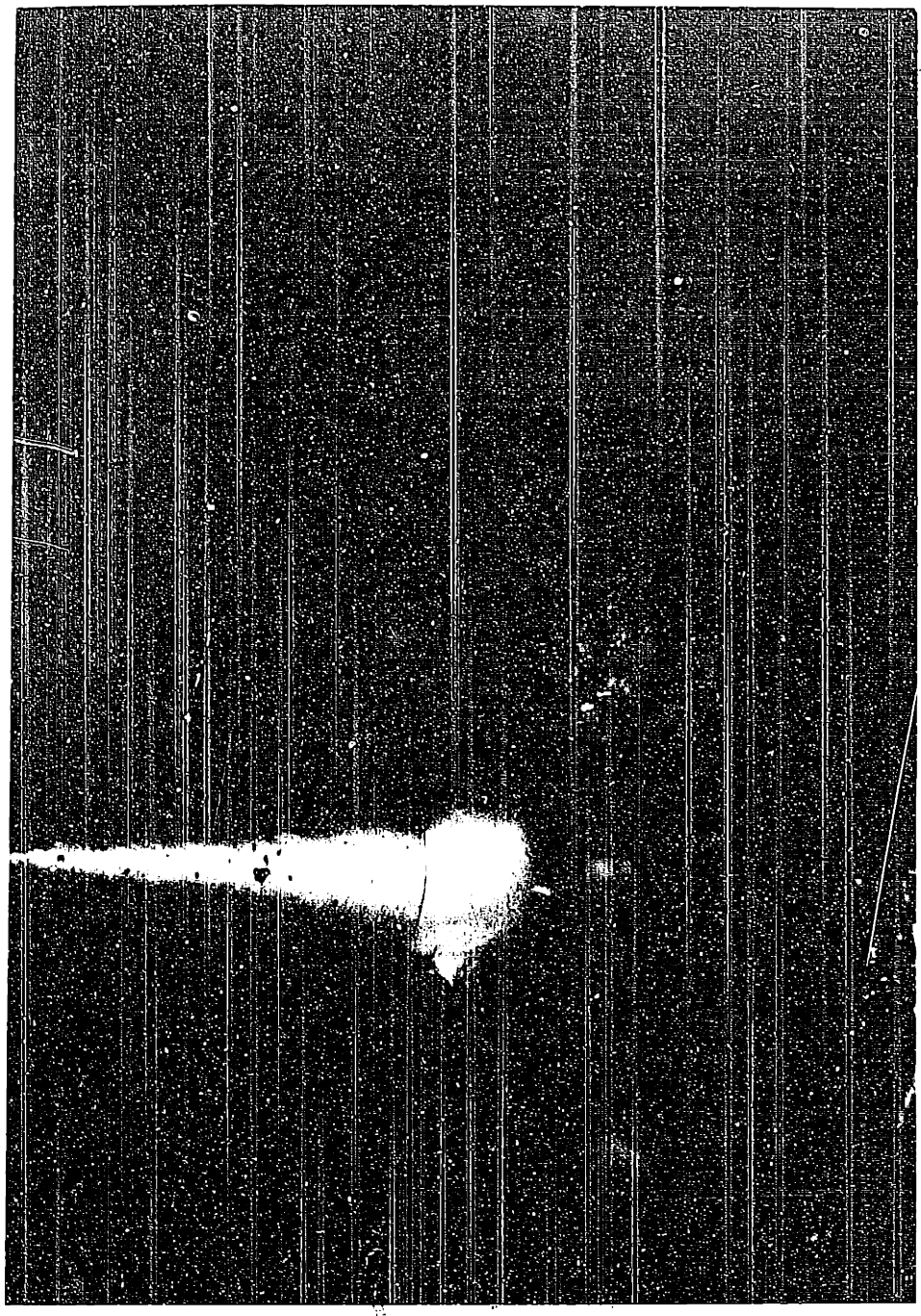

Phot. (3). - Cavitation at $\sigma_n = 0.8$, $J = 0.7$

EXPOSING FOR LIGHT PRINT

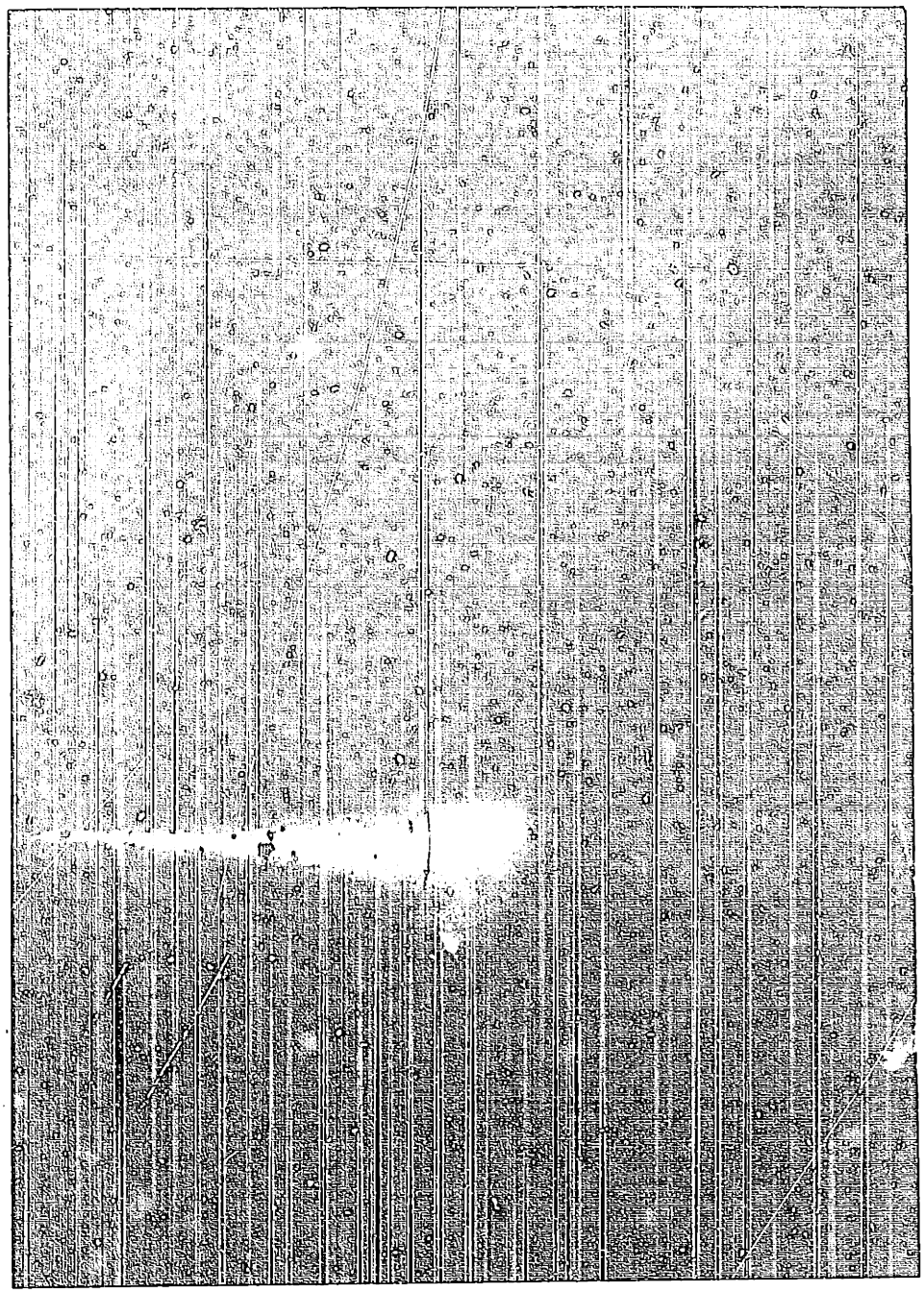

Phot. (4). - Cavitation at $\sigma_n = 0.8$, $J = 0.8$

EXPOSING FOR LIGHT

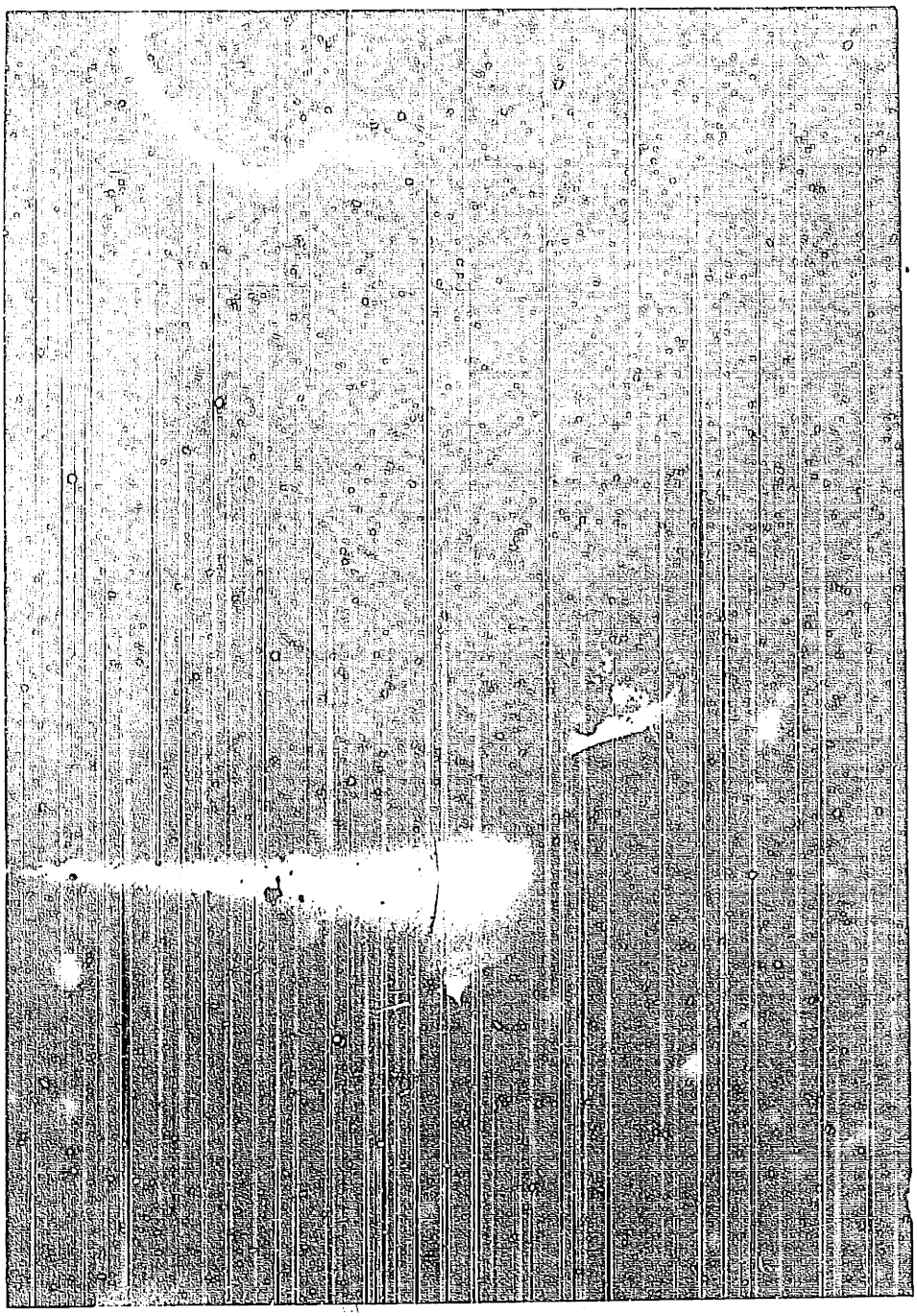

Phot. (5). - Cavitation at σ_n = 1.0, J = 0.5

EXPOSING FOR LIGHT POINT

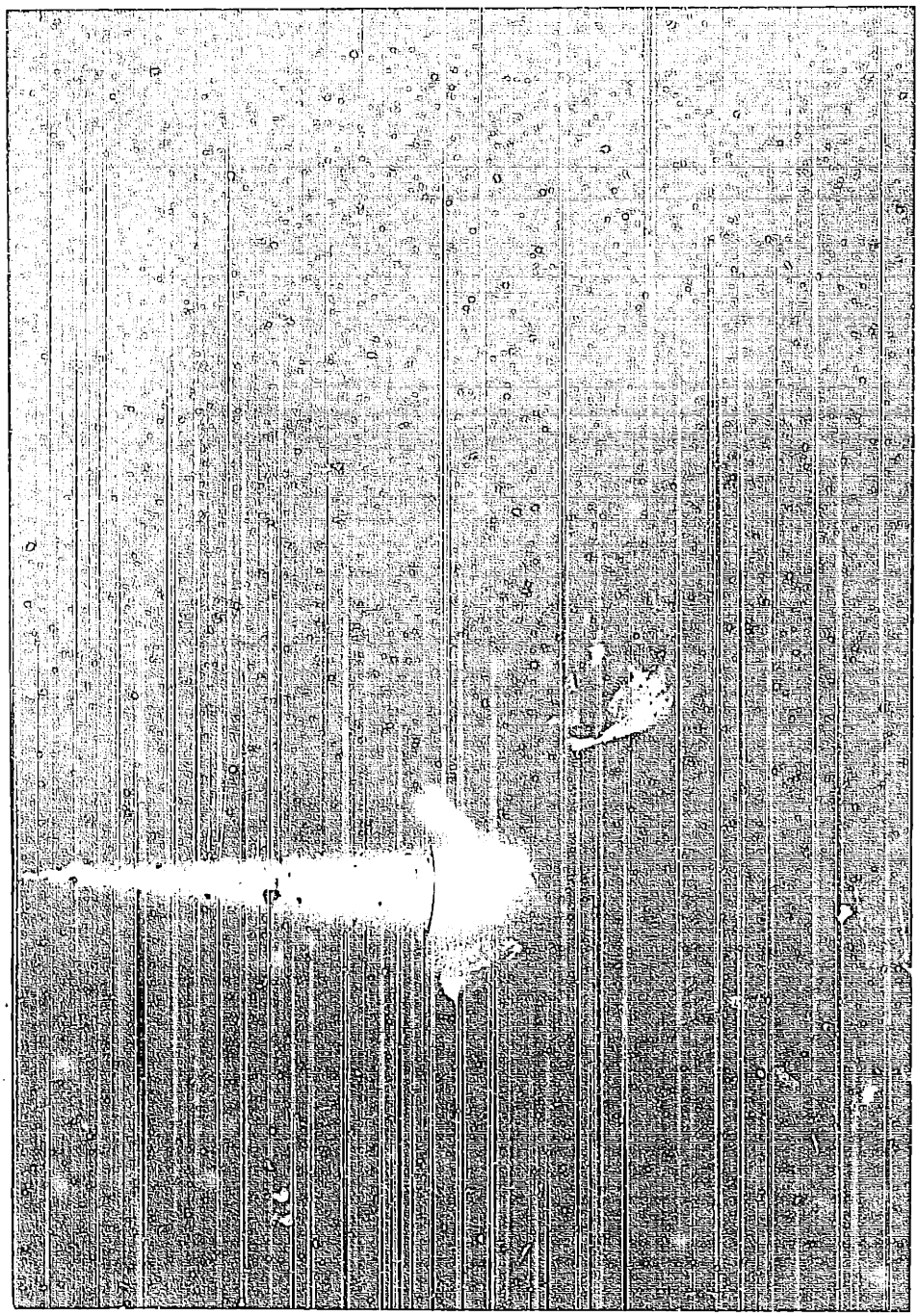

Phot. (6). - Cavitation at $\sigma_n = 1.0$, J = 0.6

EXPOSING FOR LIGHT POINT

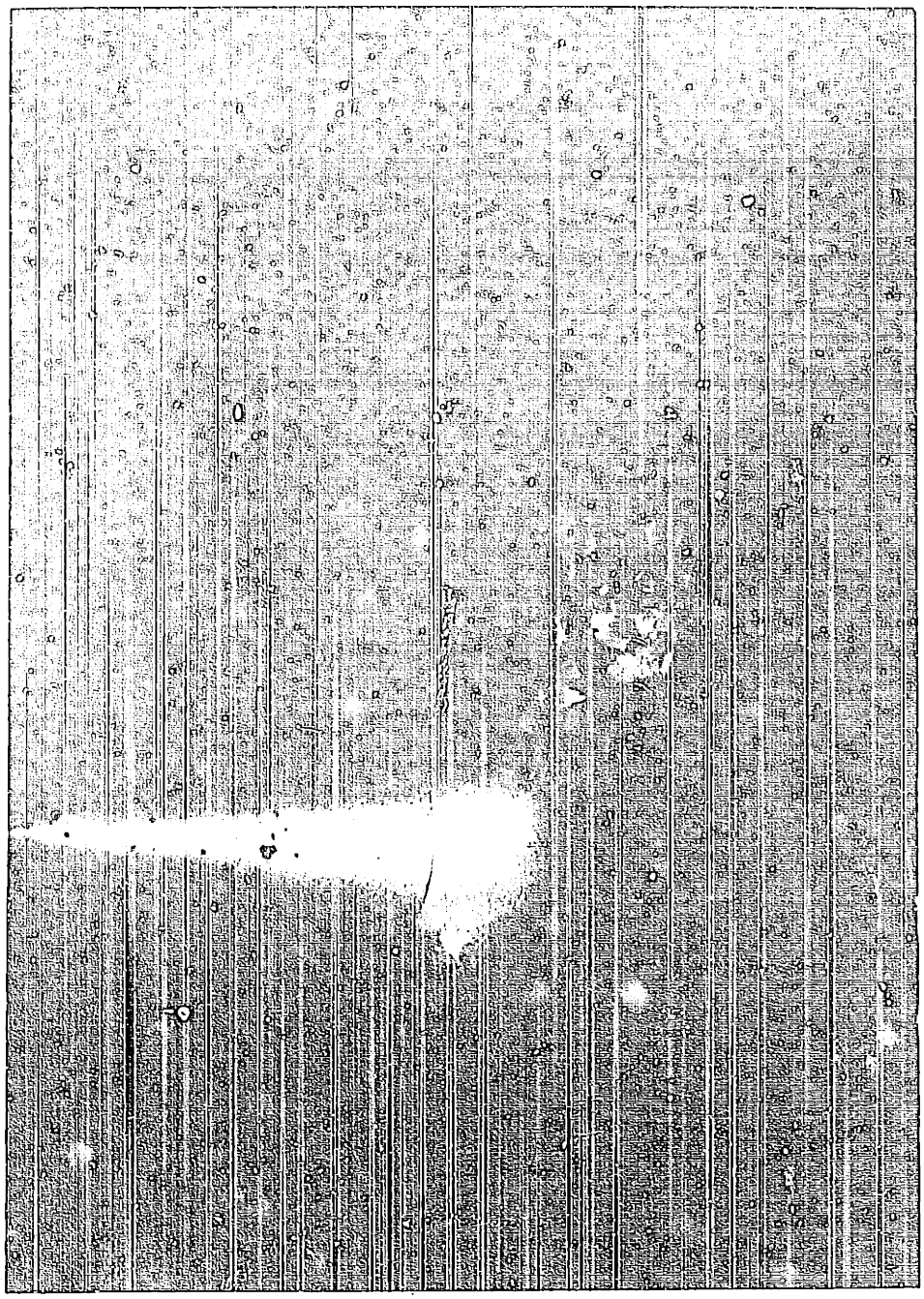

Phot. (7). - Cavitation at $\sigma_n = 1.0$, $J = 0.7$

EXPOSING FOR LIGHT POINT

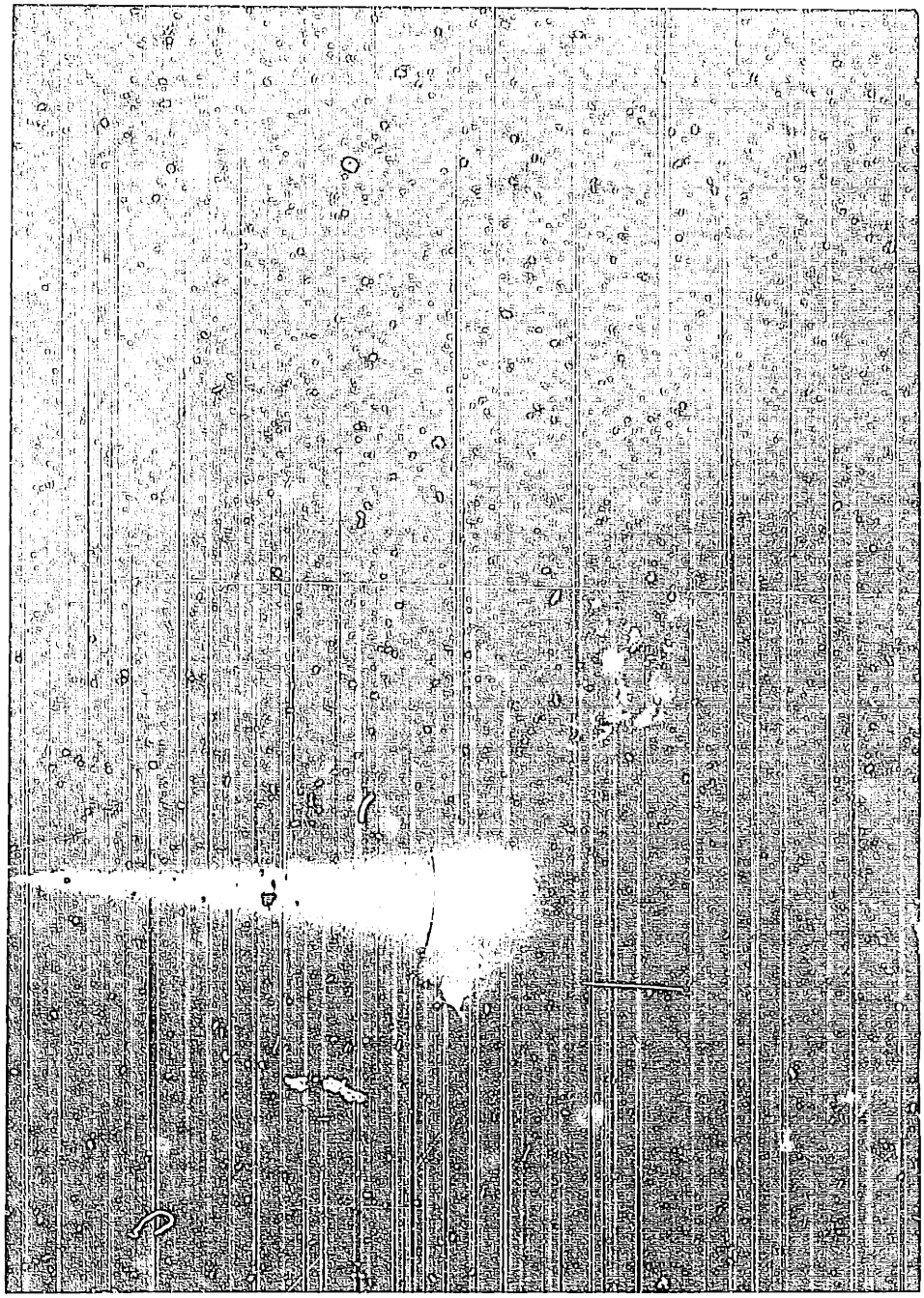

Phot. (8). - Cavitation at $\sigma_n = 1.0$, $J = 0.8$

EXPOSING FOR LIGHT

APPENDIX F.

TABLE OF RESULTS.

TABLE I.

Comparison between expressions for cavitation index.

$$\sigma_x = \frac{\sigma_v}{1 + \frac{(\pi . x)^2}{J^2}} \qquad \ldots\ldots \text{(i)}$$

$$\sigma_x = \frac{\sigma_v}{(1 - a')^2 \left\{ \frac{\tan^2 \phi}{\tan^2 \psi} + \frac{(\ .x)^2}{J^2} \right\}} \qquad \ldots\ldots \text{(ii)}$$

For $\sigma_n = 0.8$

(1) $J = 0.5$ $\sigma_v = 3.2$

x	0.3	0.5	0.6	0.7	0.8	0.9
equat. (i)	0.700	0.295	0.210	0.157	0.121	0.0970
equat. (ii)	0.785	0.315	0.221	0.163	0.126	0.0971

(2) $J = 0.6$ $\sigma_v = 2.22$

x	0.3	0.5	0.6	0.7	0.8	0.9
equat. (i)	0.641	0.282	0.204	0.154	0.120	0.0957
equat. (ii)	0.685	0.299	0.213	0.159	0.122	0.0971

(3) $J = 0.7$ $\sigma_v = 1.63$

x	0.3	0.5	0.6	0.7	0.8	0.9
equat. (i)	0.580	0.269	0.199	0.150	0.117	0.0945
equat. (ii)	0.615	0.281	0.206	0.158	0.119	0.0957

For $\sigma_n = 1.0$

(1) $J = 0.5$ $\sigma_v = 4.0$

x	0.4	0.5	0.6	0.7	0.8	0.9
equat.(i)	0.534	0.273	0.262	0.196	0.151	0.121
equat.(ii)	0.577	0.303	0.296	0.214	0.156	0.126

(2) $J = 0.6$ $\sigma_v = 2.78$

x	0.3	0.5	0.6	0.7	0.8	0.9
equat.(i)	0.801	0.353	0.256	0.193	0.150	0.119
equat.(ii)	0.870	0.374	0.270	0.198	0.151	0.123

(3) $J = 0.7$ $\sigma_v = 2.04$

x	0.3	0.5	0.6	0.7	0.8	0.9
equat.(i)	0.736	0.335	0.247	0.188	0.147	0.118
equat.(ii)	0.773	0.372	0.254	0.197	0.149	0.120

(4) $J = 0.8$ $\sigma_v = 1.56$

x	0.4	0.5	0.6	0.7	0.8	0.9
equat.(i)	0.449	0.322	0.238	0.181	0.144	0.115
equat.(ii)	0.516	0.343	0.252	0.184	0.145	0.116

TABLE II.

Comparison between expressions for hydrodynamic pitch angle in slipstream.

$$\epsilon = \phi + \beta \qquad \ldots\ldots\ldots\ldots \text{(i)}$$

$$\epsilon = \tan^{-1}\left\{ \frac{1}{(1 - 2a')} \left[2(1 - a').\tan\phi - \tan\psi \right] \right\} \ldots \text{(ii)}$$

For $\sigma_n = 0.8$

(1) $J = 0.5$ $\sigma_v = 3.2$

x	0.3	0.5	0.6	0.7	0.8	0.9
equat. (i)	56.60	36.68	30.21	25.15	21.88	19.67
equat. (ii)	57.15	37.10	30.55	25.70	22.20	19.15

(2) $J = 0.6$ $\sigma_v = 2.22$

x	0.3	0.5	0.6	0.7	0.8	0.9
equat. (i)	55.20	35.90	29.24	25.26	21.78	21.02
equat. (ii)	55.55	36.10	29.42	25.40	22.30	19.62

(3) $J = 0.7$ $\sigma_v = 1.63$

x	0.3	0.5	0.6	0.7	0.8	0.9
equat. (i)	53.85	35.20	29.08	24.99	22.15	20.08
equat. (ii)	54.00	35.55	29.15	25.40	22.70	20.00

For $\sigma_n = 1.0$

(1) $J = 0.5$ $\sigma_v = 4.0$

x	0.4	0.5	0.6	0.7	0.8	0.9
equat. (i)	46.73	38.48	31.61	26.65	22.18	19.87
equat. (ii)	47.10	38.95	31.85	26.90	22.28	19.97

(2) $J = 0.6$ $\sigma_v = 2.78$

x	0.3	0.5	0.6	0.7	0.8	0.9
equat. (i)	56.00	38.00	31.54	26.36	22.58	20.52
equat. (ii)	56.40	38.15	31.60	26.51	22.70	20.60

(3) $J = 0.7$ $\sigma_v = 2.04$

x	0.3	0.5	0.6	0.7	0.8	0.9
equat. (i)	54.75	37.30	30.68	26.19	22.95	20.72
equat. (ii)	54.85	37.55	30.95	26.32	23.10	20.78

(4) $J = 0.8$ $\sigma_v = 1.56$

x	0.4	0.5	0.6	0.7	0.8	0.9
equat. (i)	43.20	36.60	30.46	25.64	22.29	19.88
equat. (ii)	44.20	36.70	30.58	25.85	22.31	19.81

TABLE III.

Results of calculations.

$J = 0.5$ $\quad \sigma_n = 0.8$ $\quad \sigma_v = 3.2$

x	0.3	0.5	0.6	0.7	0.8	0.9
s	1.125	0.776	0.645	0.526	0.409	0.280
s_e	1.125	0.776	0.696	0.626	0.541	0.452
σ_x	0.700	0.295	0.210	0.157	0.121	0.097
α_o°	-7.60	-3.60	-2.30	-1.35	-0.85	-0.55
θ°	43.65	29.80	25.53	22.32	19.70	17.65
ψ°	28.00	17.62	14.85	12.79	11.22	10.03
α°	1.35	2.70	3.00	3.20	3.05	2.80
ϕ°	42.30	27.10	22.53	19.12	16.65	14.85
ϵ°	56.60	36.68	30.21	25.45	21.88	19.67
C_L	0.380	0.246	0.197	0.165	0.145	0.136
C_D	0.0250	0.0359	0.0300	0.0244	0.0198	0.0155
γ	3.84	8.75	8.85	8.57	7.90	6.55
a'	0.203	0.101	0.070	0.052	0.040	0.030
K_{Tx}	0.073	0.154	0.187	0.208	0.212	0.199
K_{Qx}	0.0115	0.0278	0.0341	0.0380	0.0387	0.3510
e_x	0.505	0.440	0.436	0.436	0.437	0.451

Integrated Values	K_T	K_Q	e
Calculated	0.122	0.0218	0.445
Experimental	0.125	0.0232	0.430
Difference	-2.4%	-6.0%	+1.5%

TABLE IV.

Results of calculations.

$J = 0.5$ $\quad \sigma_n = 0.8$ $\quad \sigma_v = 2.22$

x	0.3	0.5	0.6	0.7	0.8	0.9
s	1.125	0.776	0.645	0.526	0.409	0.280
s_e	1.125	0.776	0.690	0.621	0.535	0.434
σ_x	0.641	0.282	0.204	0.154	0.120	0.095
α_o^0	-7.50	-3.50	-2.40	-1.30	-0.80	-0.60
θ^0	43.65	29.80	25.53	22.32	19.70	17.65
ψ^0	32.40	20.90	17.62	15.28	13.82	11.98
α^0	-0.15	1.40	2.10	2.05	1.90	1.65
ϕ^0	43.80	28.40	23.43	20.27	17.80	16.00
ϵ^0	55.20	35.90	29.24	25.26	21.78	21.02
C_L	0.309	0.200	0.158	0.138	0.123	0.120
C_D	0.0270	0.0314	0.0275	0.0206	0.0149	0.0122
γ	5.10	9.10	10.09	8.64	7.19	5.80
a'	0.173	0.085	0.059	0.044	0.033	0.027
K_{Tx}	0.065	0.130	0.149	0.177	0.180	0.181
K_{Qx}	0.0113	0.0249	0.0297	0.0342	0.0346	0.0376
e_x	0.555	0.499	0.481	0.495	0.512	0.530

Integrated Values	K_T	K_Q	η
Calculated	0.1034	0.0199	0.497
Experimental	0.100	0.0202	0.473
Difference	+3.4%	-1.5%	+2.4%

TABLE V.

Results of calculations.

$J = 0.7$ $\quad \sigma_n = 0.8$ $\quad \sigma_V = 1.63$

x	0.3	0.5	0.6	0.7	0.8	0.9
s	1.125	0.776	0.645	0.526	0.409	0.280
s_e	1.125	0.776	0.680	0.610	0.524	0.416
σ_x	0.580	0.269	0.199	0.150	0.117	0.094
α_o^0	-7.20	-3.20	-2.30	-1.05	-0.80	-0.65
θ^0	43.65	29.80	25.53	22.32	19.70	17.65
ψ^0	36.65	24.00	20.38	17.65	15.55	13.92
α^0	-1.60	0.20	0.80	1.00	0.98	1.10
ϕ^0	45.25	29.60	24.73	21.32	18.72	16.55
ϵ^0	53.85	35.20	29.08	24.99	21.89	18.98
C_L	0.233	0.156	0.117	0.102	0.098	0.091
C_D	0.0346	0.0276	0.0230	0.0169	0.0132	0.0115
γ	8.61	10.35	11.20	9.43	7.42	7.23
a'	0.146	0.070	0.048	0.035	0.021	0.019
K_{Tx}	0.051	0.104	0.114	0.133	0.155	0.137
K_{Qx}	0.0105	0.0218	0.0248	0.0277	0.0322	0.0271
e_x	0.541	0.533	0.513	0.535	0.570	0.574

Integrated Values	K_T	K_Q	e
Calculated	0.0801	0.0164	0.545
Experimental	0.065	0.0162	0.447
Difference	+23.1%	+1.2%	+9.8%

TABLE VI.

Results of calculations.

$J = 0.5$ $\quad \sigma_n = 1.0$ $\quad \sigma_v = 4.0$

x	0.4	0.5	0.6	0.7	0.8	0.9
s	0.918	0.776	0.645	0.526	0.409	0.280
s_e	0.918	0.776	0.687	0.605	0.524	0.424
σ_x	0.534	0.369	0.262	0.196	0.151	0.121
α_o^0	-6.00	-4.02	-2.80	-1.70	-1.25	-0.80
θ^0	35.65	29.80	25.53	22.32	19.70	17.65
ψ^0	21.41	17.62	14.85	12.79	11.22	10.03
α^0	1.58	1.75	2.40	2.60	3.00	2.70
ϕ^0	34.07	28.05	23.13	19.72	16.70	14.95
ϵ^0	46.73	38.48	31.61	26.65	22.18	19.87
C_L	0.335	0.279	0.230	0.196	0.164	0.172
C_D	0.0237	0.0288	0.0284	0.0237	0.0188	0.0158
γ^0	4.12	5.46	7.17	7.02	6.57	5.31
a'	0.146	0.105	0.076	0.056	0.039	0.030
K_{Tx}	0.129	0.180	0.217	0.247	0.246	0.260
K_{Qx}	0.0202	0.0298	0.0381	0.0435	0.0421	0.0434
e_x	0.500	0.481	0.455	0.450	0.462	0.477

Integrated Values	K_T	K_Q	e
Calculated	0.147	0.0254	0.460
Experimental	0.151	0.0264	0.455
Difference	-2.65%	-4.16%	+0.5%

TABLE VII.

Results of calculations.

$J = 0.6$ $\sigma_n = 1.0$ $\sigma_v = 2.78$

x	0.3	0.5	0.6	0.7	0.8	0.9
s	1.125	0.776	0.645	0.526	0.409	0.280
s_e	1.125	0.776	0.645	0.555	0.480	0.364
σ_x	0.801	0.353	0.256	0.193	0.150	0.119
α_o°	-7.70	-4.10	-2.70	-1.65	-0.90	-0.80
θ°	43.65	29.80	25.53	22.32	19.70	17.65
ψ°	32.40	20.90	17.62	15.28	13.82	11.98
α°	-0.55	0.35	1.05	1.50	1.50	1.40
ϕ°	44.20	29.45	24.48	20.82	18.20	16.25
ϵ°	56.00	38.00	31.54	26.36	22.58	20.52
C_L	0.310	0.237	0.195	0.163	0.147	0.162
C_D	0.0190	0.0218	0.0240	0.0195	0.0170	0.0120
γ	3.56	5.34	7.14	6.83	6.65	4.24
a'	0.184	0.091	0.071	0.047	0.036	0.027
K_{Tx}	0.064	0.158	0.187	0.214	0.222	0.249
K_{Qx}	0.0106	0.0274	0.0346	0.0394	0.0411	0.0419
e_x	0.579	0.550	0.516	0.520	0.515	0.567

Integrated Values	K_T	K_Q	e
Calculated	0.125	0.0232	0.515
Experimental	0.128	0.0237	0.516
Difference	-2.3%	-2.1%	-0.1%

TABLE VIII.

Results of calculations.

$J = 0.7$ $\quad \sigma_n = 1.0$ $\quad \sigma_- = 2.04$

x	0.3	0.5	0.6	0.7	0.8	0.9
s	1.125	0.776	0.645	0.526	0.409	0.280
s_e	1.125	0.776	0.645	0.536	0.452	0.350
σ_x	0.736	0.335	0.247	0.188	0.147	0.118
α_o^o	-7.60	-3.90	-2.60	-1.60	-0.85	-0.80
θ^o	43.65	29.80	25.53	22.32	19.70	17.65
ψ^o	36.65	24.00	20.38	17.65	15.55	13.92
α^o	-2.05	-0.75	0.00	0.40	0.45	0.30
ϕ^o	45.70	30.65	25.53	21.92	19.25	17.35
ϵ^o	54.75	37.30	30.68	26.19	22.95	20.78
C_L	0.253	0.192	0.153	0.135	0.124	0.124
C_D	0.0233	0.0208	0.0194	0.0159	0.0125	0.0097
γ	6.09	6.22	7.27	6.77	5.75	4.49
a'	0.155	0.076	0.052	0.037	0.028	0.022
K_{Tx}	0.065	0.134	0.154	0.180	0.194	0.189
K_{Qx}	0.0124	0.0251	0.0298	0.0345	0.0354	0.0340
e_x	0.585	0.595	0.577	0.580	0.610	0.620

Integrated Values	K_T	K_Q	e
Calculated	0.105	0.0202	0.580
Experimental	0.098	0.0202	0.540
Difference	+7.0%	0%	+4.0%

TABLE IX.

Results of calculations.

$J = 0.8$ $\quad \sigma_n = 1.0$ $\quad \sigma_v = 1.56$

x	0.4	0.5	0.6	0.7	0.8	0.9
s	0.918	0.776	0.645	0.526	0.409	0.280
s_e	0.918	0.776	0.645	0.532	0.437	0.330
σ_x	0.449	0.322	0.238	0.181	0.144	0.115
α_o^0	-5.70	-3.95	-2.80	-1.75	-1.30	-0.85
θ^0	35.65	29.80	25.53	22.32	19.70	17.65
ψ^0	32.50	27.00	23.00	20.00	17.65	15.82
α^0	-2.20	-2.00	-1.20	-0.50	-0.27	-0.20
ϕ^0	37.85	31.80	26.73	22.82	19.97	17.85
ϵ^0	43.20	36.60	30.46	25.64	22.29	19.88
C_L	0.154	0.146	0.119	0.096	0.082	0.079
C_D	0.0242	0.0180	0.0167	0.0148	0.0105	0.0105
γ	9.05	7.07	8.05	8.75	7.03	7.60
a'	0.090	0.053	0.041	0.027	0.020	0.015
K_{Tx}	0.061	0.106	0.122	0.128	0.128	0.118
K_{Qx}	0.0142	0.0214	0.0254	0.0274	0.0272	0.0252
e_x	0.554	0.631	0.611	0.594	0.600	0.595

Integrated Values	K_T	K_Q	e
Calculated	0.0702	0.0146	0.613
Experimental	0.051	0.0143	0.455
Difference	+37.1%	+2.1%	+15.8%

TABLE X.

Results of calculations.

$J = 0.6$ $\quad \sigma_n = ---$ $\quad \sigma_v =$ Non Cavitating

x	0.3	0.5	0.6	0.7	0.8	0.9
s	1.125	0.776	0.645	0.526	0.409	0.280
s_e	1.125	0.776	0.645	0.526	0.409	0.280
σ_x	---	---	---	---	---	---
α_o^o	-7.75	-5.10	-4.10	-3.20	-2.60	-1.90
θ^o	43.65	29.80	25.53	22.32	19.70	17.65
ψ^o	32.50	20.90	17.65	15.28	13.45	12.00
α^o	-0.80	-0.50	-0.20	0.15	0.20	0.30
ϕ^o	42.65	30.30	25.73	22.17	19.70	17.35
ϵ^o	52.80	39.70	33.81	29.08	25.95	22.70
C_L	0.320	0.261	0.233	0.238	0.213	0.192
C_D	0.0200	0.0125	0.0108	0.0095	0.0090	0.0092
γ	3.60	2.76	2.66	2.30	2.42	2.75
a'	0.130	0.095	0.070	0.060	0.043	0.031
K_{Tx}	0.076	0.181	0.238	0.322	0.334	0.296
K_{Qx}	0.0127	0.0295	0.0386	0.0536	0.0544	0.0487
e_x	0.574	0.586	0.590	0.575	0.587	0.580

Integrated Values	K_T	K_Q	e
Calculated	0.176	0.0275	0.611
Experimental	0.178	0.0278	0.611
Difference	-1.1%	-1.1%	0%

TABLE XI.

Results of calculations.

$J = 0.7$ σ_n = --- σ_v = Non Cavitating

x	0.3	0.5	0.6	0.7	0.8	0.9
s	1.125	0.776	0.645	0.526	0.409	0.280
s_e	1.125	0.776	0.645	0.526	0.409	0.280
σ_x	---	---	---	---	---	---
α_o^o	-7.75	-5.10	-4.10	-3.20	-2.60	-1.90
θ^o	43.65	29.80	25.53	22.32	19.70	17.65
ψ^o	36.65	24.00	20.38	17.65	15.55	13.92
α^o	-2.25	-1.32	-1.10	-0.20	-0.30	-0.15
ϕ^o	45.90	31.10	26.63	23.52	20.00	17.80
ϵ^o	55.15	38.20	32.88	29.39	24.45	21.65
C_L	0.257	0.201	0.188	0.195	0.166	0.149
C_D	0.0248	0.0115	0.0106	0.0098	0.0097	0.0095
γ	5.62	3.29	3.23	2.90	3.34	3.65
a'	0.157	0.072	0.057	0.047	0.032	0.024
K_{Tx}	0.056	0.146	0.199	0.266	0.308	0.233
K_{Qx}	0.0105	0.0250	0.0342	0.0463	0.0532	0.0412
e_x	0.591	0.651	0.648	0.640	0.644	0.631

Integrated Values	K_T	K_Q	e
Calculated	0.135	0.0234	0.643
Experimental	0.135	0.0233	0.645
Difference	0%	0%	-0.3%

TABLE XII.

Results of calculations.

$J = 0.8$ $\quad \sigma_n = ---$ $\quad \sigma_v =$ Non Cavitating

x	0.3	0.5	0.6	0.7	0.8	0.9
s	1.125	0.776	0.645	0.526	0.409	0.280
s_e	1.125	0.776	0.645	0.526	0.409	0.280
σ_x	---	---	---	---	---	---
α^o	-7.75	-5.10	-4.10	-3.20	-2.60	-1.90
θ^o	43.65	29.80	25.53	28.32	19.70	17.65
ψ^o	40.35	27.00	23.00	20.00	17.65	15.82
α^o	-3.50	-2.25	-1.85	-1.25	-0.93	-0.63
ϕ^o	47.15	32.05	27.38	23.57	20.62	18.28
ϵ^o	53.95	37.10	31.76	27.04	23.59	20.74
C_L	0.191	0.148	0.137	0.120	0.111	0.103
C_D	0.0330	0.0155	0.0123	0.0108	0.0100	0.0095
γ	10.00	6.15	5.15	5.16	5.21	5.31
a'	0.133	0.061	0.045	0.023	0.023	0.018
K_{Tx}	0.040	0.109	0.146	0.166	0.179	0.161
K_{Qx}	0.0094	0.0214	0.0280	0.0319	0.0346	0.0317
e_x	0.548	0.650	0.665	0.664	0.659	0.649

Integrated Values	K_T	K_Q	e
Calculated	0.0905	0.0181	0.636
Experimental	0.0905	0.0185	0.622
Difference	0%	-2.2%	+1.4%